UNIVERSITÉ DE MONTRÉAL

MODELLING POLLUTANT TRANSPORT IN OVERLAND FLOW WITH INFILTRATION

MIN YAN

DÉPARTEMENT DE GÉNIE CIVIL
ÉCOLE POLYTECHNIQUE DE MONTRÉAL

MÉMOIRE PRÉSENTÉ EN VUE DE L'OBTENTION
DU DIPLÔME DE MAÎTRISE ÈS SCIENCES APPLIQUÉES (M.Sc.A.)

(GÉNIE CIVIL)
AVRIL 1995

© Min Yan 1995

National Library of Canada
Bibliothèque nationale du Canada

Acquisitions and Bibliographic Services Branch
Direction des acquisitions et des services bibliographiques

395 Wellington Street
Ottawa, Ontario
K1A 0N4

395, rue Wellington
Ottawa (Ontario)
K1A 0N4

Your file *Votre référence*

Our file *Notre référence*

The author has granted an irrevocable non-exclusive licence allowing the National Library of Canada to reproduce, loan, distribute or sell copies of his/her thesis by any means and in any form or format, making this thesis available to interested persons.

L'auteur a accordé une licence irrévocable et non exclusive permettant à la Bibliothèque nationale du Canada de reproduire, prêter, distribuer ou vendre des copies de sa thèse de quelque manière et sous quelque forme que ce soit pour mettre des exemplaires de cette thèse à la disposition des personnes intéressées.

The author retains ownership of the copyright in his/her thesis. Neither the thesis nor substantial extracts from it may be printed or otherwise reproduced without his/her permission.

L'auteur conserve la propriété du droit d'auteur qui protège sa thèse. Ni la thèse ni des extraits substantiels de celle-ci ne doivent être imprimés ou autrement reproduits sans son autorisation.

ISBN 0-612-08232-6

Canada

UNIVERSITÉ DE MONTRÉAL

ÉCOLE POLYTECHNIQUE

Ce mémoire intitulé:

MODELLING POLLUTANT TRANSPORT IN OVERLAND FLOW WITH INFILTRATION

Présenté par: YAN Min

en vue de l'obtention du diplôme de: Maîtrise ès Sciences Appliquées

a été dûment accepté par le jury d'examen constitué de:

M. ROUSSELLE Jean, Ph.D., Président

M. KAHAWITA René, Ph.D., membre et directeur de recherche

M. COMEAU Yves, Ph.D., membre

Dedicated to my husband Guo-Cheng Xu ,

my dear daughter Ying Xu

and my parents.

ACKNOWLEDGEMENTS

This work could not have been accomplished without help from a large number of people. My utmost thanks, however, go to René Kahawita, my supervisor, for his guidance, support and invaluable help during my years at École Polytechnique.

I would also like to thank the professors in my thesis defence jury for their examination of my Master's Thesis.

I greatly appreciated the help from all the colleagues in our group and my classmates during my Master study, particularly Gilles Thériault and Manuel Kotchounian.

Finally, I would like to give my special thanks to my brothers for their love, encouragement and support.

RÉSUMÉ

Un modèle mathématique du processus du transport de polluants par ruissellement et par infiltration est développé. Ce modèle couple des équations de ruissellement, d'advection-diffusion du transport des polluants, de mise en solubilité et de continuité de masse. Les équations bidimensionnelles du ruissellement, l'équation de continuité et l'équation de la quantité de mouvement sont résolues et les résultats obtenus servent à résoudre l'équation du transport des polluants. Les équations bidimensionnelles du transport des polluants dans lesquelles les propriétés physiques et chimiques sont décrites, l'équation du taux de solubilité ainsi que l'équation de continuité de masse sont modélisées. Le modèle tient également compte des apports de la pluie et de l'infiltration, l'équation de Horton et l'équation de Green-Ampt étant utilisée pour estimer les volumes infiltrés. Il est ainsi possible de prévoir la quantité des polluants dissous, infiltrés et lessivés. Pour solutionner les équations du ruissellement et du transport des polluants le traitement numérique est appliqué. En utilisant la méthode des différences finies dans une formulation explicite, implicite ou schéma boite, les équations de St-Venant ou leurs approximation pour l'onde cinématique sont résolues. La convergence est assurée par la technique itérative de Newton-Raphson pour résoudre l'ensemble des équations non linéaires. L'équation unidimensionnelle du transport des polluants est résolue par un schéma explicite

de differentiation en avant ou par le schéma implicite centré temporellement (QUICK). Ce dernier est utilisé pour résoudre l'équation bidimensionnelle du transport des polluants.

ABSTRACT

A physically based mathematical model is proposed for the process of pollutant transport in overland flow with infiltration. The model is based on the overland flow equations, the pollutant transport equation modelled with advection-diffusion, a solubility rate equation and the solid balance equation. The two-dimensional overland flow equations consist of the continuity equation and momentum equations which are solved using an implicit procedure. The results are applied to the numerical solution of the pollutant transport equation. The solubility rate equation and the solid balance equation account for the physical and chemical properties of the pollutant being simulated. The model also incorporates the effects of rainfall and infiltration. For the infiltration, the Horton equations are used during the period when the soil is unsaturated followed by the well known Green-Ampt equations after saturation.

The aim of this work has been to model the ultimate fate of a surface applied pollutant by evaluating the quantities of pollutant that is dissolved, infiltrated or washed-out. The complete St.Venant equations and the kinematic wave approximation for overland flow are solved by using an implicit finite difference method and a box scheme respectively. The global convergence of the Newton iteration technique is used to solve the nonlinear set of equations obtained with the

implicit finite difference formulation. The forward explicit and the fully time centred implicit modified QUICK finite difference schemes are used to solve the one dimensional pollutant transport equation. The fully time centred implicit modified QUICK scheme is used to solve the two dimensional pollutant transport equation. The Fortran language has been corded in and executed on a PC-based platform.

CONDENSÉ EN FRANÇAIS

Le ruissellement de surface ne cause pas seulement l'érosion du sol et des inondations mais transporte aussi les polluants qui rejoignent un cours d'eau ou la nappe phréatique par infiltration. La contamination de la nappe phréatique engendre des problèmes sérieux pour l'exploitation de cette ressource hydrique. Le contrôle des ressources d'eau est devenu une haute priorité et toute tentative pour résoudre ce problème demande une excellente compréhension du comportement hydraulique du ruissellement, de l'infiltration et du transport des polluants. De plus, la compréhension des phénomènes de base permet de déterminer les profondeurs et les vitesses de l'écoulement et sa capacité à entraîner et à transporter les polluants.

Plusieurs travaux sur la modélisation du ruissellement ont été effectués par des pionniers. Ces recherches ont conduit à une connaissance approfondie des mécanismes mis en jeu dans le comportement de ruissellement en une ou en deux dimensions. Cependant, la modélisation du transport des polluants, leur captage par l'eau et leur sort ultime une fois infiltré n'ont pas reçu une aussi grande attention. Bien que la modélisation du phénomène du transport basée sur l'équation advection-diffusion soit courante, parmi toutes les recherches réalisée, peu de recherches ont considéré les effets du ruissellement, de l'infiltration et de

taux par lequel les polluants se dissoudre dans l'écoulement.

Le but de ce travail est de modéliser le phénomène du ruissellement sur surface perméable, de modéliser le phénomène du transport des polluants avec dissolution, de proposer un modèle de mise en solubilité et de développer une séquence de procédures numériques appropriée à simuler l'effet combiné des phénomènes mis en jeu.

Cette étude décrit le développement d'un modèle numérique basé sur l'ensemble des processus de ruissellement avec transport des polluants. Ce modèle s'appuie sur les lois de la conservation de la masse et de la quantité de mouvement pour les phénomènes physico-chimiques naturels; ces phénomènes comprennent la pluie, l'infiltration, le taux de solubilité, la diffusion et l'advection. La modélisation du ruissellement est obtenue par la résolution numérique des équations de St-Venant ou des équations cinématiques.

La modélisation du transport des polluants est basée sur trois équations décrivant le phénomène du ruissellement, la dissolution des polluants et le bilan solide. Dans ces équations, le caractère transitoire du transport des polluants dans le ruissellement a été considéré en combinaison avec l'infiltration. La modélisation des aspects vraisemblablement les plus significatifs a été faite: il

s'agit du ruissellement avec infiltration, compte tenu du type de polluant, l'advection, la diffusion ainsi que le taux de solubilité. L'équation fondamentale qui décrit le phénomène du transport est celle de l'advection-diffusion. Un terme source est ajoutée à l'équation de l'advection-diffusion de façon à décrire l'effet du taux de solubilité. La solution des vitesses du ruissellement est utilisée pour décrire l'effet de l'advection non permanent. Un terme de puits (source négative) est ajouté pour décrire l'apport de la pluie. L'équation du transport des polluants proposée peut s'écrire ainsi:

$$\frac{\partial s}{\partial t}+u\frac{\partial s}{\partial x}+v\frac{\partial s}{\partial y} = \frac{\partial}{\partial x}(D_x\frac{\partial s}{\partial x})+\frac{\partial}{\partial x}(D_y\frac{\partial s}{\partial y})+\frac{S_t}{h}-\frac{sQr}{h}$$

La représentation mathématique du taux de solubilité d'un polluant est basée sur le comportement physico-chimique de ce polluant dans le ruissellement. Dans cette étude, l'ensemble des effets chimiques et physiques est pris en considération. Le taux de solubilité est présumé proportionnel au contrainte de cisaillement à la surface de ruissellement, à la différence entre la valeur de la concentration saturante et de la concentration locale, et finalement à une constante de proportionnalité qui exprime un taux de réaction dépendant du soluté et du solvant considérés. Cela conduit à l'expression mathématique suivante:

$$S_t = \frac{ds}{dt} = k\tau(c^{*}-s)$$

où

$$\tau = \gamma h s_f = \gamma \frac{n^2(u^2+v^2)}{h^{1/3}}$$

À l'aide de l'équation pour le bilan solide, la quantité de polluant dissous, infiltré et lessivé par ruissellement peut être estimée.

L'infiltration et la pluie sont des facteurs importants dans un modèle hydrologique. Ils n'affectent pas seulement le temps mais aussi la distribution et l'ampleur de la ruissellement. Ces facteurs influencent la quantité de la masse polluante en migrantion dans le sol. Ces simulations ont supposées une intensité constante de la pluie dans l'équation du ruissellement; cependant, le modèle peut accepter une intensité variable. Le taux d'infiltration est calculé en utilisant l'équation de Horton et celle de Green-Ampt. L'équation de Horton est utilisée pour prévoir la quantité de polluants infiltrés avant que l'accumulation à la surface ne se manifeste et celle de Green-Ampt est utilisée pour estimer celle infiltrée une fois l'accumulation de surface satisfaite.

Pour modéliser le ruissellement unidimensionnel, le schéma "boite", l'une des méthodes comportant une équation à une seule inconnue, inconditionnellement stable bien que limité à un intervalle de temps (Wood and Arnold, 1990), a été utilisé pour résoudre l'équation de l'onde cinématique. Dans le cas bidimensionnel, une schéma implicite est utilisé pour résoudre les équations complètes de St-Venant. Chaque modèle inclut les effets de variations topographiques dans une pente, incluant la rugosité de la surface, l'infiltration dans le sol et l'intensité de la pluie. La propriété de convergence globale de la technique d'itération de Newton-Raphson est exploitée pour résoudre l'ensemble des équations algébriques non linéaires obtenues par la discrétisation. Les solutions des équations de St-Venant pour la profondeur de l'écoulement et les deux composantes de la vitesse ont été associées à l'équation du transport des polluants, laquelle fut résolue par l'utilisation du schéma QUICK (Quadratic Upstream Interpolation For Convection Kinematics) modifié, développé originalement par Leonard (1979) et très utilisé dans la solution des problèmes reliés à l'hydraulique. Pour l'équation unidimensionnelle du transport des polluants, le même schéma QUICK cette fois avec formulation explicite et celui centré dans le temps avec une formulation implicite ont été tous les deux utilisés. Pour le cas bidimensionnel, le schéma implicite complètement centré sur le temps est utilisé.

Pour qu'un problème mathématique soit "bien posé", il est essentiel de définir correctement les conditions initiales et frontières. Dans le cas du ruissellement, il est possible de supposer une très mince couche d'eau initiale sur une surface sèche au départ, au début d'une simulation. Cette artifice évite le traitement des écoulements avec des profondeurs nulles; les simulations ont supposé une couche initiale de 10^{-4} m. Deux cas différents de conditions initiales ont été considérés dans la distribution de la masse polluante:

a) Une masse polluante initiale concentrée en un point,

b) Une masse polluante répandue uniformément sur le sol.

Les conditions limites devraient être basées sur des considérations physiques. Dans le cas du ruissellement, utilisant l'équation bidimensionnelle de St-Venant, des profondeurs de l'écoulement et des vitesses de l'écoulement sont considérés nulles. Pour l'approximation de l'onde cinématique, le débit unitaire est nul. En aval, pour l'équation unidimensionnelle de St-Venant, les gradients de profondeur de l'écoulement et les vitesses sont supposées nulles. Pour l'approximation de l'onde cinématique, les conditions limites en aval ne sont pas nécessaires. Dans le cas du transport des polluants, en amont, la condition de concentration nulle est utilisée; en aval, une gradient de concentration nulle est utilisée.

En utilisant l'intégration numérique des équations, le comportement hydraulique du ruissellement est estimé; la quantité de polluants dissous, la

quantité finale d'infiltration et celle lessivé sont déterminés. A l'aide de ces résultats, la migration des polluants appliqués à la surface dans la nature peut être analysée.

CONTENTS

ACKNOWLEDGEMENTS v

RÉSUMÉ vi

ABSTRACT viii

CONDENSÉ EN FRANÇAIS x

CONTENTS xvii

LIST OF TABLES xx

FIGURE CAPTIONS xxi

LIST OF SYMBOLS xxiv

CHAPTER 1 INTRODUCTION **1**

1.1 Generalities 1

1.2 Scope of Present Work 3

CHAPTER 2 REVIEW OF LITERATURE **7**

2.1 Modelling of Overland Flow 7

2.2 Pollutant Transport Models 13

2.3 The Effects of Rainfall-Infiltration 16

2.4 Numerical Techniques 22

CHAPTER 3 THEORETICAL FORMULATION **29**

3.1 Overland Flow Models 29

3.1.1 The St.Venant Equations in Two Dimensions 29

3.1.2 Kinematic Wave Equation 32

3.2 Infiltration Models 36

3.3 Pollutant Transport Model 43

3.3.1 Pollutant Transport Equation 43

3.3.2 Solubility Rate Model (Source Term) 48

3.3.3 Solid Balance Equation 50

3.4 Initial Condition 53

3.4.1 Overland Flow Equation 53

3.4.2 The Pollutant Transport Equation 53

3.5 Boundary Conditions 54

3.5.1 Overland Flow Equation 54

3.5.2 The Pollutant Transport Equation 58

CHAPTER 4 NUMERICAL SCHEME **60**

4.1 Box Scheme 60

4.2 Numerical Scheme for Two-Dimensional Overland flow 65

4.3 QUICK Scheme 73

4.4 Solution Technique 82

CHAPTER 5 RESULTS AND DISCUSSION **86**

5.1 Hydraulic Behaviour of Overland Flow 88

5.2 Results of Pollutant Concentration 89

5.2.1 The Migration Process of Pollutant in Overland Flow 89

5.2.2 The Effect of Diffusion Coefficient 92

5.2.3 The Effect of Solubility 93

5.2.4 The Effect of Rainfall 94

5.2.5 The Effect of Infiltration 94

5.3 The Application of Infiltration Models 95

CHAPTER 6 CONCLUSIONS AND RECOMMENDATIONS **131**

REFERENCES **133**

LIST OF TABLES

Table 2.1: Previous Research on Overland Flow 12

Table 2.2: Previous Research on Transport Phenomena 17

FIGURE CAPTIONS

Figure 1.1: Sketch of Overland Flow on a Plain 4

Figure 3.1: Definition Sketch for Two-Dimensional Overland Flow 30

Figure 3.2: Different Cases of Infiltration Behavior Under Rainfall 38

Figure 3.3: Mass Balance Over a Control Volume 45

Figure 3.4: Sketch of Representation of The Number of Unknowns 56

Figure 4.1: Sketch of Grid Representation for The Box Scheme 61

Figure 4.2: Computational Molecule for the Implicit Difference Scheme . . 67

Figure 4.3: Sketch of Grid Representation for The QUICK Scheme 75

Figure 5.1: The Sketch of Solution Procedure 87

Figure 5.1.2: Flow Depth of Overland Flow

T=1727.85s, H_{max}=0.01875m 102

Figure 5.1.3: Depth Profile of Overland Flow

T=1727.85s, H_{max}=0.01875m 103

Figure 5.1.4: Time Evolution of Runoff 104

Figure 5.1.5 Comparison of the Experimental Data with the

Numerical Solution 105

Figure 5.2.1: Variation of Concentration (1-D)

Initial Pollutant Mass Applied at One Grid Cell 106

Figure 5.2.2: The Migration of Pollutant in Overland Flow (2-D)

T=782.45s, S_{max}=0.1772kg/m^3 107

Figure 5.2.3: The Migration of Pollutant in Overland Flow (2-D)

T=1227.95s, S_{max}=0.0997kg/m^3 108

Figure 5.2.4: The Migration of Pollutant in Overland Flow (2-D)

T=1477.85s, S_{max}=0.0766kg/m^3 109

Figure 5.2.5: The Migration of Pollutant in Overland Flow (2-D)

T=2227.85s, S_{max}=0.0364kg/m^3 110

Figure 5.2.6: The Variation of Concentration (1-D)

Initial Pollutant Mass Uniformly Applied 111

Figure 5.2.7: The Migration of Pollutant in Overland Flow (2-D)

T=191.45s, S_{max}=20.0552kg/m^3 112

Figure 5.2.8: The Migration of Pollutant in Overland Flow (2-D)

T=1227.85s, S_{max}=31.22kg/m^3 113

Figure 5.2.9: The Migration of Pollutant in Overland Flow (2-D)

T=1727.85s, S_{max}=34.2072kg/m^3 114

Figure 5.2.10: The Migration of Pollutant in Overland Flow (2-D)

T=2227.85s, S_{max}=35.1082kg/m^3 115

Figure 5.3.1: The Effect of Diffusion Coefficient (1-D), D=0.5m^2/s 116

Figure 5.3.2: The Effect of Diffusion Coefficient (1-D), D=0.1m^2/s 117

Figure 5.3.3: The Effect of Diffusion Coefficient 118

Figure 5.3.4: The Effect of Diffusion Coefficient (2-D)

$D=1m^2/s$, $S_{max}=0.023kg/m^3$ 119

Figure 5.3.5: The Effect of Diffusion Coefficient (2-D)

$D=10m^2/s$, $S_{max}=0.0037kg/m^3$ 120

Figure 5.4.1: The Effect of Solubility

$C^*=745kg/m^3$, $S_{max}=0.0259kg/m^3$ 121

Figure 5.4.2: The Effect of Solubility

$C^*=34.8kg/m^3$, $S_{max}=0.0073kg/m^3$ 122

Figure 5.5.1: The Effect of Rainfall 123

Figure 5.5.2: The Effect of Infiltration 124

Figure 5.5.3: The Variation of Pollutant Infiltrated 125

Figure 5.5.4: Time Evolution of Residual Pollutant 126

Figure 5.5.5: Time Evolution of Dissolved Solute 127

Figure 5.5.6: Time Evolution of Pollutant Washout 128

Figure 5.5.7: The Trace of Maximum Concentration 129

Figure 5.5.8: Comparison of the Different Schemes 130

LIST OF SYMBOLS

C^*	solubility, kg/m^3
d_0	infiltration depth at the start of ponding, m
D_x	diffusion coefficient in the x direction, m^2/s
D_y	diffusion coefficient in the y direction, m^2/s
f_0	initial infiltration capacity, m/s
f_c	a final equilibrium capacity, m/s
f_p	infiltration capacity, m/s
F	infiltration amount, m
ΔF	potential accumulative, m
g	gravitational acceleration, m/s^2
h	flow depth, m
k_1	hydraulic conductivity, m/s
k_2	reaction rate constant, $m^2 \cdot s/kg$
k_3	time rate constant, s^{-1}
k_4	delay time constant, s
n	Manning's roughness coefficient,
q	the discharge per unit width of slope, $m^3/s/m$
Q	net lateral inflow m/s

Qi	infiltration rate, m/s
Qr	rainfall intensity, m/s
s	concentration, kg/m^3
s_e	initial effective saturation
s_f	friction slope
S_t	solubility rate, $kg/s/m^2$
s_x	the friction slope in the x direction
s_y	the friction slope in the y direction
s_{ox}	the bed slope in x direction
s_{oy}	the bed slope in y direction
t	time, s
T_e	equivalent time, s
t_p	time to ponding, s
T_s	rainfall duration, s
Δt	time interval, s
u	flow velocity in the x direction, m/s
v	flow velocity in the y direction, m/s
w_0	initial distribution of pollutant, kg/m^2
w	residue of pollutant mass, kg/m^2
w_m	initial pollutant mass, kg/m^2
Δx	space increment in x direction

Δy	space increment in y direction

Greek symbols

α	angle of slope in x direction
γ	specific weight of water, $kg/m^2/s^2$
θ	weighting coefficient
θe	effective porosity
ρ_0	soil porosity
ρ_1	effective soil porosity
ω	weighting coefficient
ϕ	angle of slope in y direction
ψ_1	wetting front capillary pressure head, m
ϵ	Courant number in x direction
η	Courant number in y direction
γ	diffusion number in x direction
ξ	diffusion number in y direction
τ	shear stress, N/m^2

Subscripts

i	node number in x direction
j	node number in y direction
M	boundary node in x direction
N	boundary node in y direction

Superscripts

k	time step number

CHAPTER 1
INTRODUCTION

1.1 GENERALITIES

Overland flow refers to that part of the streamflow which originates from rain which, having failed to infiltrate the soil surface at any point, flows over the land surface to channels (Kirkby,1979). It is well-known that overland flows not only cause surface erosion and floods but also carry pollutants, such as pesticides, fertilizers, and the debris of plants and animals into the receiving water body. Many of these pollutants are nonbiodegradable or are only slightly soluble in water; when sprayed on land, they persist in the soil for long periods of time. With heavy rainfall, these pollutants may be carried as suspended particles in the surface water, partially dissolve and infiltrate into the groundwater or join the river system. The long-term effects may be serious. Some consequences of pollution could be: (1) Oxygen depletion in water bodies due to the action of certain substances, (2) Excess plant nutrients, (3) Agents of biological dysfunction, and (4) Sedimentary and erosional processes (John, 1977).

Any attempt to define and solve this problem requires a good understanding of the laws of overland flow. A fundamental knowledge of the hydraulics of

overland flows is very important in order to be able to determine flow depths and velocities, and, hence describe the capacity of the flow to entrain and transport pollutants (Moore and Foster 1989).

Since the equations governing these types of flow are intractable to analytical solution, numerical techniques must be employed.

Much effort has been devoted to numerically solving the system of governing equations. Numerical methods have proved to be powerful tools in the simulation of diverse hydraulic and transport phenomena.

This study describes the development of a numerical model that is focused on modelling overland flow together with pollutant transport. The model is based on the continuity equation, the momentum equation and the mass conservation law. It attempts to account for the complicated natural physical and chemical phenomena, which includes rainfall, infiltration, solubility rate, diffusion and advection. Using numerical integration of the governing equations, the hydraulic behaviour of the overland flow is estimated, the amount of pollutant that is dissolved and the ultimate fate of the pollutant due to infiltration and washout is determined. With the help of these results, the migration of a surface applied pollutant in nature may be analyzed. The physical significance of this study may

be expressed by the sketch shown in figure 1.1.

It is hoped that the work presented here will have many engineering applications and provide a scientific basis for water pollution control in environmental engineering.

1.2 SCOPE OF PRESENT WORK

Different from many previous researches that treated the overland flow and transport phenomena as two individual parts, this project focus on the combination of these two parts. A numerical model for pollutant washout and transport in overland flow with infiltration is proposed in this study. The model takes full account of the two-dimensionality and transient character of the overland flow and pollutant transport.

In order to describe the hydrodynamic behaviour of overland flow, numerical solutions of the kinematic wave equations and the full two dimensional St.Venant equations were obtained. The variation of surface roughness, rainfall intensity and soil infiltration is considered. For the one-dimensional overland flow problem, a box scheme has been used to solve the kinematic wave equation. This scheme is based on an explicit time marching algorithm which is unconditionally stable (Wood

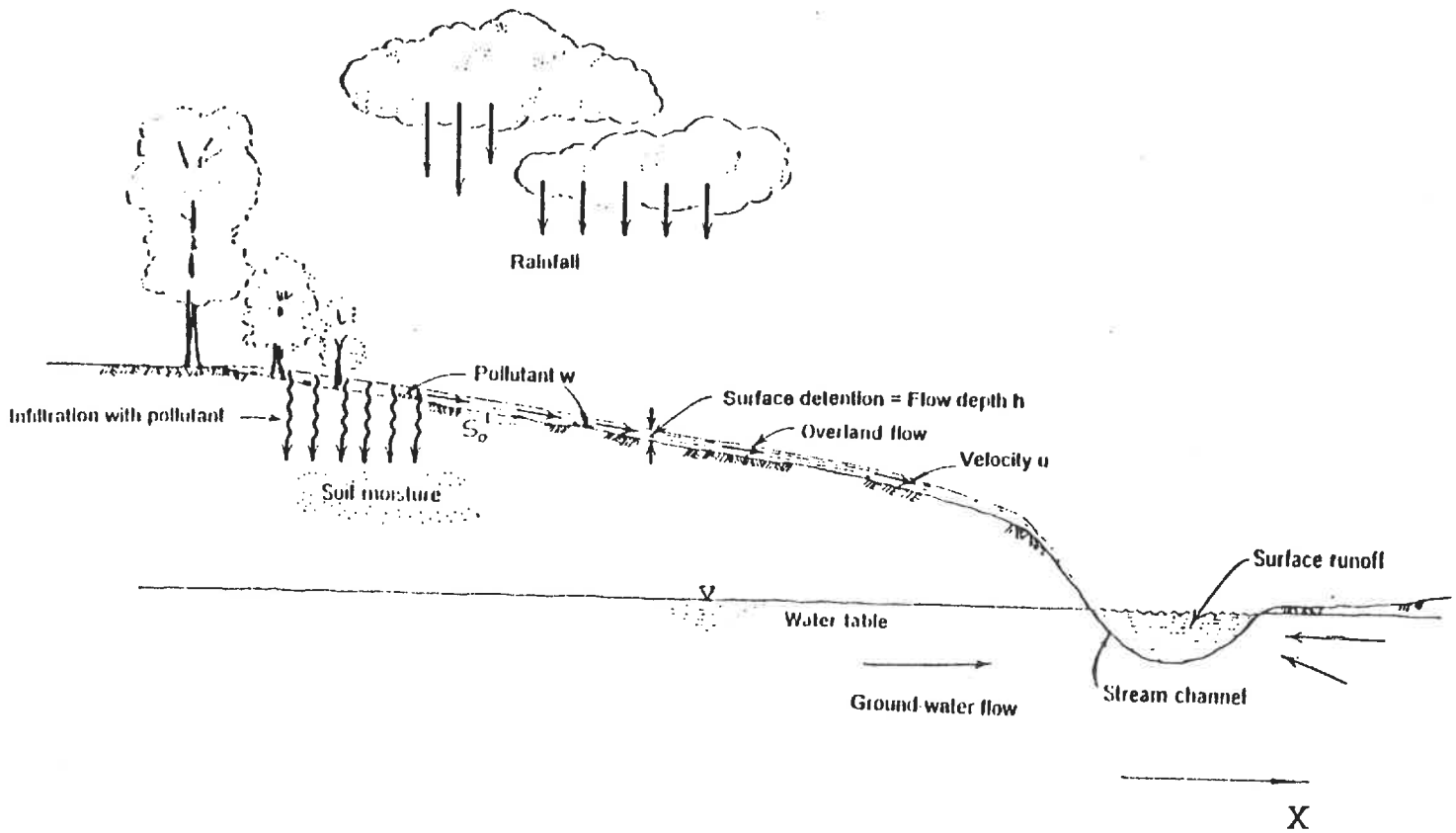

Figure 1.1 Sketch of Overland Flow on a Plain

and Arnold 1990). For the two-dimensional case, an implicit space centred finite difference scheme was used to solve the full dynamic St.Venant equations. The global convergence property of the Newton-Raphson iteration technique was exploited to solve the nonlinear set of algebraic equations.

A pollutant transport model, which is based on the mass conservation law has been proposed. This model includes the advection-diffusion equation, solubility rate equation and a solid balance equation. Pollutant transport is a complex process, which is affected by many factors. In this study, an attempt has been made to model those which are likely to be the most significant; the rainfall characteristics, the overland flow with infiltration, the type of pollutant, advection, diffusion and solubility rate.

The mathematical model for the pollutant solubility rate is proposed in this study. In most practical situations, the concentration distribution is specified as an initial condition on the basis of physical arguments, the present project is different in that a specified spatial distribution of solid pollutant is provided, and so the concept of solubility rate should be introduced. This model is constructed based on the physico-chemical behaviour of pollutant in overland flow and drawing on the analogy between heat, mass and momentum transfer, in which both physical effects such as the flow depth, the bottom bed shear stress and the density of the

pollutant as well as chemical effects, i.e. solubility and reaction rate constant were considered.

For purposes of demonstration, a constant rainfall intensity was used in the overland flow equation, infiltration rate is calculated by using Horton's equation and the Green-Ampt equation. Horton's equation is used to predict the amount of infiltrated pollutant before ponding begins and the Green-Ampt equation is used to describe the subsequent infiltration behaviour after the start of ponding.

Finally, the two parts were combined to form a pollutant concentration equation. The solutions of the St.Venant equations for the flow depth and the two velocity components were coupled with the advection-diffusion equation which was solved using a modified QUICK scheme. For one-dimensional and two-dimensional pollutant transport, the forward explicit QUICK (Quadratic Upstream Interpolation for Convection Kinematics) scheme and the fully time-centred implicit QUICK scheme were respectively used to solve the pollutant concentration equation.

Then, from the solid balance equation, the amount of dissolved, infiltrated and washed-off pollutant may be estimated.

CHAPTER 2
REVIEW OF LITERATURE

2.1 MODELLING OF OVERLAND FLOW

The physically realistic modelling of overland flow is in general, accomplished through the numerical solution of the St.Venant equation. The two-dimensional St.Venant equations that describe the motion of water with a free surface, are based on mass and momentum conservation laws and derived from the Navier-Stokes equations integrated over the depth with the assumption of a hydrostatic vertical pressure distribution.

These equations may be expressed as follows (Tayfur et al., 1993):

The continuity equation

$$\frac{\partial h}{\partial t} + \frac{\partial (hu)}{\partial x} + \frac{\partial (hv)}{\partial y} = [Qr(x,y,t) - Qi(x,y,t)]\cos(\alpha)\cos(\phi) \qquad (2\text{-}1\text{-}1)$$

The momentum equation in the x direction:

$$\frac{\partial u}{\partial t} + u\frac{\partial u}{\partial x} + v\frac{\partial u}{\partial y} + \cos(\alpha)\cos(\phi)g\frac{\partial h}{\partial x} = g\ \sin(\alpha) - S_x g - \frac{Qu}{h} \qquad (2\text{-}1\text{-}2)$$

The momentum equation in the y direction:

$$\frac{\partial v}{\partial t} + u\frac{\partial v}{\partial x} + v\frac{\partial v}{\partial y} + \cos(\alpha)\cos(\phi)g\frac{\partial h}{\partial y} = g\ \sin(\phi) - S_y g - \frac{Qv}{h} \qquad (2\text{-}1\text{-}3)$$

Where

h = flow depth

u = flow velocity in the x-direction

v = flow velocity in the y-direction

Qr = rainfall intensity

Qi = infiltration rate

Q = net lateral inflow (rainfall-infiltration)

α = angle of the slope with respect to the x-direction

ϕ = angle of the slope with respect to the y-direction

g = gravitational acceleration

S_x = the friction slope in the x direction

S_y = the friction slope in the y direction

The system is nonlinear so that no analytical solutions are generally available, except those with highly restrictive assumptions.

The kinematic wave approximation is a popular approximation to the St.Venant equation, and has been commonly used because of its simplicity. It assumes that all terms in the momentum equation are very small compared to the friction and gravity terms (Moore and Foster 1989). This results in the uniform flow approximation for the momentum equation together with the continuity equation to complete the set. The diffusion wave equation is another approximation to the

St.Venant equations. It assumes that the inertial terms are small compared to the pressure, friction and gravity terms (Moore and Foster, 1989). This results in the transformation of the original equations into a transport-diffusion set. This form of the equation has found application in the modelling of routing of flood waves where the propagation and attenuation is modelled with two parameters.

Obtaining solutions to the full St.Venant equations applied to overland flow is not trivial. The difficulties arise from its following physical characteristics:

1) Overland flow is very shallow. It is not uncommon for the depth of overland flow to be of the order of a few centimeters or even millimeters. Consequently, even very small numerical oscillations will result in negative computed flow depths, thus causing the numerical solution to fail.

2) The effect of shear stress induced by the bed roughness is larger than that for the case of deep water. This often causes numerical difficulties leading to complete failure during the computation.

3) Rainfall and infiltration represent a significant mathematical "source" and "sink", respectively (Zhang and Cundy 1989) and must be carefully treated numerically.

There has been many research studies for modelling overland flows. Liggett and Woolhiser (1967) used the one-dimensional hydrodynamic equation for modeling overland flow. They conducted extensive numerical experimentation

to compare the behaviour of different numerical schemes for solving the hydrodynamic equations. Although this study provided valuable experience and guidelines for obtaining solutions to the hydrodynamic equation for overland flow, it was limited to homogeneous plane surfaces.

Akan and Yen (1981) developed a one-dimensional overland flow model, in which both surface and subsurface flows were described by a set of dynamic wave equations. However, only one- dimensional flow with homogeneous plane surfaces was considered.

Chow and Zvi (1973) indicated the feasibility of two-dimensional hydrodynamic modelling of watershed flow with a proposed theoretical model. However, they used a much simplified version of the hydrodynamic equation in which all terms related to the convective acceleration were dropped from the hydrodynamic equation. These terms may be significant in flows with spatial variations in hillslope characteristics.

Kawahara and Yokoyama (1980) presented a model for two-dimensional overland flow. They assumed a depth averaged velocity of the flow at any point of the watershed. The pressure was postulated to be hydrostatic neglecting the rainfall impact. Spatial variability of infiltration rate and roughness were ignored

in their model.

Wood and Arnold (1990) have modeled overland flow given by rainfall-runoff on a sloping plane using a one dimensional kinematic wave equation.

Zhang and Cundy (1989) solved the two dimensional overland flow equation using the explicit MacCormack scheme. Their results were partially verified with field experiments. More recently, the two dimensional kinematic wave equation was modelled by Tayfur et al. (1993) and supplemented with field experiments. Both studies included the effects of variations in hillslope feature, including surface roughness, infiltration and microtopography.

The research cited above has provided considerable insight into the mechanism, behaviour and modelling of overland flow in one and two dimensions. However the aspect of pollutant transport and their ultimate fate through infiltration and runoff into a receving water body has not been investigated. Table 2.1 summarizes previous work realised on overland flow. This study is devoted to the investigation of this problem.

Table 2.1 Previous Research on Overland Flow

Author	Year	Dimension	Physical Condition
Liggett and Woolhiser	1967	1-D	Overland flow with homogeneous plane surfaces
Akan and Yen	1981	1-D	Overland flow with homogeneous plane surfaces, both subsurface and surface flows were described
Chow and Bon-Zvi	1973	2-D	Overland flow in which all terms related to the convective acceleration were dropped
Wood and Arnold	1990	1-D	Kinematic wave approximation
Kawahara and Yokoyama	1980	2-D	Overland flow without spatial variability of infiltration rate and roughness
Zhang and Cundy	1989	2-D	Overland flow including surface roughness, infiltration and microtopography , the results were partially verified with field experiments
Tayfur et al	1993	2-D	Kinematic wave equations including surface roughness, infiltration and microtopography with field experiments.

2.2 POLLUTANT TRANSPORT MODELS

Predicting the evolution and fate of a surface applied pollutant in overland flow is a complex problem, since it encompasses the surface transport, infiltration and washout. Usually, transport in overland flow takes place as a result of two phenomena: advection and diffusion. Advection is that transport of a contaminant which results from fluid motion. Diffusion is one of the most basic phenomena occurring in nature. It is a process by which a substance in solution or in suspension, migrates in response to a concentration gradient through the solvent in a direction that would tend to nullify the concentration gradient. A complete model for pollutant transport should account for the advection, dispersion, diffusion, solubility rate and the chemical and biological reactions of the pollutant as well as the two velocity components and flow depth of the overland flow. However, the effects of dispersion and biochemical reactions may be neglected for all practical purposes, when the pollutants are transported in a shallow overland flow over a short time period. (Akan 1987). The process of pollutant infiltration and washout is affected by many factors, chief among which are the rainfall characteristics, the type of flow, the infiltration properties of the soil and the type of pollutant.

In recent years, considerable effort has focused on numerically solving fluid

transport problems. The model equation describing transport phenomena is the advection-diffusion equation, it may be written as follows:

$$\frac{\partial s}{\partial t} + u\frac{\partial s}{\partial x} + v\frac{\partial s}{\partial y} = \frac{\partial}{\partial x}\left(D_x\frac{\partial s}{\partial x}\right) + \frac{\partial}{\partial y}\left(D_y\frac{\partial s}{\partial y}\right) \qquad (2\text{-}2\text{-}1)$$

where s = concentration (kg/m^3)

u, v = the advection velocity in the x- and y-direction respectively (m/s)

with D_x and D_y are diffusion coefficient in the x and y direction, respectively.

Siemons (1970) was one of the earlier researchers who attempted the numerical solution of the advection-diffusion equation. He presented the numerical solutions for two special cases: the one-dimensional diffusion-advection equation, and the two-dimensional diffusion-advection equation with zero velocity. In his research, the numerical solution of the two-dimensional diffusion-advection equation with advection in two directions was not treated.

Li (1990) simulated the advective transport of a scalar. His results however, were limited to the one-dimensional pure advection of a scalar with constant velocity.

Holly and Preissmann (1977) presented a numerical method for the accurate calculation of advection and diffusion in one and two dimensions. Their research considered the following problem: a neutrally buoyant marked fluid, assumed to be uniformly distributed over the depth, is subjected to turbulent diffusion and differential advection in a two-dimensional, time-dependent velocity field that is assumed to be known. High accuracy was obtained by using the derivative as the dependant variable.

Chen and Falconer (1992) modelled the transient one-dimensional source-free transport of a scalar mass of pollutant concentration in an open channel, and the simplified governing two-dimensional advection equation. In both cases, constant velocities were used. All of the above work has been concerned with transport phenomena in rivers and estuaries.

Farthermore, the individual phenomena were modelled seperately and not in combination as acoupled system.

Akan (1987) proposed a mathematical model to predict pollutant washout from impervious areas by overland flow, this model was based on the one dimensional equations for kinematic overland flow and the pollutant transport equation. However, the infiltration rate, solubility rate and diffusion coefficient

were not taken into consideration. This study addressed only a single element of the complex process of stormwater pollution and therefore the proposed model could be useful only if used as part of a more comprehensive urban-runoff model. The summarization of previous researches about the portion of transport phenomena is listed in Table 2.2.

Modelling pollutant transport phenomena with advection-diffusion is currently the most popular approach used. Simulation of pollutant transport in overland flow where the velocities can be highly variable and with the effects of infiltration, rainfall and solubility incorporated into the model has not received much attention. Such a model would facilitate the assessment of the fate of surface applied pollutants and lead to better management of the environment.

2.3 THE EFFECTS OF RAINFALL-INFILTRATION

Infiltration refers to the passage of water through the soil surface into the soil and is an important hydrological component which affects overland flow. The actual process is very complex, even when it is assumed that the soil is a homogeneous medium with a uniform initial moisture content. There are three stages of infiltration for many rainfall events. Initially, the rainfall intensity is less than the saturated conductivity of the soil. Consequently all the rainfall penetrates

Table 2.2 Previous Research on Transport Phenomena

Author	Year	Dimension	Physical Condition
Siemons	1970	1-D 2-D	Diffusion-advection equation Diffusion-advection with zero velocity or with advection in one direction
Holly	1977	1-D 2-D	Diffusion and advection equation in sea
Chi	1990	1-D	Pure advection with constant velocity
Chen and Falconer	1992	1-D 2- D	Source-free transport of a scalar mass of pollutant concentration in an open channel Advection equation

the soil and runoff is not generated. At the second stage, the rainfall intensity is larger than the saturated conductivity of the soil but less than the infiltration capacity. The capacity of the soil to absorb water decreases as more and more infiltration takes place. Finally, the rainfall intensity exceeds the saturated conductivity and infiltration capacity, consequently, water begins to accumulate on the soil surface and runoff is initiated.

Many attempts have been made to model infiltration. In the early 1930's, Horton (Viessman,1989) studied the infiltration process and proposed an empirical equation. It indicates that if the rainfall supply exceeds the infiltration capacity, infiltration tends to decrease in an exponential manner:

$$f_p = f_c + (f_0 - f_c)\cdot e^{-k_3 \cdot t} \qquad (2\text{-}3\text{-}1)$$

where f_p = infiltration capacity, m/s

f_0 = initial infiltration capacity, m/s

f_c = a final equilibrium capacity, m/s

k_3 = time rate constant, s^{-1}

t = time, s

Although simple in form, difficulties in determining useful values for the initial infiltration capacity and time constant restrict the use of this equation.

Following Horton's work, in 1954 Philip (Viessman, 1989) developed an infiltration equation with predictable parameters for a homogeneous soil assuming an excess of water supply at the surface:

$$F(t) = St^{1/2} + Kt \qquad (2\text{-}3\text{-}2)$$

Yet, computing these parameters is difficult and their values are more commonly obtained by data fitting (Mein and Larson, 1973). The assumption of excess water supply at the surface is another difficulty that the modeller must contend with. Holtan (Viessman, 1989) provided an empirical equation which expresses the infiltration capacity as a function not of time, but of the unoccupied pore space in the soil. A model of this type is convenient for a watershed model, but determining the control depth is uncertain (Mein and Larson, 1973).

The most popular equation in current use is that developed by Green and Ampt in 1911 and is based on Darcy's law. The infiltration rate may be expressed as (Tayfur et al., 1993):

$$Qi = k_1 \cdot [1 + \frac{\psi_1}{(d_0^2 + \frac{2 \cdot k_1 \cdot \psi_1}{\rho_1} \Delta t)^{1/2}}] \qquad (2\text{-}3\text{-}3)$$

where Q_i = infiltration rate (m/s)

k_1 = saturated conductivity (m/s)

ρ_0 = soil porosity

ψ_1 = wetting front capillary pressure head (m)

d_0 = infiltration depth at the start of ponding (m)

Mein and Larson (1973) showed the applicability of the equation for the conditions of constant rainfall intensity and homogeneous soil. They also developed a procedure for determining the value of the capillary suction parameter used in the model. Chu (1978) demonstrated the applicability of the model for use under conditions of unsteady rainfall. As a result of these and other efforts, the Green-Ampt model is now employed in such widely used continuous simulation models as the Storm Water Management Model (Viessman,1989).

Mullem (1991) used the Green-Ampt infiltration model to predict runoff from rangelands and cropland watersheds, he stated that the Green-Ampt model predicted both the runoff volume and peak discharge better than other empirical

equations since the parameters were physically based and could be obtained from measurable properties of the soil.

Akan (1986) developed a mathematical model to calculate the time of concentration of overland flow based on the kinematic wave equation and Green-Ampt infiltration. He confirmed that the Green-Ampt model has a well-accepted physical basis, and that its results agree well with those of the Richards soil moisture equation under a variety of infiltration situations. He proposed the mathematical model for the time of concentration of overland flow: At the early stages of the rainfall runoff process, complete infiltration will occur due to the high infiltration capacity of an initially unsaturated soil. The rainfall excess and consequently the surface runoff will commence after the potential infiltration rate of the soil drops below the rate of rainfall. The time at which the potential infiltration rate becomes equal to the rainfall rate is referred to as the time to ponding. The model is assumed to have uniform surface and subsurface properties, and infiltration is the only type of rainfall loss; it is also assumed that the rainfall is of constant intensity.

The simulation of the process of rainfall-infiltration was modeled by Tayfur et al. (1993). In this work, constant infiltration rates were taken from the given data with constant rainfall intensities being assumed for the simulations. After the

start of ponding, the Green-Ampt infiltration formula was used for modeling the infiltration rates.

Application of the Green and Ampt infiltration model requires estimates of certain parameters such as the saturated hydraulic conductivity, porosity, and wetting front capillary pressure head.

Pioneering work on evaluating the Green and Ampt parameters was first reported by Bouwer (1966). Additional work, relating the parameters to soil texture has been reported by Clapp and Hornberger (1978) and McCuen, et al (1981). Rawls et al. (1983) summarized a procedure for determining the Green-Ampt parameters based on soil properties utilizing the full spectrum of soil survey information.

These studies have provided valuable insight into the mechanics of overland flow, although they are limited to the field of infiltration.

2.4 NUMERICAL TECHNIQUES

In order to analyze overland flow and pollutant transport characteristics, many numerical approaches have been proposed. Basically, the overland flow

equation has been solved in one-dimension using several numerical methods or in two-dimensions with either expicit or implicit finite difference schemes. In explicit methods, the unknown values of the dependant variables at the new time level occur explicitly in the difference equation and are determined sequentially. Liggett and Woolhiser (1967) state that although explicit methods are easy to code in the solution procedure, they suffer from (sometimes) extreme stability restrictions. The implicit method expresses unknown values in terms of other unknowns at the same time level. A set of simultaneous equations is thus obtained with the required closure being provided by the boundary conditions: such a solution is generally stable although formal stability can only be proved for linear equations. Because of its great efficiency, the implicit method is especially suited for application to large time-scale phenomena for which explicit methods were found to be impractical and time-consuming.

The box scheme is one of the more popular methods because it is explicit with only one unknown per equation and is unconditionally stable. Nevertheless practical considerations dictate a limit on the time step. (Wood and Arnold, 1990)

The QUICK (Quadratic Upstream Interpolation for Convection Kinetics) scheme, which is widely used in solving hydraulic problems, was originally developed by Leonard (1979), This scheme which uses quadratic upstream

interpolation has the benefits of mass conservation, reasonably high accuracy and computational efficiency in comparison with many other higher-order-accurate schemes (Chen and Falconer 1992). However a Von Neumann stability analysis indicates that the explicit QUICK scheme has a severe stability constraint which is dependent on the diffusion coefficient. It can be proved that this scheme is numerically unstable for the case of pure advection. As a consequence, various modified forms of the implicit QUICK scheme have been formulated by Chen and Falconer (1992), which are claimed to overcome the stability problems of the explicit form and may be applied both to pure advection and to combined advection-diffusion. The various forms of the QUICK scheme include:

i). Forward explicit QUICK scheme

ii). Fully time-centred implicit QUICK scheme

iii). Backward implicit QUICK scheme

iv). Semi-time-centred QUICK scheme

v). Semi-backward implicit QUICK scheme.

Liggett and Woolhiser (1967) used the method of characteristics, as well as explicit and implicit finite difference methods for modelling one-dimensional overland flow. They stated that both the characteristic scheme and the implicit scheme will provide stable solutions to the equations over a rather wide range of parameters. The characteristic scheme has the advantage of greater speed

whereas the implicit scheme offers the advantage of regular point spacing.

Akan and Yen (1981) employed a four-point implicit finite difference scheme for the solution of the surface runoff equations.

Chow and Zvi (1973) employed a scheme based on the combination of the Lax-Wendroff scheme with Burstein and Lapidus modifications for modelling of watershed flow. They obtained a solution to the two-dimensional watershed flow model which would have been extremely difficult to solve by the method of characteristics.

Wood and Arnold (1990) solved the one-dimensional kinematic wave approximation by using the box scheme.

Katopodes and Strelkoff (1979) solved the two-dimensional St.Venant equations using a characteristics method. They pointed out that the method of characteristics precisely follows the paths along which information propagates and provides an accurate and efficient method of computation in shallow water problems. However, since the characteristic surfaces in two dimensions form a case, the formulation is quite complex while demanding significant computer resoures.

Kawahara and Yokoyama (1980) applied the finite element method to spatial functions of flow depth and velocity for two-dimensional overland flow or direct runoff flow over the watershed.

Hromadka et al (1987) developed a diffusion hydrodynamic model which is based on an explicit, integrated finite-difference scheme.

Zhang and Cundy (1989) solved the two- dimensional overland flow equations by using the second order accurate, MacCormack explicit finite difference method.

Tayfur et al. (1993) solved a two-dimensional overland flow equation by using the implicit finite difference method of Amein (1968) which does not suffer from any instability problems.

Siemons (1970) made use of finite difference methods which are developed from the one-dimensional diffusion-advection equation for the solution of the two-dimensional advection-diffusion equation.

Li (1990) simulated the advective transport of a scalar by using the minimax-characteristics method, which is an explicit and efficient finite difference

scheme derived from the local "min max" approximation of the exact solution to the pure advection equation. The method is developed within the finite element framework. However, numerical stability requires that the Courant number must be less than unity, moreover, the advection and diffusion processes must be computed separately, thereby requiring additional computer resources (Chen and Falconer 1992).

Holly and Preissmann (1977) presented the results of a tentative exploration into a new finite difference method for the calculation of advection and diffusion. The favorable characteristics of the two-point fourth-order scheme as demonstrated for calculation in one dimension, extend also to calculations in two dimensions. The idea of characteristic propagation and the Hermitian cubic polynomial representation for the scalar distribution within the computational domain were used and promising results were produced. However, it is computationally more complicated and expensive for two-dimensional flows, where additional sets of equations are required to simulate not only the scalar quantity but also its spatial derivatives for the advection and diffusion processes.

Chen and Falconer (1992) presented the modified QUICK scheme to solve the advection-diffusion equation. The various modified forms of the implicit QUICK schemes were tested for the one dimensional pure advection equation.

A two-dimensional version of the semi-time-centred QUICK scheme had been applied to a two-dimensional test case. They stated that the modified QUICK scheme could overcome the stability problem of the explicit form and be applicable both to pure advection and to combined advection and diffusion.

In this study, a mathematical model of pollutant transport in overland flow with infiltration is proposed, which is based on three groups of governing equations: the two-dimensional St.Venant overland flow equation, the pollutant transport equation and an equation for the solid balance. The two-dimensional overland flow equations consist of the continuity and momentum equations in which complicated physical conditions such as roughness, infiltration and addition of rainfall is allowed. The equation for pollutant transport is a combination of the advection-diffusion equation with a solubility rate equation, source and sink term, and the effect of rainfall. The source term incorparates a solubility rate equation based on the analogy between mass and momentum transfer. The main advantage of the proposed model is its ability to simultaneously handle not only overland flow but also pollutant transport while accounting for complicated physical and chemical effects.

CHAPTER 3
THEORETICAL FORMULATION

3.1 OVERLAND FLOW MODELS

3.1.1 The St.Venant Equations in Two Dimensions

The two-dimensional St.Venant equations consist of the continuity and momentum conservation equations in the x- and y-directions.

For the physical configuration of the watershed shown in Fig 3.1, these equations may be expressed as follows (Tayfur et al., 1993):

The continuity equation:

$$\frac{\partial h}{\partial t} + \frac{\partial (hu)}{\partial x} + \frac{\partial (hv)}{\partial y} = [Qr(x,y,t) - Qi(x,y,t)]\cos(\alpha)\cos(\phi) \qquad (3\text{-}1\text{-}1)$$

The momentum equation in the x direction:

$$\frac{\partial u}{\partial t} + u\frac{\partial u}{\partial x} + v\frac{\partial u}{\partial y} + \cos(\alpha)\cos(\phi)g\frac{\partial h}{\partial x} = g\ \sin(\alpha) - S_x g - \frac{Qu}{h} \qquad (3\text{-}1\text{-}2)$$

The momentum equation in the y direction:

$$\frac{\partial v}{\partial t} + u\frac{\partial v}{\partial x} + v\frac{\partial v}{\partial y} + \cos(\alpha)\cos(\phi)g\frac{\partial h}{\partial y} = g\ \sin(\phi) - S_y g - \frac{Qv}{h} \qquad (3\text{-}1\text{-}3)$$

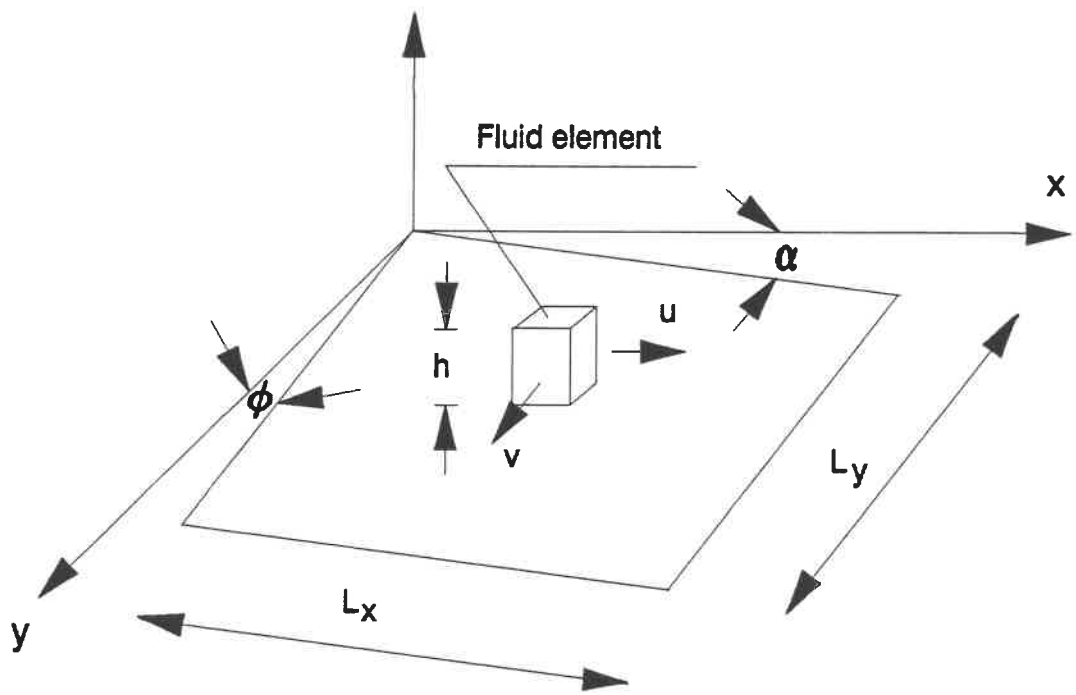

Figure 3.1 Definition Sketch for Two-Dimensional Overland Flow

Where

h = flow depth

u = flow velocity in the x-direction

v = flow velocity in the y-direction

Qr = rainfall intensity

Qi = infiltration rate

Q = net lateral inflow (rainfall-infiltration)

α = angle of the slope with respect to the x-direction

ϕ = angle of the slope with respect to the y-direction

g = gravitational acceleration

S_x = the friction slope in the x direction

S_y = the friction slope in the y direction

For turbulent flow, bed shear stress dominates and viscous stresses may be negligible. The friction slopes using Manning's roughness relationships may be expressed as:

$$S_x = \frac{n^2 u\sqrt{u^2+v^2}}{h^{4/3}} \qquad (3\text{-}1\text{-}4)$$

and

$$S_y = \frac{n^2 v\sqrt{u^2+v^2}}{h^{4/3}} \qquad (3\text{-}1\text{-}5)$$

Where n = Manning's roughness coefficient.

Since α and ϕ are considered small, the following approximations may be made,

$\sin(\alpha) \cong \tan(\alpha) = s_{ox}$

$\sin(\phi) \cong \tan(\phi) = s_{oy}$

$\cos(\alpha) \cdot \cos(\phi) = 1.0$

Where s_{ox} and s_{oy} are the bed slopes in the x and y-directions respectively.

3.1.2 Kinematic Wave Equation

Although overland flow could ideally be represented by the St.Venant equation, the kinematic wave approximation was shown to provide very reliable results for most hydrologically significant cases (Akan,1986). Due to its simplicity, it has become a popular alternative to the St.Venant equations for numerical simulation of overland flow.

The kinematic wave equation assumes that all terms in the momentum equations are small compared with the friction and gravity terms (Moore and Foster,1989). This results in:

$$g\sin(\alpha) = s_x g \qquad (3\text{-}1\text{-}6)$$

and

$$g\sin(\Phi) = s_y g \qquad (3\text{-}1\text{-}7)$$

since

$$\sin(\alpha) = s_{ox}$$

$$\sin(\phi) = s_{oy}$$

so

$$s_{ox} = s_x \qquad (3\text{-}1\text{-}8)$$

$$s_{oy} = s_y \qquad (3\text{-}1\text{-}9)$$

Substituting equation (3-1-8) and (3-1-9) into (3-1-4) and (3-1-5) , the equations may be expressed as:

$$s_{ox} = \frac{n^2 u\sqrt{u^2 + v^2}}{h^{4/3}} \qquad (3\text{-}1\text{-}10)$$

$$s_{oy} = \frac{n^2 v\sqrt{u^2+v^2}}{h^{4/3}} \qquad (3\text{-}1\text{-}11)$$

combining equations (3-1-10) and (3-1-11), we obtain:

$$v = u\frac{s_{oy}}{s_{ox}} \qquad (3\text{-}1\text{-}12)$$

by substituting (3-1-12) into equation (3-1-10)

$$u = \frac{s_{ox}^{\frac{1}{2}}\, h^{\frac{2}{3}}}{n[1 + (\frac{s_{oy}}{s_{ox}})^2]^{\frac{1}{4}}} \qquad (3\text{-}1\text{-}13)$$

and similarly:

$$v = \frac{s_{oy}^{\frac{1}{2}}\, h^{\frac{2}{3}}}{n[1 + (\frac{s_{ox}}{s_{oy}})^2]^{\frac{1}{4}}} \qquad (3\text{-}1\text{-}14)$$

Then, substituting equations (3-1-13) and (3-1-14) into the continuity equation (3-1-1), the kinematic wave equation is obtained as follows:

$$\frac{\partial h}{\partial t} + \frac{s_{ox}^{\frac{1}{2}}}{n\,[1 + (\frac{s_{oy}}{s_{ox}})^{2}]^{\frac{1}{4}}}\frac{\partial h^{\frac{5}{3}}}{\partial x} + \frac{s_{oy}^{\frac{1}{2}}}{n\,[1 + (\frac{s_{ox}}{s_{oy}})^{2}]^{\frac{1}{4}}}\frac{\partial h^{\frac{5}{3}}}{\partial y} = Qr\text{-}Qi \qquad (3\text{-}1\text{-}15)$$

An alternate representation in one dimension is (Wood and Arnold, 1990):

$$\frac{\partial q}{\partial t} + u(q)\,(\frac{\partial q}{\partial x} - Q) = 0 \qquad (3\text{-}1\text{-}16)$$

where q = the discharge per unit width

t = time

x = the distance from the top of the slope

Q = net lateral inflow

and

$$u(q) = \frac{q^{2/5} s_{ox}^{3/10}}{n^{3/5}} \qquad (3\text{-}1\text{-}17)$$

Here, the friction effect has been modelled using Manning's formula with n as a roughness parameter and s_{ox} as the bed slope. The use of Manning's formule is probably questionable in overland flow due to the small depths involved. The flow is "hydraulically rough" and a pressure force type equation should be used. However, for the present, we have continued this work with the standard formulation.

3.2 INFILTRATION MODELS

Infiltration is an important component of a hydrologic model. It can affect not only the timing, but also the distribution and magnitude of surface runoff, and influence the quantities of pollutant mass penetrating the soil. For this reason reliable estimates of infiltration must be incorporated into any watershed model.

The infiltration rate is the rate at which water enters the soil at the surface. If water accumulates on the surface, a phenomenon called ponding occurs and the infiltration occurs at the potential infiltration rate. If the rate of supply of water at the surface is less than the potential infiltration rate, then the actual infiltration rate will also be less than the potential rate. Most infiltration equations describe the potential rate. Infiltration capacity is the maximum rate at which a given soil can absorb falling rain when it is in a specified condition (Kirkby, 1979).

Mein and Larson (1973) described three distinct cases or stages of infiltration when a rainfall of intensity Qr is applied to a soil having a saturated conductivity k_1, and an infiltration capacity f_p.

Case A: $Qr < k_1$, all the rainfall infiltrates, runoff will not occur, but the soil moisture level is being altered.

Case B: $k_1 < Qr < f_p$, all the rainfall infiltrates into the soil, the moisture content at the surface increases during rainfall until surface saturation is reached.

Case C: $k_1 < f_p \leq Qr$, the infiltration rate is at its maximum capacity and decreasing, the surface has become saturated. Runoff is being generated. Fig 3.2 shows the different cases of infiltration behaviour under rainfall, line A shows case A, line B shows case B, curve C and D show case C.

In this study, the infiltration rate has been calculated with two equations. At the first stage, Horton's equation is used to predict the infiltration rate before ponding begins. At the second stage, the Green-Ampt equation is used for describing the subsequent infiltration behaviour after the ponding time.

Because of the high infiltrability of an initially unsaturated soil, all the rain will infiltrate at the early stage. Surface runoff will commence after the potential infiltration rate of the soil drops below the rate of rainfall. The ponding time t_p is the elapsed time between the time rainfall begins and the time water begins to pond

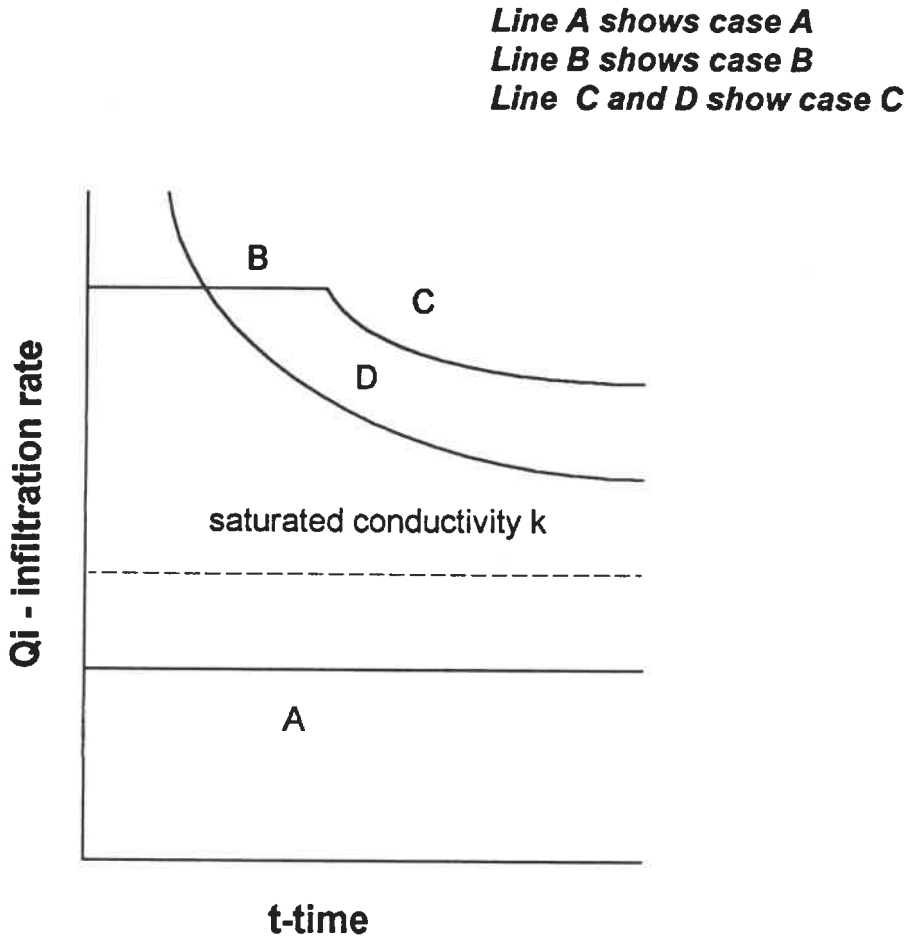

Figure 3.2 Different Cases of Infiltration Behavior Under Rainfall

on the soil surface. This time is critical and relates to rainfall intensity Qr and to the soil properties. If the rainfall intensity is large, the ponding time appears earlier and vice versa.

It may be evaluated from

$$t_p = \frac{\Psi_1 \cdot \rho_0}{Qr \cdot (\frac{Qr}{k_1} - 1)} \qquad (3\text{-}2\text{-}1)$$

with

$$\rho_0 = (1 - S_e) \cdot \rho_1$$

where t_p = time to ponding

s_e = initial effective saturation

Qr = rainfall intensity, m/s

k_1 = hydraulic conductivity of the soil

ρ_1 = effective soil porosity

ρ_0 = soil porosity

Ψ_1 = wetting front capillary pressure head,m

During the period leading up to ponding, large amounts of pollutant is infiltrated. In order to predict the amount of infiltrated pollutant during this stage, Horton's equation is used.

Horton (Viessman,1989) showed that when the rainfall rate exceeds the infiltration rate, water infiltrates the surface soil at a rate that generally decreases with time. He proposed the infiltration equation,

$$f_p = f_c + (f_0 - f_c)\cdot e^{-k_3 \cdot t} \qquad (3\text{-}2\text{-}2)$$

where f_p = infiltration capacity, m/s

f_0 = initial infiltration capacity, m/s

f_c = a final equilibrium capacity, m/s

k_3 = time rate constant, s^{-1}

k_3 is an empirical constant representing the rate of decrease in capacity, it indicates that if the rainfall supply exceeds the infiltration capacity, infiltration tends to decrease in an exponential manner.

Typical values of the parameters of f_0, f_c and k_3 in the Horton model have been cited in the book by Bedient (1988). Although simple in form, difficulties in determining useful values for f_0 and time rate constant k_3 restrict the use of Horton's equation (Viessman et al, 1989). Furthermore, the form of equation (3-2-2) is not suitable for the case when the rainfall intensity is less than the computed value of infiltration capacity f_0, since then all the rainfall may infiltrate, i.e. f = Qr. The infiltration capacity should be reduced as a function of the actual amount of

water available for infiltration and not only on the basis of time. In this study, some adjustments to the infiltration behaviour have been used. The actual infiltration can be expressed by

$$f(t) = \min\ [f_p(t),\ Qr(t)] \qquad (3\text{-}2\text{-}3)$$

where f (t) is the actual infiltration into the soil and Qr(t) is the rainfall intensity. By using equation (3-2-3), the infiltration rate at any time is set equal to the lesser of the infiltration capacity f_p (t) or the rainfall intensity Qr(t).

Besides using Horton's model, the Green-Ampt model, which is based on a Darcy-type water flux, is applied after ponding time.

The Green-Ampt infiltration model has been found to have wide applicability for modelling the infiltration process. A major advantage of the Green-Ampt model is that the necessary parameters may be determined from physical measuremeters in the soil, rather than empirically as for the Horton parameters. The Green-Ampt formula is:

$$Qi = k_1 \cdot (1 + \frac{\rho_0 \cdot \Phi_1}{F}) \qquad (3\text{-}2\text{-}4)$$

where Qi = infiltration rate (m/s)

F = infiltration amount (m)

k_1 = saturated conductivity (m/s)

ρ_0 = soil porosity

Ψ_1 = wetting front capillary pressure head (m)

The following expression is obtained for the infiltration depth after ponding (Tayfur et al., 1993):

$$d = [d_0^2 + \frac{2 \cdot k_1 \cdot \Psi_1}{\rho_0} (t - t_0)]^{1/2} \qquad (3\text{-}2\text{-}5)$$

here d_0 = infiltration depth at the start of ponding.

The infiltration rate for times after the start of ponding is obtained as (Tayfur et al., 1993):

$$Qi = k_1 \cdot [1 + \frac{\Psi_1}{(d_0^2 + \frac{2 \cdot k_1 \cdot \Psi_1}{\rho_0} \Delta t)^{1/2}}] \qquad (3\text{-}2\text{-}6)$$

where Qi = infiltration rate (m/s)

k_1 = saturated conductivity (m/s)

ρ_0 = soil porosity

Ψ_1 = wetting front capillary pressure head (m)

d_o = infiltration depth at hte start of ponding, m

$\Delta t = (t-t_0)$ is time increment (s).

Application of the Green-Ampt infiltration model requires estimates of the hydraulic conductivity k_1, effective porosity ρ_1, and wetting front capillary pressure head Ψ_1. In our case, the values of Ψ_1, ρ_1, k_1 and d_0 used in this study were from published soil properties (Rawls et al,1983). Since the overland flow depth is small compared to the capillary head, a constant capillary pressure head Ψ_1 = 0.15m ~ 0.17m was taken, soil porosity ρ_0 being considered equal to 0.3 ~ 0.45.

3.3 POLLUTANT TRANSPORT MODEL

The mathematical model of pollutant transport is based on three governing equations representing the transport of pollutant in overland flow, the pollutant dissolution and solid balance.

3.3.1 Pollutant Transport Equation

The fundamental equation describing pollutant transport is the advection-diffusion equation. However, the complete modelling of pollutant transport leading up to the ultimate fate of the pollutant should consider not only the

advection and the diffusion but also the solubility rate, i.e. the process of pollutant dissolution, the type of pollutant, the characteristics of the rainfall intensity, the infiltration and the overland flow.

The pollutant transport equation is established by writing a mass balance over a stationary volume element Δx, Δy through which the fluid is flowing. The control volume approach was used, as shown in Fig 3.3. In time Δt, the mass of constituent entering the control volume is:

$$s \cdot u \cdot h \cdot \Delta y \cdot \Delta t + s \cdot v \cdot h \cdot \Delta x \cdot \Delta t + s_t \cdot \Delta t \cdot \Delta x \cdot \Delta y$$

while that leaving is

$$[s \cdot u \cdot h \cdot \Delta y + \frac{\partial(s \cdot u \cdot h)}{\partial x} \Delta x \cdot \Delta y]\Delta t + [s \cdot v \cdot h \cdot \Delta x + \frac{\partial(s \cdot v \cdot h)}{\partial y} \Delta y \cdot \Delta x]\Delta t + s \cdot Qi \cdot \Delta t \cdot \Delta x \cdot \Delta y$$

where s = concentration (kg/m^3)

u, v = the advection velocity in the x- and y-direction respectively (m/s)

Qi = infiltration rate (m/s)

S_t = solubility rate (kg/s/m^2)

h = flow depth (m)

Δt = time interval (m)

During time Δt, a control volume balance (without diffusion) results in:

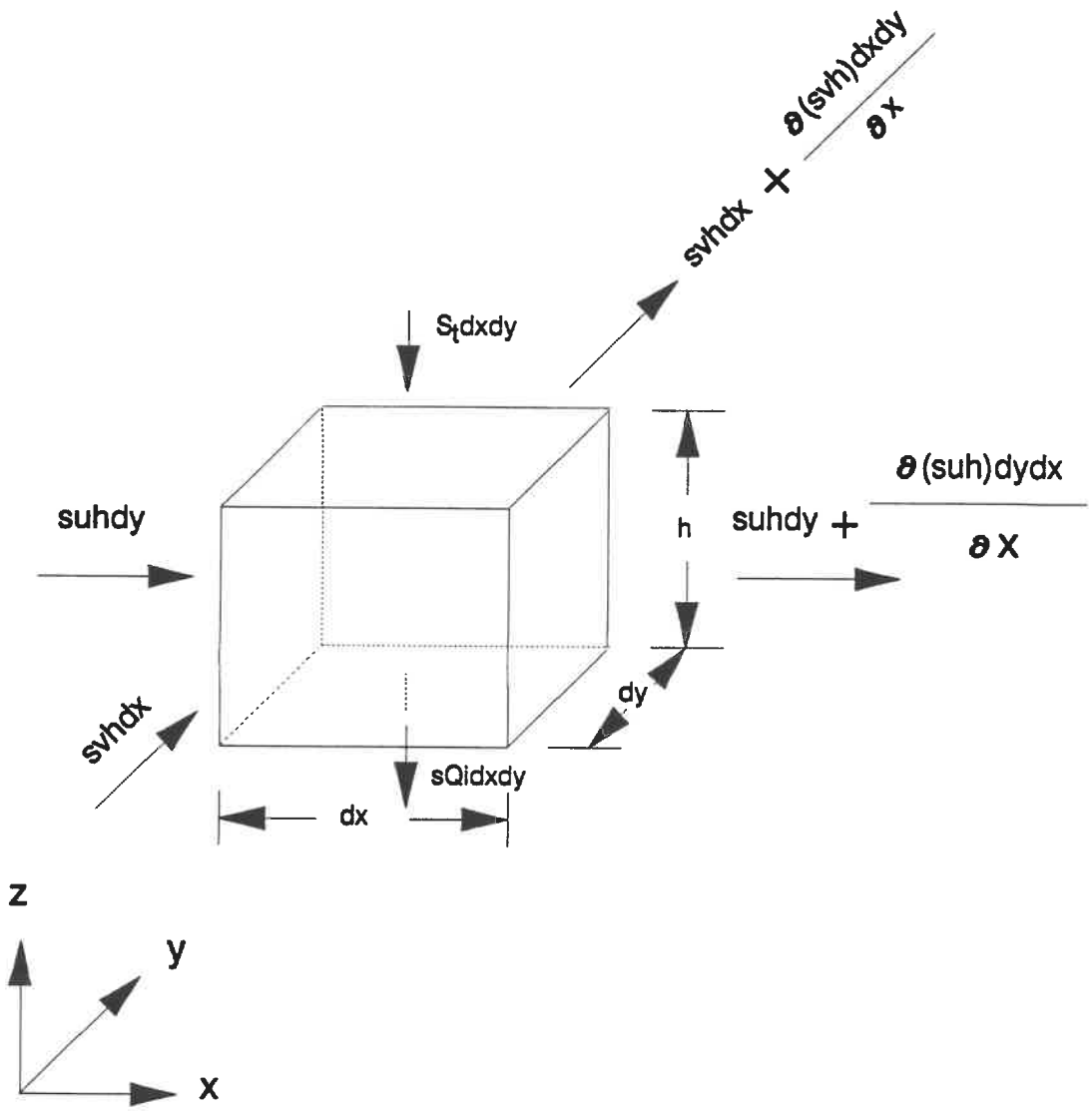

Figure 3.3 Mass Balance Over a Control Volume

$$s \cdot u \cdot h \cdot \Delta y \cdot \Delta t + \frac{\partial(suh)}{\partial x}\Delta x \Delta t \Delta y + s \cdot v \cdot h \cdot \Delta x \cdot \Delta t + \frac{\partial(svh)}{\partial y}\Delta x \Delta y \Delta t$$
$$+ s \cdot Qi \cdot \Delta t \cdot \Delta x \cdot \Delta y - s \cdot u \cdot h \cdot \Delta y \cdot \Delta t - s \cdot v \cdot h \cdot \Delta x \cdot \Delta t - s_t \Delta x \cdot \Delta y \cdot \Delta t \qquad (3\text{-}3\text{-}1)$$
$$= -(s \cdot h \cdot \Delta x \cdot \Delta y)$$

Rearranging equation (3-3-1), we have:

$$\frac{\partial sh}{\partial t} + \frac{\partial suh}{\partial x} + \frac{\partial svh}{\partial y} = s_t - s \cdot Qi \qquad (3\text{-}3\text{-}2)$$

this equation may also be written as:

$$h\frac{\partial s}{\partial t} + uh\frac{\partial s}{\partial x} + vh\frac{\partial s}{\partial y} + s\left(\frac{\partial h}{\partial t} + \frac{\partial uh}{\partial x} + \frac{\partial vh}{\partial y}\right) = s_t - s \cdot Qi \qquad (3\text{-}3\text{-}3)$$

Since the shallow water equation for mass continuity may be expressed as follows:

$$\frac{\partial h}{\partial t} + \frac{\partial uh}{\partial x} + \frac{\partial vh}{\partial y} = Qr - Qi \qquad (3\text{-}3\text{-}4)$$

substituting (3-3-4) to (3-3-3), we obtain

$$h\frac{\partial s}{\partial t} + uh\frac{\partial s}{\partial x} + vh\frac{\partial s}{\partial y} + s \cdot Qr = s_t \qquad (3\text{-}3\text{-}5)$$

or:

$$\frac{\partial s}{\partial t} + u\frac{\partial s}{\partial x} + v\frac{\partial s}{\partial y} = \frac{s_t}{h} - \frac{s \cdot Qr}{h} \qquad (3\text{-}3\text{-}6)$$

Fick's first law of diffusion states that mass transport occurs because of a gradient in mass concentration. The mass diffusivity D can be regarded as the proportionality factor between mass flux and mass concentration gradient. Based on Fick's law, the complete pollutant transport equation may be written as follows:

$$\frac{\partial s}{\partial t} + u\frac{\partial s}{\partial x} + v\frac{\partial s}{\partial y} = \frac{\partial}{\partial x}\left(D_x\frac{\partial s}{\partial x}\right) + \frac{\partial}{\partial y}\left(D_y\frac{\partial s}{\partial y}\right) + \frac{s_t}{h} - \frac{s \cdot Qr}{h} \qquad (3\text{-}3\text{-}7)$$

where D_x, D_y -- diffusion coefficient (m^2/s) in the x- and y-directions respectively. In this study, a constant diffusion coefficient D has been used. In equation (3-3-7), the solubility rate is a source term and the rainfall is a sink term.

For the one-dimensional case, the equation becomes:

$$\frac{\partial s}{\partial t} + u\frac{\partial s}{\partial x} = \frac{\partial}{\partial x}\left(D\frac{\partial s}{\partial x}\right) + \frac{S_t}{h} - \frac{s \cdot Q_r}{h} \qquad (3\text{-}3\text{-}8)$$

3.3.2 Solubility Rate Model (Source Term)

The process of pollutant dissolution in overland flow is neither a pure physical process nor a pure chemical one, it is a complicated physico-chemical process in which solubility rate plays an important part. The amount of solute dissolved in a saturated solution at a certain temperature is known as the solubility of the substance. Solubility is usually expressed as the number of grams of solute dissolved per 100g of solvent at a particular temperature. Solubility rate may be defined as the mass of solute that will dissolve per unit time per unit area at a fixed temperature. Factors affecting solubility are temperature, pressure and the chemical nature of the solute and solvent. The chemical natures of the possible solutes are so varied that it is impossible to develop detailed rules of solubility (William, 1967). The solubility of solids is only slightly affected by pressure change. So, in this study, any effects of pressure are neglected and it is assumed that during the process of dissolution no new substance is created and temperature keeps constant. The value of the saturated concentration of a solute in a particular solvent has been assigned the symbol c^*.

The mathematical behaviour for pollutant solubility rate has been constructed based on the physico-chemical behaviour of the pollutant in overland flow. The solubility rate is assumed to be proportional to the bottom bed shear

stress of the overland flow, the reaction rate constant and the difference between the saturated and local concentration.

This leads to the expression:

$$S_t = k_2 \cdot \tau \cdot (c^* - s) \qquad (3\text{-}3\text{-}9)$$

where the shear stress may be evaluated (using the Manning equation) as:

$$\tau = \gamma h s_f = \gamma \frac{n^2(u^2+v^2)}{h^{1/3}} \qquad (3\text{-}3\text{-}10)$$

here S_t = solubility rate (kg/m^2/s)

τ = shear stress (N/m^2)

γ = specific weight of water (kg/m^2/s^2)

S_f = friction slope

h = flow depth (m)

u, v = flow velocities in both x- and y- direction (m/s)

n = Manning's roughness coefficient

k_2 = reaction rate constant (m^2·s/kg)

c* = solubility (kg/m^3)

s = local concentration (kg/m^3)

The concentration of a solution is a measure of how much solute is dissolved in a unit amount of solvent. If in unit time there are more particles of solute entering the solvent than leaving it to return to the lattice, the solute is dissolving. At any specific temperature, enough solid may be present so that the same number of particles is leaving the lattice as returning. The solid phase and the liquid phase are then said to be in dynamic equilibrium. Once solids are dissolved in water, a point is finally reached at which no more solute dissolves and the undissolved solute remains in equilibrium with the solution, in this state of equilibrium the solution is said to be saturated , $c^* = s$. In the present study, the reaction rate constant k is presumed to depend only on the pollutant characteristics.

3.3.3 Solid Balance Equation

Pollutant infiltration into the ground during a rainfall event can be treated in two distinct stages: a stage before surface ponding and a stage after surface ponding. Let the initial distribution of pollutant be w_0 kg/m^2, assume a concentration of c^* to prevail before ponding. Before ponding time, in the time interval Δt, the mass that goes into the ground is:

$$A = c^* \cdot k_4 \cdot f_p \cdot \Delta t \cdot \Delta x \cdot \Delta y \qquad (3\text{-}3\text{-}11)$$

After ponding time, in the time interval Δt, the mass infiltrating into the ground: where the solution is now considered unsaturated is:

$$B = \Sigma s \cdot Qi \cdot \Delta x \cdot \Delta y \cdot \Delta t \qquad (3\text{-}3\text{-}12)$$

and where the solution is saturated:

$$C = \Sigma c^{*} \cdot Qi \cdot \Delta x \cdot \Delta y \cdot \Delta t \qquad (3\text{-}3\text{-}13)$$

the amount of pollutant washout is:

$$D = \Sigma s \cdot h_n \cdot v_n \Delta x \cdot \Delta t + \Sigma s \cdot h_m \cdot u_m \cdot \Delta y \cdot \Delta t \qquad (3\text{-}3\text{-}14)$$

while the amount of dissolved pollutant is:

$$E = \Sigma k_2 \cdot \mathrm{T} \cdot (c^{*} - s) \cdot \Delta x \cdot \Delta y \cdot \Delta t \qquad (3\text{-}3\text{-}15)$$

the mass balance equation for the solid pollutant is:

$$w = w_0 - \Sigma A - E \qquad (3\text{-}3\text{-}16)$$

in which

c^* = solubility (kg/m^3),

s = concentration (kg/m^3),

k_4 = delay time coefficient,

f_p = infiltration capacity (m/s),

τ = bed shear stress ($kg/m/s^2$),

k_2 = reaction rate constant ($m^2 \cdot s/kg$),

Qi = infiltration rate (m/s),

S_t = solubility rate (kg/m^2 /s),

Δt = time interval (s),

Δx, Δy = space interval in the x- and y- direction respectively,

w_0 = initial pollutant mass (kg/m^2),

w = residue of pollutant mass (kg/m^2),

term A represents pollutant mass infiltrated before ponding time,

term B represents pollutant mass infiltrated with local concentration after ponding time,

term C represents pollutant mass infiltrated at saturated concentration after ponding time,

term D represents pollutant mass washed-out by overland flow,

term E represents pollutant mass dissolved.

At the end of time step Δt, the solid remaining will be w kg/m^2. When w becomes zero, no more solid pollutant is dissolved.

3.4 INITIAL CONDITION

3.4.1 Overland Flow Equation

In the case of overland flow, it is possible to assume a very thin layer of water to be ponded on an initially dry surface at the beginning of the rainfall. The results are not affected by the assumption of this very thin film of water (Akan and Yen.1981). The same assumption was applied by Liggett and Woolhiser (1967), Brutsaert (1971), Chow and Zri (1973), Zhang and Cundy (1989) and Tayfer et al. (1993). In this study, a layer of depth 0.0001m is assumed to cover the flow surface, and the following initial conditions have been adopted:

for the two-dimensional St.Venant equation:

$$u(x, y, 0) = 0$$

$$v(x, y, 0) = 0$$

$$h(x, y, 0) = 0.0001\text{m}$$

for the kinematic wave approximation:

$$q(x, 0) = 0$$

3.4.2 The Pollutant Transport Equation

Two different cases of initial conditions were considered for the pollutant mass distribution:

a). Non-zero initial pollutant mass applied at a discrete location:

$$w_0(L,L,0) = w_m$$

b). Non-zero initial pollutant mass uniformly applied:

$$w_0(x,y,0) = w_m$$

in which w_m is the mass of pollutant.

3.5 BOUNDARY CONDITIONS

3.5.1 Overland Flow Equation

Specified boundary conditions should be based on the physics of the situation, especially when the finite difference method is used. With the wrong boundary conditions, it is likely that numerical difficulties will be encountered or physically unrealistic results obtained.

For two-dimensional overland flows, the continuity equation (3-1-1), the momentum equation (3-1-2) and (3-1-3) are solved by using a finite difference scheme that provides the solutions for the interior nodes simultaneously. There are 3•M•N unknown results, these unknowns are the flow depth and flow velocities at each node in both the x- and y-directions. By writing the continuity and momentum equations at the centre of the cells, 3•(M-1)•(N-1) equations are obtained. The remaining 3•(M+N-1) equations are obtained from the boundary

conditions. However, the solutions at the boundary nodes require special treatment. Fig 3.4 is an illustrative sketch for the number of unknowns.

The numerical approximation of the boundary conditions for overland flow has been widely discussed in the literature. The upstream boundary condition has been frequently taken to be of the "zero flux" type. Brutsaert (1971) used zero velocities at the upstream end. Woolhiser (1975) handled the upstream boundary conditions with h=0, u=0. Zhang and Cundy (1989) took zero flux as the appropriate upstream boundary condition. The upstream boundary condition h(0,t)=0,0 has been shown to be physically valid for steep slopes (Govindaraju et al, 1990).

For the downstream end, several boundary conditions have been implemented, the most popular being a zero depth gradient. Morris (1979) showed that the zero depth gradient condition is applicable to a large class of problems. Recently, Tayfur et al. (1993) used the zero depth gradient condition at the downstream end with satisfactory results..

In this study, the following boundary conditions have been adopted:
for the two-dimensional St.Venant equation, the flow depth and the flow velocities in both x- and y-directions are taken as zero at the upstream end,

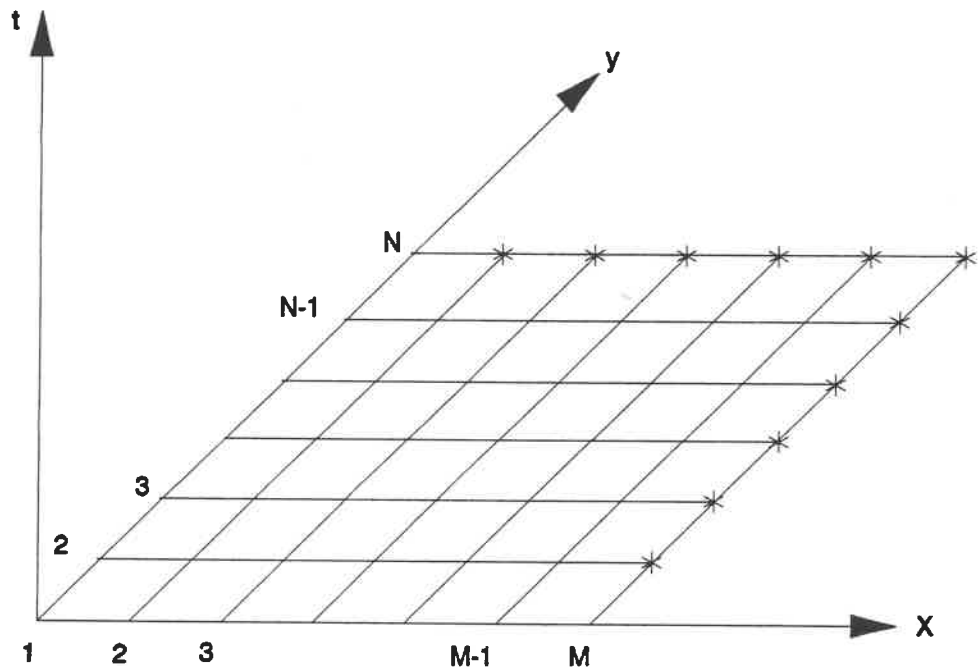

Figure 3.4 Sketch of Representation of The Number of Unknowns

u (0,y,t) = 0

v (0,y,t) = 0

h (0,y,t) = 0

u (x,0,t) = 0

v (x,0,t) = 0

h (x,0,t) = 0

For the kinematic wave approximation:

q (0,t) = 0

At the downstream, the boundary conditions are as follows:

$$\frac{\partial h}{\partial x} = 0 \qquad (3\text{-}5\text{-}1)$$

$$\frac{\partial h}{\partial y} = 0 \qquad (3\text{-}5\text{-}2)$$

$$\frac{\partial u}{\partial x} = 0 \qquad (3\text{-}5\text{-}3)$$

$$\frac{\partial u}{\partial y} = 0 \qquad (3\text{-}5\text{-}4)$$

$$\frac{\partial v}{\partial x} = 0 \qquad (3\text{-}5\text{-}5)$$

$$\frac{\partial v}{\partial y} = 0 \qquad (3\text{-}5\text{-}6)$$

Solutions at the downstream end have also been initiated using the quasiuniform approximation:

$$\frac{\partial h}{\partial x} = -s_{fx} \qquad (3\text{-}5\text{-}7)$$

$$\frac{\partial h}{\partial y} = -S_{fy} \qquad (3\text{-}5\text{-}8)$$

This approach was also found to work well.

When the kinematic wave approximation is used, it is not necessary to specify the downstream boundary conditions because the backwater effects were not taken into consideration.

3.5.2 The Pollutant Transport Equation

In previous research, a zero concentration condition has commonly been used upstream. This has been the boundary condition of choice of Chen and Falconer (1992), and Akan (1987) who used it for the one-dimensional case. At the downstream boundary, Chen and Falconer (1992) assumed zero derivatives.

In this work, the concentration has been set to zero upstream:

$$s\,(x,0,t) = 0$$

$$s\,(0,y,t) = 0$$

At the downstream boundary, zero concentration gradient is used:

$$\frac{\partial s}{\partial x} = 0 \qquad (3\text{-}5\text{-}9)$$

$$\frac{\partial s}{\partial y} = 0 \qquad (3\text{-}5\text{-}10)$$

CHAPTER 4
NUMERICAL SCHEME

4.1 BOX SCHEME

The box scheme is used for the numerical solution of the kinematic wave approximation which is obtained from the St.Venant equations after simplifying assumptions are made. The stability and convergence properties of this scheme have been discussed by Wood and Arnold (1990). They indicate that although the box scheme is unconditionally stable a limit on the time step is necessary due to considerations of accuracy. The numerical solution of the kinematic wave equation is obtained over a discrete net of points in the (x, t) plane. The net is constructed by lines drawn parallel to the x- and t-axes. The first line represents the upstream boundary and is located at x = 0, whereas the last line represents the downstream boundary. A four-point grid is used in the development of the numerical procedure. Each point on the net is identified by a subscript and a superscript, the x-position of the point is given by the subscript and its t-value by the superscript. Fig 4.1 shows the sketch of grid representation for the scheme.

We rewrite the one-dimensional kinematic wave approximation to overland flow resulting from rainfall-runoff on a sloping plane as:

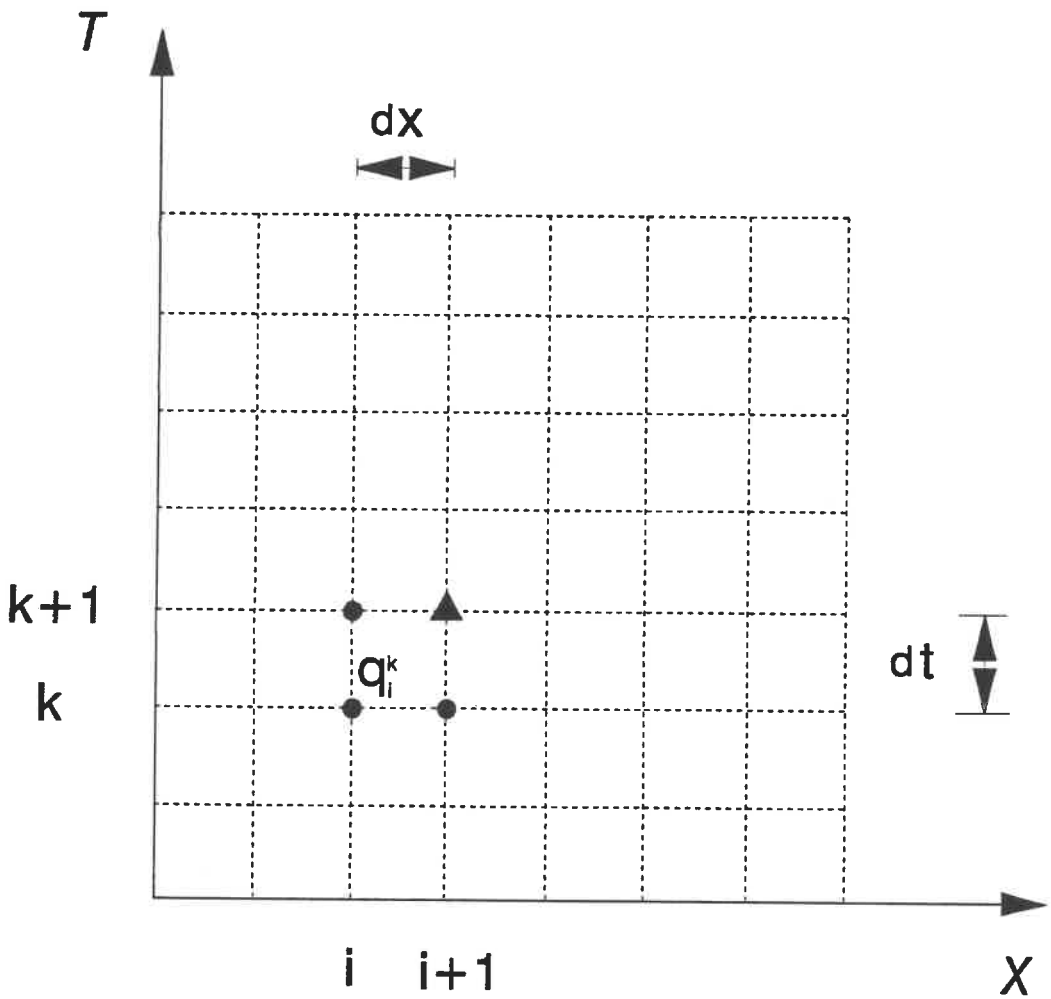

Figure 4.1 Sketch of Grid Representation for the Box Scheme

$$\frac{\partial q}{\partial t} + u(q)(\frac{\partial q}{\partial x} - Q) = 0 \qquad (3\text{-}1\text{-}17)$$

with

$$u(q) = \frac{q^{2/5} s_{ox}^{3/10}}{n^{3/5}} \qquad (3\text{-}1\text{-}18)$$

where q is the discharge per unit width of slope,

t is time,

x is the distance measured from the top of the slope,

Q is net inflow,

n is Manning coefficient, and

s_{ox} is bed slope,

The box scheme of equation (3-1-17) can be written as (Wood and Arnold, 1990):

$$\begin{aligned}
&(1 - \theta)\frac{q_i^{k+1} - q_i^{k}}{\Delta t} + \theta\frac{q_{i+1}^{k+1} - q_{i+1}^{k}}{\Delta t} \\
&+ (1 - \omega)\ u(\bar{q}^{k})[\frac{(q_{i+1}^{k} - q_i^{k})}{\Delta x} - Q] \qquad (4\text{-}1\text{-}1) \\
&+ \omega\ u(\bar{q}^{k+1})[\frac{(q_{i+1}^{k+1} - q_i^{k+1})}{\Delta x} - Q] = 0
\end{aligned}$$

where

$$u(\bar{q}^{k}) = \frac{\left[\frac{q_i^{k} + q_{i+1}^{k}}{2}\right]^{2/5} s_{ox}^{3/10}}{n^{3/5}} \tag{4-1-2}$$

and

$$u(\bar{q}^{k+1}) = \frac{\left[\frac{q_i^{k+1} + q_{i+1}^{k+1}}{2}\right]^{2/5} s_{ox}^{3/10}}{n^{3/5}} \tag{4-1-3}$$

Equation (4-1-1) may also be written as:

$$\begin{aligned}
&\left(\frac{1}{\Delta t} - \frac{\theta}{\Delta t} - \frac{\omega\ u(\bar{q}^{k+1})}{\Delta x}\right) q_i^{k+1} + \left(\frac{\theta}{\Delta t} - \frac{1}{\Delta t} - \frac{u(\bar{q}^{k})}{\Delta x} + \frac{\omega\ u(\bar{q}^{k})}{\Delta x}\right) q_i^{k} \\
&+ \left(\frac{u(\bar{q}^{k})}{\Delta x} - \frac{\theta}{\Delta t} - \frac{\omega\ u(\bar{q}^{k})}{\Delta x}\right) q_{i+1}^{k} + \left(\frac{\theta}{\Delta t} + \frac{\omega\ u(\bar{q}^{k+1})}{\Delta x}\right) q_{i+1}^{k+1} \\
&+ (\omega\ u(\bar{q}^{k}) - \omega\ u(\bar{q}^{k+1}) - u(\bar{q}^{k}))Q = 0
\end{aligned} \tag{4-1-4}$$

where Δx and Δt are the space and time step, respectively.

ω is weighting parameter for the time, ω=1 implies a fully implicit scheme, while ω=0 results in an explicit scheme, here ω=1/2 has been used as in the Crank-Nicholson scheme. θ weights the forward time difference between the i and i+1 grid points, again θ =1/2 provides the optimum weighting.

In this study, two weighting parameters θ and ω were used to improve the stability of the equation. Both θ and ω were set to 0.5. For each time step, there is only one unknown occurring explicitly in the difference equation, it may be solved by using three known values from the previous step. Equation (4-1-4) is nonlinear and is solved by the method of successive substitution by rearranging (4-1-4) to read:

$$q_{i+1}^{k+1} = \frac{1}{E}(Aq_i^{k+1} + Bq_i^{k} + Gq_{i+1}^{k} + C) \qquad (4\text{-}1\text{-}5)$$

where

$$A = -\frac{(1-\theta)}{dt} + \omega\frac{u(\overline{q}^{k+1})}{dx} \qquad (4\text{-}1\text{-}6)$$

$$B = \frac{(1-\theta)}{dt} + \frac{u(\overline{q}^{k})}{dx}(1-\omega) \qquad (4\text{-}1\text{-}7)$$

$$G = \frac{\theta}{dt} - \frac{u(\overline{q}^k)}{dx}(1 - \omega) \tag{4-1-8}$$

$$E = \frac{\theta}{dt} + \omega \frac{u(\overline{q}^{k+1})}{dx} \tag{4-1-9}$$

$$C = [\omega \cdot u(\overline{q}^{k+1}) + u(\overline{q}^k) - \omega \cdot u(\overline{q}^k)]\ Q \tag{4-1-10}$$

a trial q_{i+1}^{k+1} is substituted on the right side of equation (4-1-4), and a new value of q_{i+1}^{k+1} calculated on the left-hand, which is substituted as a trial value on the right side, and so on, until the calculated value of q_{i+1}^{k+1} converges. In this scheme, the stability condition is:

$$c\ \frac{\Delta t}{\Delta x} \leq 1 \tag{4-1-11}$$

4.2 NUMERICAL SCHEME FOR TWO-DIMENSIONAL OVERLAND FLOW

In this section, the implicit centred finite difference scheme has been used to solve the full St.Venant equations. The stability and convergence properties of this scheme have been discussed by Amein (1968). A representation of the

computational "molecule" is shown in Fig 4.2.

i refers to the node number in the x direction,

j refers to the node number in the y direction, and

k is the time step number

θ is a weighting coefficient, whose value varies from 0.5 to 1.0 (Joliffe, 1984). Numerical experimentation has indicated that a value of θ =0.75 gives the most stable solutions (Tayfur, 1993). This implies that the scheme has a more implicit character since the solution is weighted more towards future values than towards present ones.

The implicit finite difference method assumes that at each node, the initial values at the present time are known, to find the unknown values at a future time step. To initiate the calculations, initial values at the present time step are provided from the mathematically or physically specified initial conditions. For the unknown values at the future time step, trial values are given, and iterations are performed until the desired accuracy is achieved. Once new values within the limits of prescribed accuracy are found for the unknowns, these values are taken as trial values for the unknowns at the next time step. Once again iterations are performed until the desired accuracy is reached, to find the new unknown values. This procedure is repeated at each time step. The finite difference form of the continuity equation (3-1-1) is written as follows:

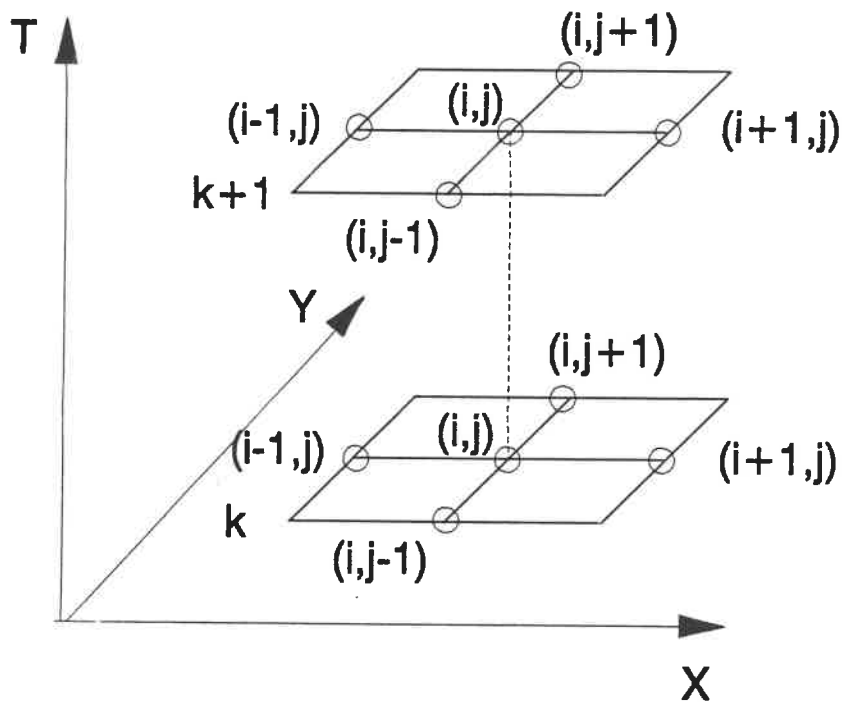

Figure 4.2 Computational Molecule for the Implicit Finite Difference Scheme

$$\frac{h_{ij}^{k+1} - h_{ij}^{k}}{\Delta t} + \frac{\theta u_{ij}^{k+1}(h_{i+1j}^{k+1} - h_{i-1j}^{k+1})}{2\Delta x} + \frac{(1-\theta)u_{ij}^{k}(h_{i+1j}^{k} - h_{i-1j}^{k})}{2\Delta x}$$
$$+ \frac{h_{ij}^{k+1}\theta(u_{i+1j}^{k+1} - u_{i-1j}^{k+1})}{2\Delta x} + \frac{h_{ij}^{k}(1 - \theta)(u_{i+1j}^{k} - u_{i-1j}^{k})}{2\Delta x}$$
$$+ \frac{\theta v_{ij}^{k+1}(h_{ij+1}^{k+1} - h_{ij-1}^{k+1})}{2\Delta y} + \frac{v_{ij}^{k}(1-\theta)(h_{ij+1}^{k} - h_{ij-1}^{k})}{2\Delta y}$$
$$+ \frac{\theta h_{ij}^{k+1}(v_{ij+1}^{k+1} - v_{ij-1}^{k+1})}{2\Delta y} + \frac{h_{ij}^{k}(1 - \theta)(v_{ij+1}^{k} - v_{ij-1}^{k})}{2\Delta y} + Qi_{ij}^{k} - Qr_{ij}^{k} = 0 \qquad (4\text{-}2\text{-}1)$$

there are M •N unknowns, which are the flow depths at each node. (M-1) •(n-1) equations may be solved at each internal node, the remaining equations are obtained from the boundary conditions. Equation (4-2-1) may also be written as:

$$A \cdot h_{i-1j}^{k+1} + B \cdot h_{ij}^{k+1} + C \cdot h_{i+1j}^{k+1} = D \qquad (4\text{-}2\text{-}2)$$

where

$$A = \frac{u_{ij}^{k+1}\theta}{2\Delta x} \qquad (4\text{-}2\text{-}3)$$

$$B = -\frac{1}{\Delta t} - \frac{\theta(u_{i+1j}^{k+1} - u_{i-1j}^{k+1})}{2\Delta x} - \frac{\theta(v_{ij+1}^{k+1} - v_{ij-1}^{k+1})}{2\Delta y} \qquad (4\text{-}2\text{-}4)$$

$$C = -\frac{u_{i,j}^{k+1}\theta}{2\Delta x} \tag{4-2-5}$$

$$\begin{aligned} D = & -\frac{h_{i,j}^{k}}{\Delta t} + \frac{u_{i,j}^{k}(1-\theta)(h_{i+1,j}^{k} - h_{i-1,j}^{k})}{2\Delta x} \\ & + \frac{h_{i,j}^{k}(1-\theta)(U_{i+1,j}^{k} - u_{i-1,k}^{k})}{2\Delta x} + \frac{v_{i,j}^{k+1}\theta(h_{i,j+1}^{k+1} - h_{i,j-1}^{k+1})}{2\Delta y} \\ & + \frac{v_{i,j}^{k}(1-\theta)(h_{i,j+1}^{k} - h_{i,j-1}^{k})}{2\Delta y} + \frac{h_{i,j}^{k}(1-\theta)(v_{i,j+1}^{k} - v_{i,j-1}^{k})}{2\Delta y} - Qr_{i,j}^{k} + Qi_{i,j}^{K} \end{aligned} \tag{4-2-6}$$

equation (4-2-6) can be written as a tridiagonal matrix equation:

$$\begin{bmatrix} [B_2] & [C_2] & & & & & \\ & [A_3] & [B_3] & [C_3] & & & \\ & & \ddots & \ddots & \ddots & & \\ & & & \ddots & \ddots & \ddots & \\ & & & & \ddots & \ddots & \ddots \\ & & & & [A_{m-2}] & [B_{m-2}] & [C_{m-2}] \\ & & & & & [A_{m-1}] & [B_{m-1}] \end{bmatrix} \begin{bmatrix} [h_2] \\ [h_3] \\ \vdots \\ \vdots \\ \vdots \\ [h_{m-2}] \\ [h_{m-1}] \end{bmatrix} = \begin{bmatrix} [D_2 - A_2 * h_1] \\ [D_3] \\ \vdots \\ \vdots \\ \vdots \\ [D_{m-1}] \\ [D_{m-1} - C_{m-1} * h_m] \end{bmatrix}$$

(4-2-7)

This tridiagonal matrix equation may be solved by combining the values specified as boundary conditions at each end of the computational domain. This results in a set of flow depths h_i at each internal node. Then, the flow depths h are substituted in the momentum equations. The discretized form of the momentum equation in the x-direction is:

$$u_{i,j}^{k+1}\,(u_{i,j}^2 + v_{i,j}^2)^{1/2} = \frac{h_{i,j}^{4/3}}{n^2}\,[s_{ox} - \frac{h_{i+1,j} - h_{i-1,j}}{2\Delta x} - \frac{u_{i,j}\,(u_{i+1,j} - u_{i-1,j})}{2g\Delta x} - \frac{v_{i,j}\,(u_{i,j+1} - u_{i,j-1})}{2g\Delta y} - \frac{(u_{i,j}^{k+1} - u_{i,j}^{k})}{g\Delta t} - \frac{Q_{i,j}\,u_{i,j}}{gh_{i,j}}] \qquad (4\text{-}2\text{-}8)$$

or

$$u_{i,j}^{k+1} = \frac{h_{i,j}^{4/3}}{n^2}\,[s_{ox} - \frac{(h_{i+1,j} - h_{i-1,j})}{2\Delta x} - \frac{u_{i,j}}{2g\Delta x}\,(u_{i+1,j} - u_{i-1,j}) - \frac{v_{i,j}}{2g\Delta y}\,(u_{i,j+1} - u_{i,j-1}) + \frac{u_{i,j}^{k}}{g\Delta t} - \frac{Q_{i,j}\,\mu_{i,j}}{gh_{i,j}}]\ /\ [(u_{i,j}^2 + v_{i,j}^2)^{1/2} + \frac{h_{i,j}^{4/3}}{g\Delta t n^2}] \qquad (4\text{-}2\text{-}9)$$

The discretized form of the momentum equation in the y-direction is:

$$v_{i,j}^{k+1}\,(u_{i,j}^2 + v_{i,j}^2)^{1/2} = \frac{h_{i,j}^{4/3}}{n^2}\,[s_{oy} - \frac{h_{i,j+1} - h_{i,j-1}}{2\Delta y} - \frac{u_{i,j}\,(v_{i+1,j} - v_{i-1,j})}{2g\Delta x} - \frac{v_{i,j}\,(v_{i,j+1} - v_{i,j-1})}{2g\Delta y} - \frac{(v_{i,j}^{k+1} - v_{i,j}^{k})}{g\Delta t} - \frac{Q_{i,j}\,v_{i,j}}{gh_{i,j}}]$$

(4-2-10)

or

$$v_{i,j}^{k+1} = \frac{h_{i,j}^{4/3}}{n^2}\,[s_{oy} - \frac{(h_{i,j+1} - h_{i,j-1})}{2\Delta y} - \frac{u_{i,j}}{2g\Delta x}\,(v_{i+1,j} - v_{i-1,j}) - \frac{v_{i,j}}{2g\Delta y}\,(v_{i,j+1} - v_{i,j-1}) + \frac{v_{i,j}^{k}}{g\Delta t} - \frac{Q_{i,j}\,v_{i,j}}{gh_{i,j}}]\ /\ [(u_{i,j}^2 + v_{i,j}^2)^{1/2} + \frac{h_{i,j}^{4/3}}{g\Delta t n^2}]$$

(4-2-11)

The downstream boundary condition of depth gradients are specified in finite difference form as:

$$\frac{\partial h}{\partial x} = \frac{h_{m,j} - h_{m-1,j}}{\Delta x} \qquad (4\text{-}2\text{-}12)$$

or $\qquad h_{m,j} = h_{m-1,j}$

if zero gradient is assumed.

and

$$\frac{\partial h}{\partial y} = \frac{h_{i,n} - h_{i,n-1}}{\Delta y} \qquad (4\text{-}2\text{-}13)$$

or $$h_{i,n} = h_{i,n-1}$$

similarly,

$$u_{m,j} = u_{m-1,j}$$

$$u_{i,n} = u_{i,n-1}$$

and $$v_{m,j} = v_{m-1,j}$$

$$v_{i,n} = v_{i,n-1}$$

the following boundary condition may also be used:

$$h_{m,j} = h_{m-1,j} - \frac{\Delta x n^2 u \sqrt{u^2 + v^2}}{h^{4/3}} \qquad (4\text{-}2\text{-}14)$$

or

$$h_{i,n} = h_{i,n-1} - \frac{\Delta y n^2 v \sqrt{u^2 + v^2}}{h^{4/3}} \qquad (4\text{-}2\text{-}15)$$

This equates the gradient of flow depth to the friction slope. By solving equations (4-2-9) and (4-2-11) together with the boundary equations, velocities in both the x- and y-directions may be obtained. By repeating this procedure, all unknown values, flow depths and flow velocities are found over all nodes of the overland flow domain for each time step.

4.3 QUICK Scheme

The QUICK finite difference scheme has been widely used in solving the advection-diffusion equation. This scheme has the benefits of mass conservation, reasonably high accuracy and computational efficiency in comparison with other higher order-accurate schemes.

In this study, the forward explicit QUICK scheme and the fully time-centred implicit QUICK scheme are used to solve the one-dimensional pollutant transport equation. The full time-centred implicit QUICK scheme is used to solve the two-dimensional pollutant transport equation. The transient one-dimensional pollutant transport equation may be written as:

$$\frac{\partial s}{\partial t} + \frac{\partial (us)}{\partial x} = \frac{\partial}{\partial x}\left(D \frac{\partial s}{\partial x}\right) + \frac{S_t}{h} - \frac{sQr}{h} \qquad (4\text{-}3\text{-}1)$$

The finite difference representation of equation (4-3-1) over a time step is written as:

$$s_i^{k+1} + \alpha\,(\varepsilon_{i+1/2}^{k+1}\, s_{i+1/2}^{k+1} - \varepsilon_{i-1/2}^{k+1}\, s_{i-1/2}^{k+1}) - \alpha\,[\gamma_{i+1/2}^{K+1}\,(s_{i+1}^{k+1} - s_i^{k+1}) - \gamma_{i-1/2}^{k+1}\,(s_i^{k+1} - s_{i-1}^{k+1})]$$
$$= s_i^{k} - (1-\alpha)\,(\varepsilon_{i+1/2}^{k}\, s_{i+1/2}^{k} - \varepsilon_{i-1/2}^{k}\, s_{i-1/2}^{k}) + (1-\alpha)\,[\gamma_{i+1/2}^{k}\,(s_{i+1}^{k} - s_i^{k})$$
$$- \gamma_{i-1/2}^{k}\,(s_i^{k} - s_{i-1}^{k})] + \frac{S_t}{h_i} + s\,\frac{Qr}{h_i}$$

(4-3-2)

when $\alpha = 0$, it expresses a forward explicit scheme,

$\alpha = 0.5$, expresses a fully time-centred implicit scheme,

$\alpha = 1$, expresses a backward implicit scheme.

$$\varepsilon_{i+1/2}^{k} = u_{i+1/2}^{k}\,\frac{\Delta t}{\Delta x}$$

and

$$\gamma_{i+1/2}^{k} = D_{i+1/2}^{k}\,\frac{\Delta t}{\Delta x^2}$$

are the Courant and diffusion numbers respectively, $s_{i+1/2}^{k}$ and $u_{i+1/2}^{k}$ are the concentration and velocity values respectively at grid point i+1/2 as illustrated in Fig 4.3.

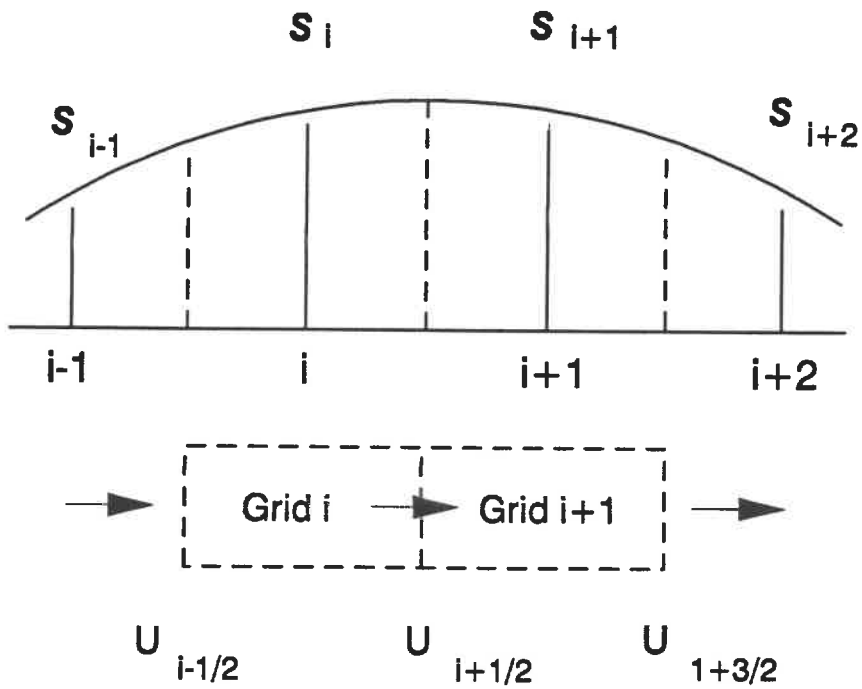

Figure 4.3 Sketch of Grid Representation for the QUICK Scheme

In the case of the one-dimensional fully time-centred implicit QUICK scheme, the unknowns occur implicitly, and they are solved simultaneously. The fully time-centred implicit QUICK scheme for one-dimensional pollutant transport can be written as:

$$
\begin{aligned}
s_i^{k+1} &+ \frac{1}{4}[\epsilon_{i+1/2}^{k+1}(s_{i+1}^{k+1} + s_i^{k+1}) - \epsilon_{i-1/2}^{k+1}(s_i^{k+1} + s_{i-1}^{k+1})] - \frac{1}{16}(\epsilon_{i+1/2}^{k+1}\nabla^2 s_i^{k+1} \\
&- \epsilon_{i-1/2}^{k+1}\nabla^2 s_{i-1}^{k+1}) - \frac{V_{i+1/2}^{k+1}}{2}(s_{i+1}^{k+1} - s_i^{k+1}) + \frac{V_{i-1/2}^{k+1}}{2}(s_i^{k+1} - s_{i-1}^{k+1}) \\
&= s_i^k - \frac{1}{4}[\epsilon_{i+1/2}^{k}(s_{i+1}^{k} + s_i^{k}) - \epsilon_{i-1/2}^{k}(s_i^{k} + s_{i-1}^{k})] + \frac{1}{16}(\epsilon_{i+1/2}^{k}\nabla^2 s_i^{k} \\
&- \epsilon_{i-1/2}^{k}\nabla^2 s_{i-1}^{k}) + \frac{V_{i+1/2}^{k}}{2}(s_{i+1}^{k} - s_i^{k}) - \frac{V_{i-1/2}^{k}}{2}(s_i^{k} - s_{i-1}^{k})
\end{aligned}
\tag{4-3-3}
$$

In the one-dimensional forward explicit scheme, the unknown occurs explicitly and is obtained from the known values at the previous time step. The forward explicit scheme for one-dimensional advection-diffusion is written as:

$$
\begin{aligned}
s_i^{k+1} = s_i^k &- \frac{1}{2}[\epsilon_{i+1/2}^{k}(s_{i+1}^{k}+s_i^{k}) - \epsilon_{i-1/2}^{k}(s_i^{k}+s_{i-1}^{k})] \\
&+ \frac{1}{8}(\epsilon_{i+1/2}^{k}\nabla^2 s_i^{k} - \epsilon_{i-1/2}^{k}\nabla^2 s_{i-1}^{k}) + V_{i+1/2}^{k}(s_{i+1}^{k}-s_i^{k}) \\
&- V_{i-1/2}^{k}(s_i^{k}-s_{i-1}^{k}) + \frac{S_t}{h} - \frac{s_i Qr}{h_i}
\end{aligned}
\tag{4-3-4}
$$

Equation (4-3-2) may be extended to two dimensions. When α=0.5, the representation of the two dimensional pollutant transport equation in a fully time centred implicit scheme is:

$$
\begin{aligned}
S_{i,j}^{k+1} &+ \frac{1}{2}\left(\varepsilon_{i+1/2,j}^{k+1}\, S_{i+1/2,j}^{k+1} - \varepsilon_{i-1/2,j}^{k+1}\, S_{i-1/2,j}^{k+1}\right) + \frac{1}{2}\left(\eta_{i,j+1/2}^{k+1}\, S_{i,j+1/2}^{k+1} - \eta_{i,j-1/2}^{k+1}\, S_{i,j-1/2}^{k+1}\right) \\
&- \frac{1}{2}\left[\gamma_{i+1/2,j}^{k+1}\left(S_{i+1,j}^{k+1} - S_{i,j}^{k+1}\right) - \gamma_{i-1/2,j}^{k+1}\left(S_{i,j}^{k+1} - S_{i-1,j}^{k+1}\right)\right] \\
&- \frac{1}{2}\left[\xi_{i,j+1/2}^{k+1}\left(S_{i,j+1}^{k+1} - S_{i,j}^{k+1}\right) - \xi_{i,j-1/2}^{k+1}\left(S_{i,j}^{k+1} - S_{i,j-1}^{k+1}\right)\right] \\
&= S_{i,j}^{k} - \frac{1}{2}\left(\varepsilon_{i+1/2,j}^{k}\, S_{i+1/2,j}^{k} - \varepsilon_{i-1/2,j}^{k}\, S_{i-1/2,j}^{k}\right) \\
&+ \frac{1}{2}\left[\gamma_{i+1/2,j}^{k}\left(S_{i+1,j}^{k} - S_{i,j}^{k}\right) - \gamma_{i-1/2,j}^{k}\left(S_{i,j}^{k} - S_{i-1,j}^{k}\right)\right] \\
&- \frac{1}{2}\left(\eta_{i,j+1/2}^{k}\, S_{i,j+1/2}^{k} - \eta_{i,j-1/2}^{k}\, S_{i,j-1/2}^{k}\right) \\
&+ \frac{1}{2}\left[\xi_{i,j+1/2}^{k}\left(S_{i,j+1}^{k} - S_{i,j}^{k}\right) - \xi_{i,j-1/2}^{k}\left(S_{i,j}^{k} - S_{i,j-1}^{k}\right)\right]
\end{aligned}
\tag{4-3-5}
$$

where

$$\varepsilon_{i+1/2,\,j}^{k} = u_{i+1/2,\,j}^{k}\,\frac{\Delta t}{\Delta x} \tag{4-3-6}$$

$$\gamma_{i+1/2,\,j}^{k} = D_{i+1/2,\,j}^{k}\,\frac{\Delta t}{\Delta x^2} \tag{4-3-7}$$

$$\eta_{i,\,j+1/2}^{k} = v_{i,\,j+1/2}^{k}\,\frac{\Delta t}{\Delta y} \tag{4-3-8}$$

$$\xi^{k}_{i,\,j+1/2} = D^{k}_{i,\,j+1/2}\,\frac{\Delta t}{\Delta y^2} \qquad (4\text{-}3\text{-}9)$$

ϵ, η are the Courant numbers in the x- and y-direction and γ, ξ are diffusion numbers in the x- and y- directions respectively, Δt the time step and Δx, Δy the grid size, k is the time step number, D is diffusion coefficient. The values at the cell faces may be obtained by quadratic upstream interpolation as following:

$$S^{k}_{i+1/2,\,j} = \frac{1}{2}\,(S^{k}_{i+1,\,j} + s^{k}_{i,\,j}) - \frac{1}{8}\,\nabla^2\,S^{k}_{i,\,j} \qquad (4\text{-}3\text{-}10)$$

$$S^{k}_{i-1/2,\,j} = \frac{1}{2}\,(S^{k}_{i-1,\,j} + s^{k}_{i,\,j}) - \frac{1}{8}\,\nabla^2\,S^{k}_{i-1,\,j} \qquad (4\text{-}3\text{-}11)$$

$$S^{k}_{i,\,j+1/2} = \frac{1}{2}(S^{k}_{i,\,j+1} + s^{k}_{i,\,j}) - \frac{1}{8}\,\nabla^2\,S^{k}_{i,j} \qquad (4\text{-}3\text{-}12)$$

$$S^{k}_{i,\,j-1/2} = \frac{1}{2}\,(S^{k}_{i,\,j-1} + s^{k}_{i,\,j}) - \frac{1}{8}\,\nabla^2\,S^{k}_{i,\,j-1} \qquad (4\text{-}3\text{-}13)$$

in which

$$\nabla^2 S_{i,j}^{k} = S_{i+1,j}^{k} - 2\, S_{i,j}^{k} + S_{i-1,j}^{k} \qquad (4\text{-}3\text{-}14)$$

$$\nabla^2 S_{i-1,j}^{k} = S_{i,j}^{k} - 2\, S_{i-1,j}^{k} + S_{i-2,j}^{k} \qquad (4\text{-}3\text{-}15)$$

the terms $\varepsilon_{i+1/2,j}^{k+1}$, $\gamma_{i+1/2,j}^{k+1}$, $\eta_{i,j+1/2}^{k+1}$, $\xi_{i,j+1/2}^{k+1}$, $s_{i,j}^{k+1}$, $\nabla^2 s_{i,j}^{k+1}$ correspond to those given in equations (4-3-6) to equation (4-3-15). Rearranging equation (4-3-5), we have

$$A\, s_{i-1,j}^{k+1} + B\, s_{i,j}^{k+1} + C\, s_{i+1,j}^{k+1} = D \qquad (4\text{-}3\text{-}16)$$

where

$$A = -\frac{1}{16}\,\varepsilon_{i+1/2,j}^{k+1} - \frac{3}{8}\,\varepsilon_{i-1/2,j}^{k+1} - \frac{\gamma_{i-1/2,j}^{k+1}}{2} \qquad (4\text{-}3\text{-}17)$$

$$\begin{aligned} B = 1 &- \frac{3}{16}\,\varepsilon_{i-1/2,j}^{k+1} + \frac{3}{8}\,\varepsilon_{i+1/2,j}^{k+1} + \frac{3}{8}\,\eta_{i,j+1/2}^{k+1} \\ &- \frac{3}{16}\,\eta_{i,j-1/2}^{k+1} + \frac{\gamma_{i+1/2,j}^{k+1}}{2} + \frac{\gamma_{i-1/2,j}^{k+1}}{2} + \frac{\xi_{i,j+1/2}^{k+1}}{2} + \frac{\xi_{i,j-1/2}^{k+1}}{2} \end{aligned} \qquad (4\text{-}3\text{-}18)$$

$$C = \frac{3}{16}\varepsilon_{i+1/2,j}^{k+1} - \gamma_{i+1/2,j}^{k+1} \qquad (4\text{-}3\text{-}19)$$

$$
\begin{aligned}
D = {} & S_{ij} - \frac{1}{4}\left[\varepsilon^{k}_{i+1/2j}\left(S^{k}_{i+1j} + S^{k}_{ij}\right) - \varepsilon^{k}_{i-1/2j}\left(S^{k}_{ij} + S^{k}_{i-1j}\right)\right] - \frac{1}{4}\left[\eta^{k}_{ij+1/2}\left(S^{k}_{ij+1} + S^{k}_{ij}\right)\right. \\
& \left. - \eta^{k}_{ij-1/2}\left(S^{k}_{ij} + S^{k}_{ij-1}\right)\right] + \frac{1}{16}\left(\varepsilon^{k}_{i+1/2j}\nabla^{2}S^{k}_{ij} - \varepsilon^{k}_{i-1/2j}\nabla^{2}S^{k}_{i-1j} + \eta^{k}_{ij+1/2}\nabla^{2}S^{k}_{ij}\right. \\
& \left. - \eta^{k}_{ij-1/2}\nabla^{2}S^{k}_{ij-1}\right) + \frac{\gamma^{k}_{i+1/2j}}{2}\left(S^{k}_{i+1j} - S^{k}_{ij}\right) - \frac{\gamma^{k}_{i-1/2j}}{2}\left(S^{k}_{ij} - S^{k}_{i-1j}\right) \\
& + \frac{\xi^{k}_{ij+1/2}}{2}\left(S^{k}_{ij+1} - S^{k}_{ij}\right) - \frac{\xi^{k}_{ij-1/2}}{2}\left(S^{k}_{ij} - S^{k}_{ij-1}\right) + \frac{S_{t}}{h_{ij}} - \frac{S_{ij}Qr}{h_{ij}} \\
& - \frac{1}{4}\eta^{k+1}_{ij+1/2}S^{k+1}_{ij+1} + \frac{1}{4}\eta^{k+1}_{ij-1/2}S^{k+1}_{ij-1} - \frac{1}{8}\eta^{k+1}_{ij-1/2}S^{k+1}_{ij-1} - \frac{1}{16}\eta^{k+1}_{ij-1/2}S^{k+1}_{ij-2} \\
& - \frac{1}{16}\varepsilon^{k+1}_{i-1/2j}S^{k+1}_{i-2j} + \frac{1}{16}\eta^{k+1}_{ij+1/2}S^{k+1}_{ij+1} + \frac{1}{16}\eta^{k+1}_{ij+1/2}S^{k+1}_{ij-1} + \frac{\xi^{k+1}_{ij+1/2}}{2}S^{k+1}_{ij+1} + \frac{\xi^{k+1}_{ij-1/2}}{2}S^{k+1}_{ij-1}
\end{aligned}
\tag{4-3-20}
$$

equation (4-3-16) is in tridiagonal matrix form:

$$
\begin{bmatrix}
[B_2] & [C_2] & & & & & \\
 & [A_3] & [B_3] & [C_3] & & & \\
 & & \ddots & \ddots & \ddots & & \\
 & & & \ddots & \ddots & \ddots & \\
 & & & & \ddots & \ddots & \ddots \\
 & & & & [A_{m-2}] & [B_{m-2}] & [C_{m-2}] \\
 & & & & & [A_{m-1}] & [B_{m-1}]
\end{bmatrix}
\begin{bmatrix}
[s_2] \\ [s_3] \\ \vdots \\ \vdots \\ \vdots \\ [s_{m-2}] \\ [s_{m-1}]
\end{bmatrix}
=
\begin{bmatrix}
[D_2 - A_2 * s_1] \\ [D_3] \\ \vdots \\ \vdots \\ \vdots \\ [D_{m-1}] \\ [D_{m-1} - C_{m-1} * s_m]
\end{bmatrix}
\tag{4-3-21}
$$

As before, specification of the boundary conditions completely determines the

solution domain.

The finite difference form of the downstream boundary conditions for the concentration gradient are as follows:

$$\frac{\partial s}{\partial x} = \frac{s_{m,j} - s_{m-1,j}}{\Delta x} \qquad (4\text{-}3\text{-}22)$$

$$\frac{\partial s}{\partial y} = \frac{s_{i,n} - s_{i,n-1}}{\Delta y} \qquad (4\text{-}3\text{-}23)$$

or

$$s_{m,j} = s_{m-1,j}$$

and

$$s_{i,n} = s_{i,n-1}$$

4.4 Solution Technique

Globally convergent methods are well-known numerical methods for solving nonlinear equations. These methods generally converge to a solution from almost any starting point. They combine the rapid local convergence of Newton's method with a global convergence strategy that will guarantee some progress towards the solution at each iteration.

In this project, the globally convergent Newton routine was used; the routine computes the necessary partial derivatives of the equation by finite differences and computes the Jacobian. The method is started with an initial guess x(1:n) for a root in 3 dimensions. The values of the initial guess are taken from the output data by solving equation (4-2-1), (4-2-9) and (4-2-11) together with the boundary conditions. The steps for the global method are:

$$F(x) = 0$$

we rewrite equation (4-2-1),(4-2-9) and (4-2-11), and get

$$F(1) = AA \cdot x(1) + BB \cdot x(1) \cdot x(3)^{4/3} - CC \cdot x(3)^{4/3} + DD \cdot X(3)^{1/3} \qquad (4\text{-}4\text{-}1)$$

where

$$AA = (u_{ij}^2 + v_{ij}^2)^{1/2} \tag{4-4-2}$$

$$BB = \frac{1}{g\Delta t n^2} \tag{4-4-3}$$

$$CC = \frac{1}{n^2}\left[s_{ox} - \frac{1}{2\Delta x}(h_{i+1j} - h_{i-1j}) - \frac{u_{ij}}{2g\Delta x}(u_{i+1j} - u_{i-1j}) - \frac{v_{ij}}{2g\Delta y}(u_{ij+1} - u_{ij-1}) + \frac{u_{ij}^k}{g\Delta t}\right. \tag{4-4-4}$$

$$DD = \frac{q_{ij}u_{ij}}{gn^2} \tag{4-4-5}$$

$$F(2) = AA\cdot x(2) + BB\cdot x(2)\cdot x(3)^{4/3} - SS\cdot x(3)^{4/3} + RR\cdot x(3)^{1/3} \tag{4-4-6}$$

$$SS = \frac{1}{n^2}\left[s_{oy} - \frac{1}{2\Delta y}(h_{ij+1} - h_{ij-1}) - \frac{u_{ij}}{2g\Delta x}(v_{i+1j} - v_{i-1j}) - \frac{v_{ij}}{2g\Delta y}(v_{ij+1} - v_{ij-1}) + \frac{v_{ij}^k}{g\Delta t}\right. \tag{4-4-7}$$

where

$$RR = \frac{q_{i,j} v_{i,j}}{g n^2} \tag{4-4-8}$$

$$F(3) = PP \cdot x(1) + QQ \cdot x(2) + EE \cdot x(3) + GG \tag{4-4-9}$$

in which

$$PP = \frac{\theta}{2\Delta x} (h_{i+1,j} - h_{i-1,j}) \tag{4-4-10}$$

$$QQ = \frac{\theta}{2\Delta y} (h_{i,j+1} - h_{i,j-1}) \tag{4-4-11}$$

$$EE = \frac{1}{\Delta t} + \frac{\theta}{2\Delta x} (u_{i+1,j} - u_{i-1,j}) + \frac{\theta}{2\Delta y} (v_{i,j+1} - v_{i,j-1}) \tag{4-4-12}$$

$$GG = -\frac{h_{ij}}{\Delta t} + \frac{u_{ij}\,(1-\theta)\,(h_{i+1j} - h_{i-1j})}{2\Delta x} + \frac{h_{ij}\,(1-\theta)\,(U_{i+1j} - u_{i-1j})}{2\Delta x}$$
$$+ \frac{v_{ij}\,(1-\theta)\,(h_{ij+1} + h_{ij-1})}{2\Delta y} + \frac{h_{ij}\,(1-\theta)\,(v_{ij+1} - v_{ij-1})}{2\Delta y} + Qi_{ij} - Qr_{ij} \qquad (4\text{-}4\text{-}13)$$

after solving equation (4-4-1),(4-4-6) and (4-4-9), the set of h_i, u_i, v_i, are obtained, these values are taken as the next approximation, this procedure is continued until the successive values are sufficiently close to each other.

CHAPTER 5
RESULTS AND DISCUSSION

The set of equations arising from the mathematical model of pollutant transport in overland flow with infiltration is solved using numerical methods. The usefulness of the proposed model lies in its capability of producing general results that can be used to predict the fate of a pollutant that is infiltrated, dissolved and washed-out by overland flow.

The overland flow was modelled with the St.Venant equation and with the kinematic wave approximation. The pollutant transport was modelled with the advection-diffusion equation, a solubility rate equation and a solid balance equation. The solution procedure is illustrated in Fig 5.1.

The following cases were simulated:

1. The hydraulic behaviour of overland flow,
2. The migration process of pollutant in overland flow,
3. Effect of diffusion coefficient,
4. Effect of solubility,
5. Effect of rainfall,
6. Effect of infiltration.

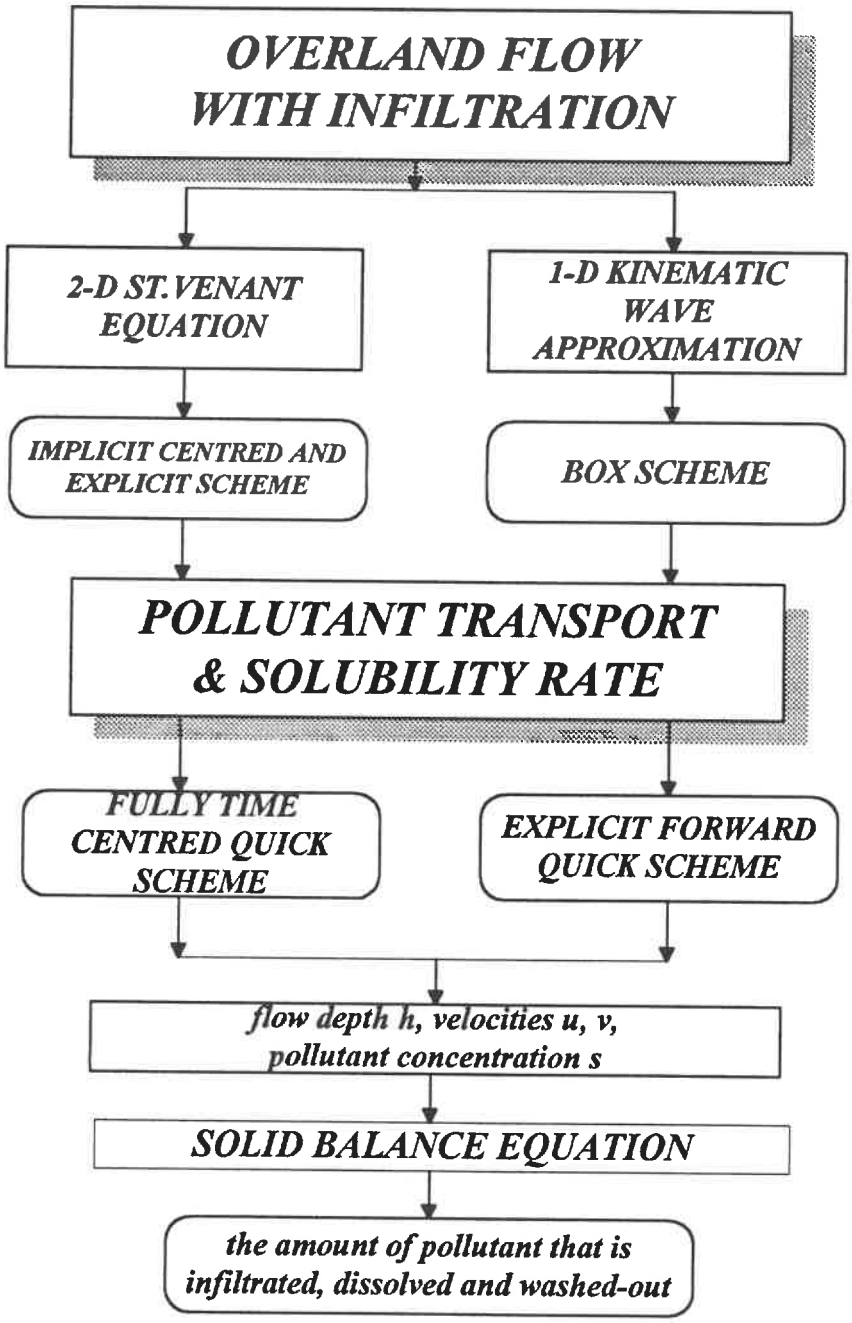

Figure 5.1 The Sketch of Solution Procedure

5.1 HYDRAULIC BEHAVIOUR OF OVERLAND FLOW

Previous research has treated overland flow and transport phenomena on a separate basis. In this work, both phenomena have been integrated into the study. Solution to the equations for overland flow is first obtained, these results are then combined with the pollutant transport equation to obtain solutions for the pollutant concentration field as influenced by rainfall, runoff, infiltration and dissolution. The hydraulic behaviour of overland flow is illustrated by Fig 5.1.2 and Fig 5.1.3, which are three dimensional representations of flow depth and isolines of flow depth, respectively. These results were obtained assuming a constant rainfall intensity and the Green-Ampt infiltration equation on a x-y plane with bed slope of 0.0068 in both the x- and y-directions. The dimensions of the plane were 500 m square, the time interval Δt used was 5s, the computational grid number M×N was 50×50, while the Manning roughness coefficient had a constant value of 0.04. A zero velocity gradient and a zero depth gradient boundary condition were imposed at the downstream end. Fig 5.1.2 is a three dimensional representation of the spatial variation of depth due to runoff. As expected, the flow depth increases with increase of distance and time.

The results obtained with the one dimensional kinematic wave equation with constant rainfall rate and the Green-Ampt infiltration equation using the box

scheme are shown in Fig 5.1.4. The length of land surface is 500m, the bed slope is 0.0068, and the Manning roughness coefficient is 0.025. A time step Δt of 3s, with a computational grid number M of 50 was used. A constant rainfall intensity of 0.000028m/s, that stopped after 2000s was assumed. As seen in figure 5.1.4, when time equals 600s, a mostly uniform water layer covers the land surface except at the upstream end. Since the surface is tilted, the flow depth gradually increases in the slope direction with increase of time and "accumulates" downstream. After 2000s, the rainfall stops, so the upstream flow depth gradually decreases and tends to dry out, while downstream, the accumulated water decreases. This family of curves may be used to predict runoff at different time steps, similar charts may be developed for other types of rainfall intensity distributions. The hydraulic part of the model has been validated against the published data of Tayfur et al. in 1993. This is illustrated in figure 5.1.5.

5.2 RESULTS OF POLLUTANT TRANSPORT

5.2.1 The Migration Process of Pollutant in Overland Flow

Transport phenomena is commonly modelled using the advection-diffusion equation which provides the variation of concentration as a function of space and time. In most practical situations, the concentration distribution is specified as an initial condition on the basis of physical arguments. The present project is different

in that a specified spatial distribution of solid pollutant (for example a pesticide or fertilizer) is provided. This requires the introduction of the concept of a solubility rate St which is added to the advection-diffusion equation as a source term and describes the process of pollutant dissolution. This process is expected to depend on the degree of turbulence characterized by the turbulent skin friction, solubility and local concentration. Fig 5.2.1 to Fig 5.2.10 show that the mass of dissolved pollutant is affected by the solubility rate St and that the magnitude and position of the peak concentration varies with increasing time. Two different initial conditions have been modelled:

i) initial pollutant mass applied at one grid cell,

ii) initial pollutant mass uniformly applied over the land surface. The test domain consists of a 50×50 grid (with $\Delta x = \Delta y$), solubility C^* is 357 kg/m^3, diffusion coefficient D is 0.5 m^2/s, reaction rate constant k_2=0.00001$m^2 \cdot s/kg$, and an initial density of coverage W_0 of 0.05kg per grid cell area is used, which is Δx multiplied by Δy.

In the first case the solid pollutant is supposed to be applied on one grid cell. Fig 5.2.1 shows the results for the one-dimensional situation. These results have been obtained from the advection-diffusion equation using the box scheme and a fully time centred implicit QUICK scheme. As the rainfall excess is converted to surface runoff, the pollutant dissolves and an aqueous concentration of pollutant

begins to spread around its initial position. For example, Fig 5.2.1 indicates that at time of 600s, the peak concentration is about 0.5 kg/m^3 and is situated near the upstream. As the rainfall continues and fresh water continues to replenish the runoff, the combined effect of advection and diffusion results in the position and magnitude of the peak concentration changing, the peak concentration moving downstream with the magnitude being reduced. When time equals 2100s, the peak concentration becomes less than 0.1 kg/m^3 and is situated close to the downstream end. The process of pollutant dilution is faster at the initial stage than at a later stage. Figs 5.2.2 to Fig 5.2.5 show the variation of pollutant concentration for the two dimensional simulations. These figures indicate the same generally expected behaviour, namely that with increasing time, the peak concentration decreases and migrates downstream.

In the second case, initial pollutant mass is uniformly applied over the computational domain. Fig 5.2.6 shows the variation of concentration in the one-dimensional situation. With runoff, the pollutant is supposed to be uniformly dissolved at the beginning. With increase of time, the pollutant concentration migrates and accumulates downstream where it finally leaves the domain. Figs 5.2.7 to 5.2.10 show the two-dimensional case. The peak concentration always occurs (as expected) at the downstream end. The results of the two-dimensional case agree well with that of the one-dimensional situation.

5.2.2 The Effect of Diffusion Coefficient

After the process of pollutant dissolution, diffusion becomes a sensitive factor. Generally speaking, diffusion is caused by local concentration gradients which are in turn caused by mixing on a molecular and a turbulent scale. In shallow overland flow, the bed shear stress is large which leads to strong turbulent mixing vertically and then horizontally. In this study, given the shallow depth of flow, the pollutant concentration is assumed to be uniformly distributed vertically. The effect of varying diffusion coefficient is illustrated in Fig 5.3.1, 5.3.2 and 5.3.3. These results were obtained by using the box scheme and a fully time centred implicit QUICK scheme with a solubility C* of 1.85kg/m^3 and a reaction rate constant k_2 of 0.01m^2·s/kg.

For the one-dimensional case, at the same time step of T=480s, in Fig 5.3.1, with a diffusion coefficient D of 0.5 m^2/s, the maximum concentration is about 0.35 kg/m^3; while in Fig 5.3.2, a diffusion coefficient D of 0.1m^2/s, results in a maximum concentration of about 0.7kg/m^3. Fig 5.3.3 displays the relationship between diffusion coefficient D and maximum concentration S_{max}. It is evident that as expected, the larger the diffusion coefficient D, the lower the maximum concentration of pollutant. Numerical tests confirm that the diffusion coefficient improves the stability properties of all the finite difference schemes tested and also

reduces the amplitude of grid-scale oscillations.

For the two dimensional case, the results are presented at 1727.85s, using a solubility $c^* = 357 kg/m^3$ and a reaction rate constant k = 0.0001. Fig 5.3.4 was obtained using a diffusion coefficient D of $1 m^2/s$, Fig 5.3.5 used a D = 10 m^2/s. From comparing the two figures it may be seen that the concentration in Fig 5.3.5 is more diffused than that in Fig 5.3.4.

5.2.3 The Effect of Solubility

The maximum amount of a solute that may be dissolved in a solvent so that a saturated solution is obtained is expressed as the solubility. The solubility depends on the solute (pollutant) and the temperature. For example, Calcium Chloride $CaCl_2$ has a solubility of 745 kg/m^3 at a temperature of 20°C. That is, at most 745g solute can be dissolved in 1litre water. In this study, values of solubility of typical chemical compounds were used to test the behaviour of different types of pollutant. Figs 5.4.1 and 5.4.2 is a comparison of the results obtained for two different solutes Barium Oxide (BaO, C^* solubility = $34.8 kg/m^3$) and Calcium Chloride (CaCl2, $C^* = 745 kg/m^3$). The results were obtained for the same hydraulic conditions, time=1727.85s and constants k and D with respective values of $0.00001 m^2 \cdot s/kg$ and $1.0 m^2/s$. A larger solubility results in faster dissolution of

the pollutant and higher concentration.

5.2.4 The Effect of Rainfall

Fig 5.5.1 shows the effect of rainfall on pollutant concentration. The following conditions were used: time interval Δt 5s, solubility 357 kg/m^3, reaction rate constant k_2 0.00001 m^2·s/kg, Qr 0.000028m/s. The asterisk lines are for the case when the rainfall is stopped at a time greater than 1000s, while the solid circle lines represent the behaviour with a constant rainfall rate. Higher rainfall intensity will result in larger dilution of the concentration. When the rainfall stops, there is no freshwater inflow, so the rate of dilution will be slowed down. Comparison of the two curves at a point in time after the rainfall ceases indicates that the pollutant concentration remains higher if rainfall ceases than if it had continued.

5.2.5 The Effect of Infiltration

Fig 5.5.2 indicates the influence of infiltration on pollutant concentration. The conditions are the same as in Fig 5.5.1. The solid circles are with the presence of infiltration, the asterisks are for an impervious surface. These results indicate that pollutant concentration in the presence of infiltration is higher than in its absence, since for the same amount of solute, as the amount of available

solvent decreases, the concentration increases.

5.3 THE APPLICATION OF INFILTRATION MODELS

At the present time a complete model to estimate the amount of infiltrated pollutant is unavailable. The model proposed in this study may be regarded as a first step in a quantitative analysis of the infiltration behaviour of different pollutants. In the process of infiltration, the ponding time tp is a critical parameter which may be determined from equation (3-2-1). It is related to the rainfall intensity Qr, rainfall duration and to the soil property. The rainfall intensity Qr may be evaluated from

the formula:

$$Qr = \frac{86}{Ts + 12} \qquad (5\text{-}1)$$

where

Qr = rainfall intensity

T_s = rainfall duration

If the rainfall duration is longer, the ponding time appears later and vice versa. The Green-Ampt infiltration model describes the infiltration process and can be used to estimate the amount of infiltrated pollutant. Normally, the application of the

Green-Ampt equation is limited to times greater than the ponding time, because in its original form, it was intended for use where infiltration resulted from an excess of water at the ground surface at all times (Viessman, 1977). It indicates that the rate of infiltration decreases with increasing time, therefore, the total amount of infiltrated pollutant increases at a slower rate with an increase of time since we assume it to be proportional to the infiltration rate of water.

With this model therefore, it is expected that the pollutant infiltration will occur during the time period leading up to ponding. In order to predict the amount of infiltrated pollutant during this stage, Horton's equation is used. This equation indicates that when the rainfall rate exceeds the infiltration rate, water infiltrates into subsurface at a rate that generally decreases with time (Bedient, 1988), which is physically reasonable.

In this work therefore, a two stage computation of the infiltration process is proposed. Before the start of ponding, Horton's equation (3-2-2) is used to estimate the total pollutant mass infiltrated. Once ponding has occurred, the Green-Ampt equation (3-2-6) is used to evaluate the pollutant mass "lost" due to infiltration.

At the first stage, before ponding, the infiltration capacity is reduced in

proportion to the cumulative infiltration volume F, which may be obtained by integrating Horton's equation (3-2-2),

$$F(t) = f_c t + (f_0 - f_c)/k(1 - e^{-kt}) \qquad (5-2)$$

Equation (5-2) may be solved iteratively for a time t as a function of F. The potential cumulative ΔF is determined from the difference between the value of F at time $t+\Delta t$ and time t. The initial value of t is the starting time zero. The actual infiltration volume increment over the time interval ΔF_{act} is determined as the minimum of

$$\Delta F_{act} = \min\ (\text{potential } \Delta F, \text{ rainfall volume})$$

Rainfall volume is equal to rainfall rate multiplied by the time interval. This permits determination of the actual amount of available water for infiltration. By solving equation (5-2) iteratively, the equivalent time T_e can be obtained which is required to infiltrate the actual cumulative infiltration volume of the Horton parameter. The Newton-Raphson method has been used to obtain the root of equation (5-2). The intial guess is $Te+\Delta t/2$. Iterations converge rapidly to within four decimal places. During the next time interval, the value of F corresponds to the equivalent time and not to the real time. By solving equation (5-2) for each value of t, the infiltration capacity at any time may be found.

During the period before ponding, especially at the start of rainfall, it is assumed that pollutant infiltrates into the soil as an aqueous solution with saturated concentration. In an attempt to realistically model the process of dissolution of the pollutant to a final saturated state, a delay time coefficient k_4 has been introduced. k_4 decribes the time taken for a solute after initial contact with a solvent, to develop into a saturated solution. It is also assumed that no pollutant mass is lost due to runoff at times less than the ponding time. In other words, the only mechanism for pollutant to be consumed is by infiltration.

Before ponding, the amount of pollutant that has infiltrated into the soil may be calculated from equation (3-3-11):

$$A = c^{*} \cdot k_4 \cdot f_p \cdot \Delta t \cdot \Delta x \cdot \Delta y$$

the amount of remaining pollutant decreases with an increase in the amount of infiltrated pollutant; once the pollutant mass decreases to zero, further infiltration is only of pure water.

After the start of the rainfall excess period, the Green-Ampt equation (3-2-6) is used, in which Δt is the interval between the local time and ponding time. During this stage, infiltration capacity is a function of time. After ponding, the amount of pollutant infiltrating into the soil may be calculated in the following

manner:

For an unsaturated solution:

$$B = s \cdot Qi \cdot \Delta x \cdot \Delta y \cdot \Delta t$$

For a saturated solution:

$$C = c^{*} \cdot Qi \cdot \Delta x \cdot \Delta y \cdot \Delta t$$

The total infiltrated pollutant mass can be evaluated from:

$$QDL = \Sigma A + \Sigma B + \Sigma C$$

A test case with the following data has been investigated: the length of land surface is 500m with a bed slope of 0.0068 and a Manning roughness coefficient of 0.04. The initial pollutant mass is applied at a local spot with a density of 0.05 kg per grid cell area, which is Δx multiplied by Δy. The treated area is located 100m from the upstream end. The solubility of the pollutant C* is 745kg/m^3, the diffusion coefficient D is 0.4m^2 /s and the reaction rate constant k_2 is 0.000001m^2·s/kg. The rainfall intensity is 0.000013m/s with a duration of 2000s. The Horton parameters are such that the initial infiltration capacity f_0 of a watershed is given as 0.0000245m/s, final capacity f_c is 0.00001856m/s, the time

constant k_3 is 0.000389s and the delay time coefficient k_4 is 0.0005. Before runoff reaches equilibrium, i,e. before ponding time, the amount of infiltrated pollutant may be estimated from the infiltration capacity, according to the Horton equation. Fig 5.5.3 shows that curve A represents the amount of infiltrated pollutant before ponding time, i,e. time from zero to 438s. Curve B represents the amount of infiltrated pollutant after ponding time. Before ponding, the residual pollutant mass decreases with infiltration. Once ponding occurs, the pollutant dissolves and then washout by the overland flow occurs as well as infiltration. This is computed to establish the residual mass of pollutant. As seen from Fig 5.5.3, before ponding, the amount of infiltrated pollutant is 0.38kg, while after ponding occurs, the amount of infiltrated pollutant is about 3.18kg. Fig 5.5.4 represents the time evolution of residual pollutant, the total applied pollutant mass 5kg being consumed within 851s. Fig 5.5.5 represents the time evolution of the dissolved solute, the total mass of dissolved solute is 4.62kg. Fig 5.5.6 represents the time evolution of washed out pollutant, the total amount of pollutant washed out is 1.55kg. Our results indicate that during the time period leading up to ponding, the amount of pollutant infiltrating into the soil depends on the solubility, the infiltration capacity of the soil as well as on the time delay coefficient. For example, when k_4 equals 1, the total pollutant mass is lost by infiltration into the soil. The period before ponding is therefore important and cannot be ignored in a practical situation.

At every time step, in the computational domain, there is a value of maximum concentration. The trace of maximum concentrations are shown in Fig 5.5.7, they describe the evolution of maximum concentration with time. Fig 5.5.8 shows the results using different numerical schemes, the asterisk lines represent the results obtained by using the forward explicit QUICK scheme and the solid lines represent the results obtained by using the fully time centred implicit QUICK scheme. Comparison of the results with different schemes indicates good agreement. The results in this study are physically realistic, while the numerical algorithms used are stable and robust .

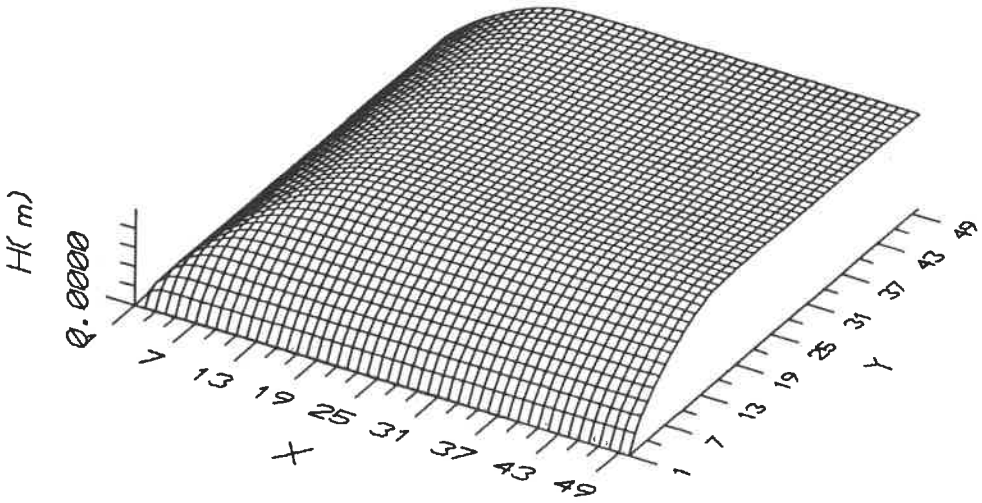

Figure 5.1.2 Flow Depth of Overland Flow
T=1727.85s, Hmax=0.01875m

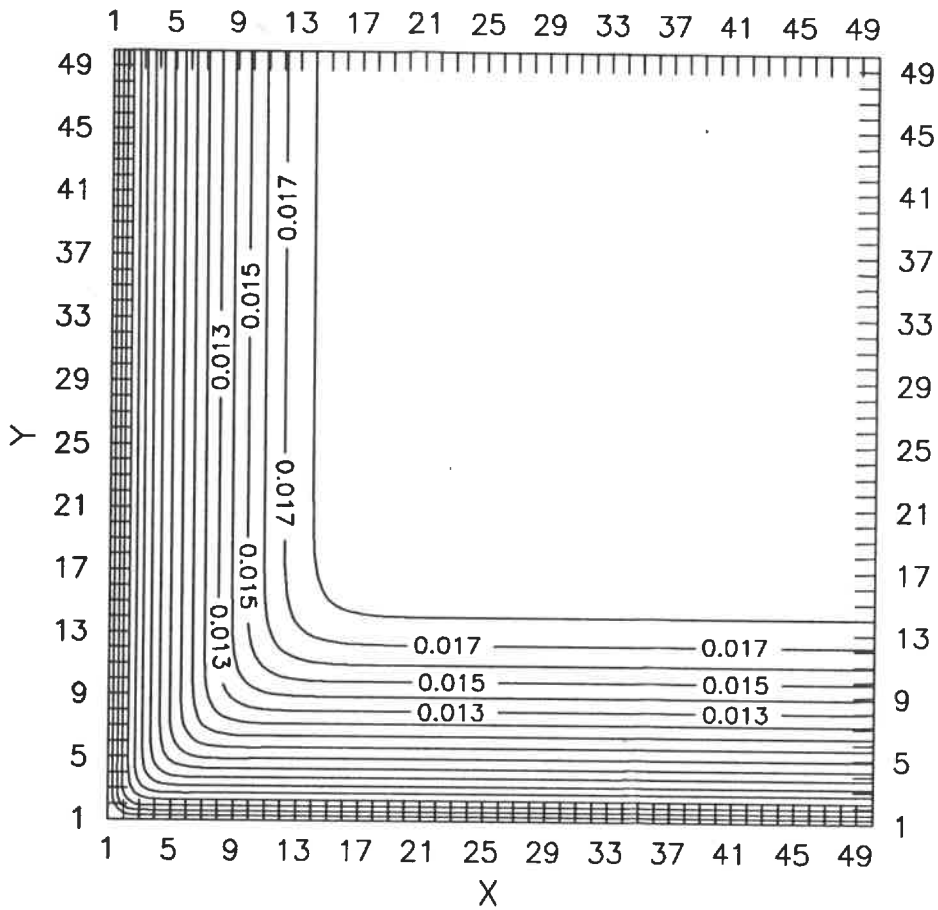

Figure 5.1.3 Depth Profile of Overland Flow
T=1727.85s, Hmax=0.01875m

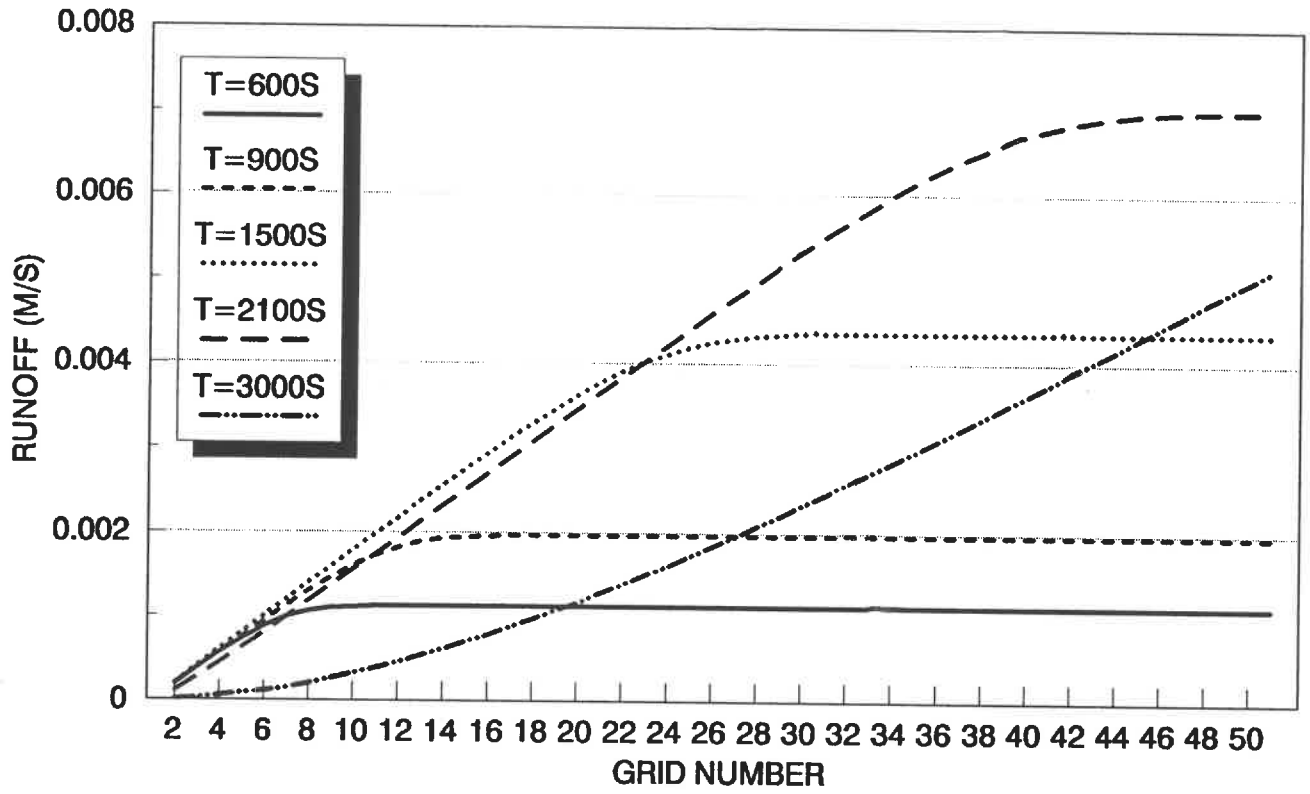

Figure 5.1.4 Time Evolution of Runoff

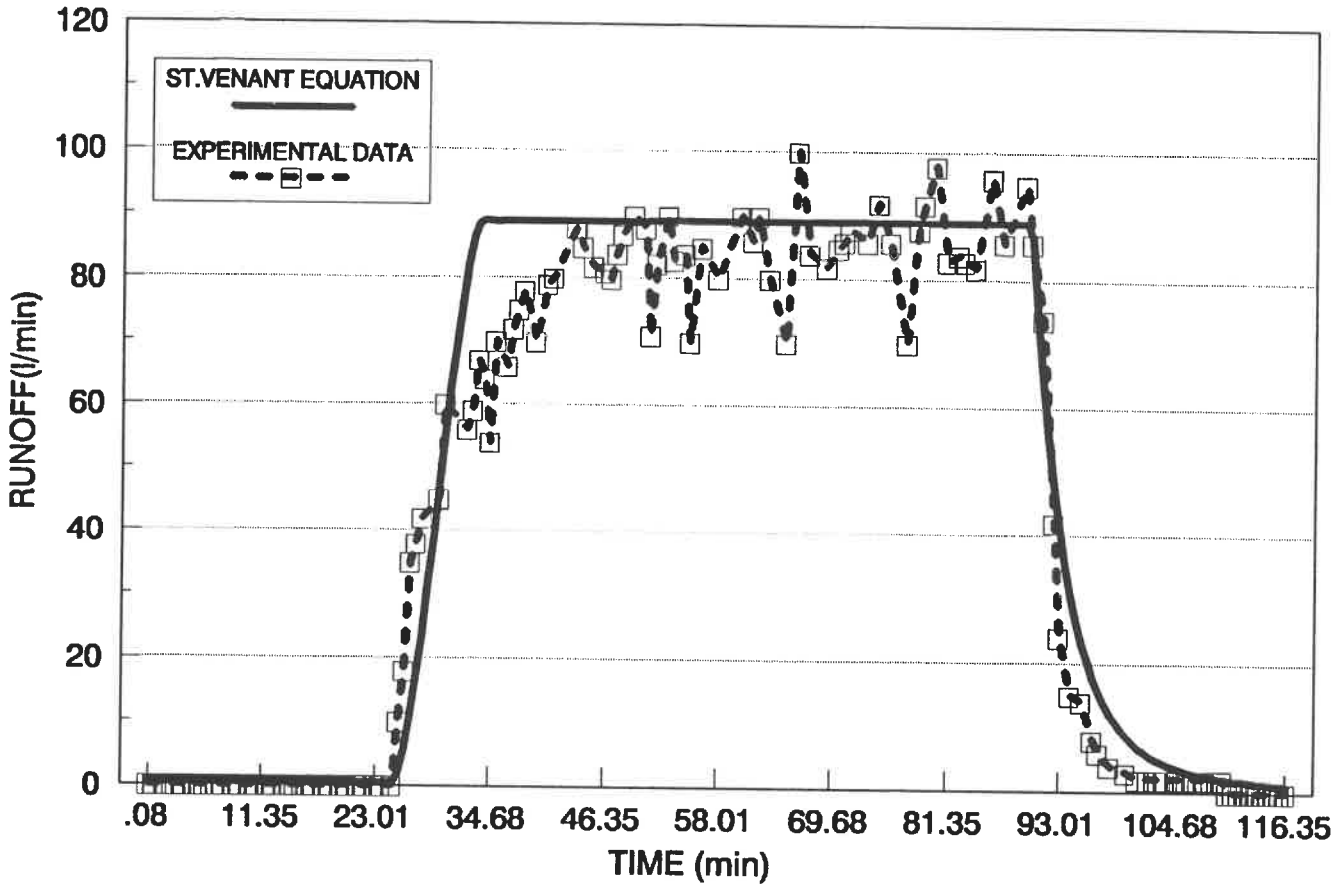

Figure 5.1.5 Comparison of the Experimental Data with the Numerical Solution

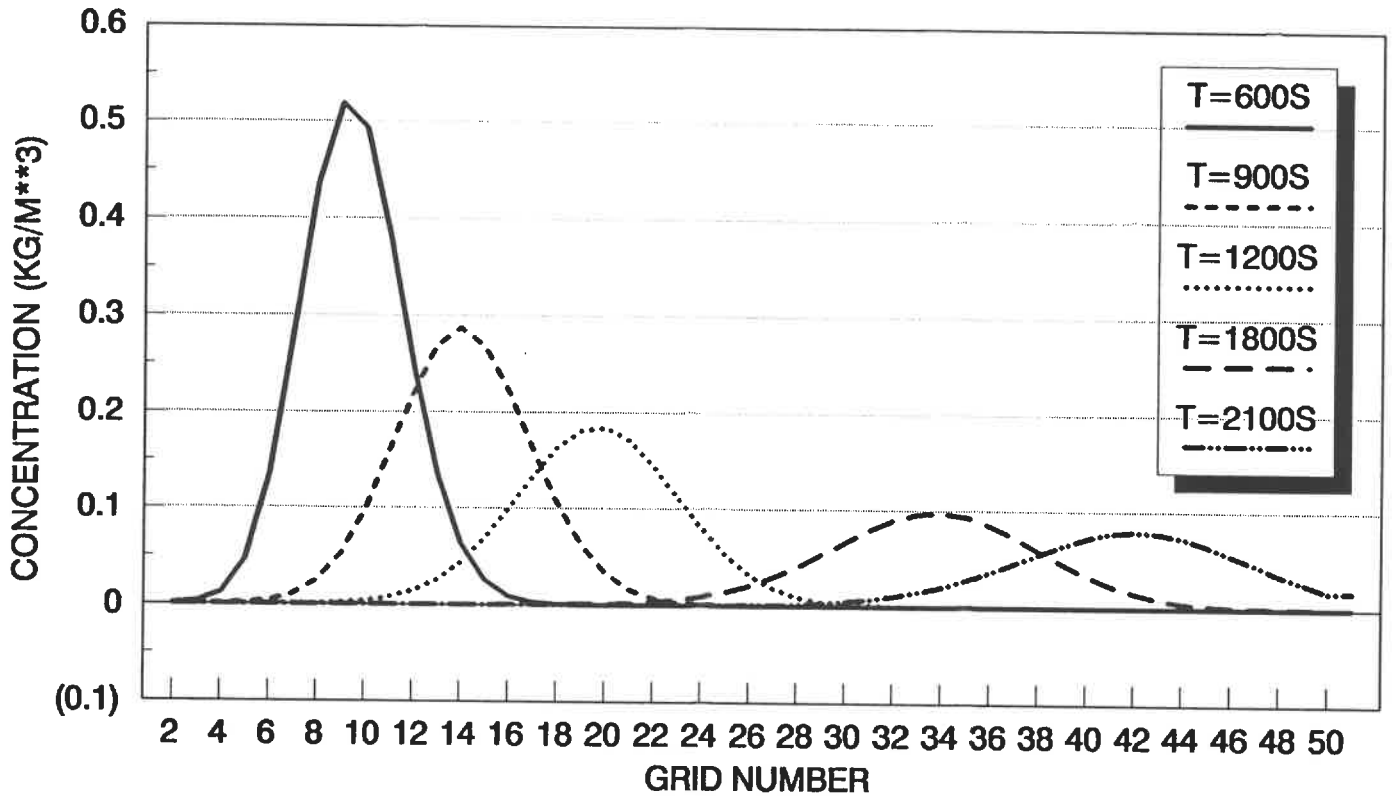

Figure 5.2.1 Variation of Concentration (1-D)

Initial Pollutant Mass Applied at One Grid Cell

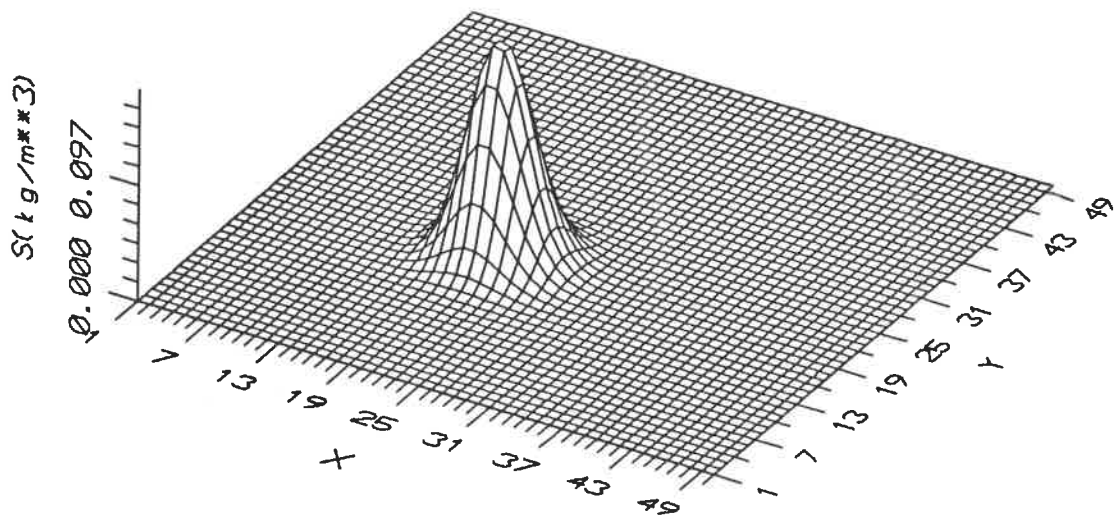

Figure 5.2.2 The Migration of Pollutant
in Overland Flow (2-D)
T=782.45s, Smax=0.1772kg/m**3

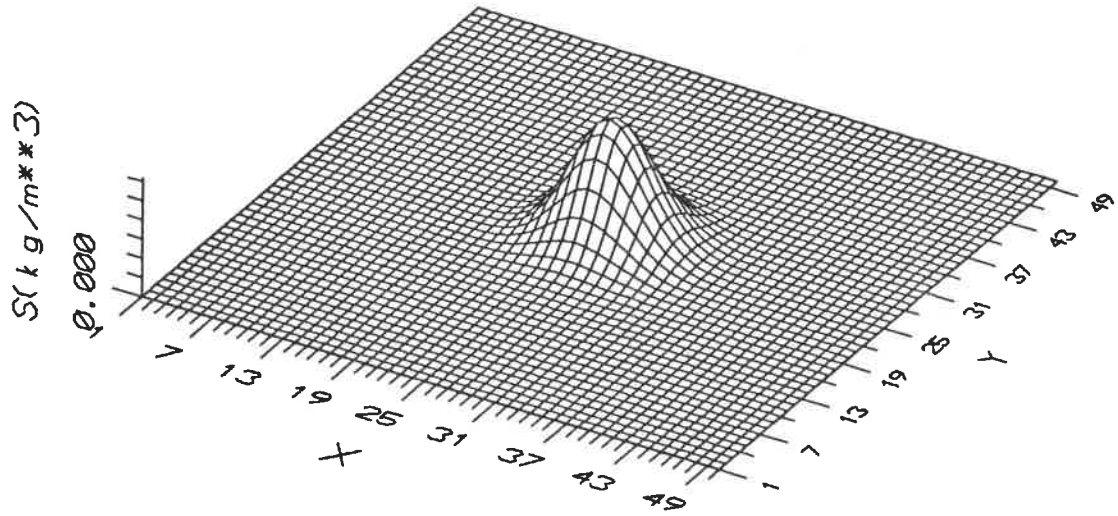

Figure 5.2.3 The Migration of Pollutant
in Overland Flow (2-D)
T=1227.95s, Smax=0.0997kg/m**3

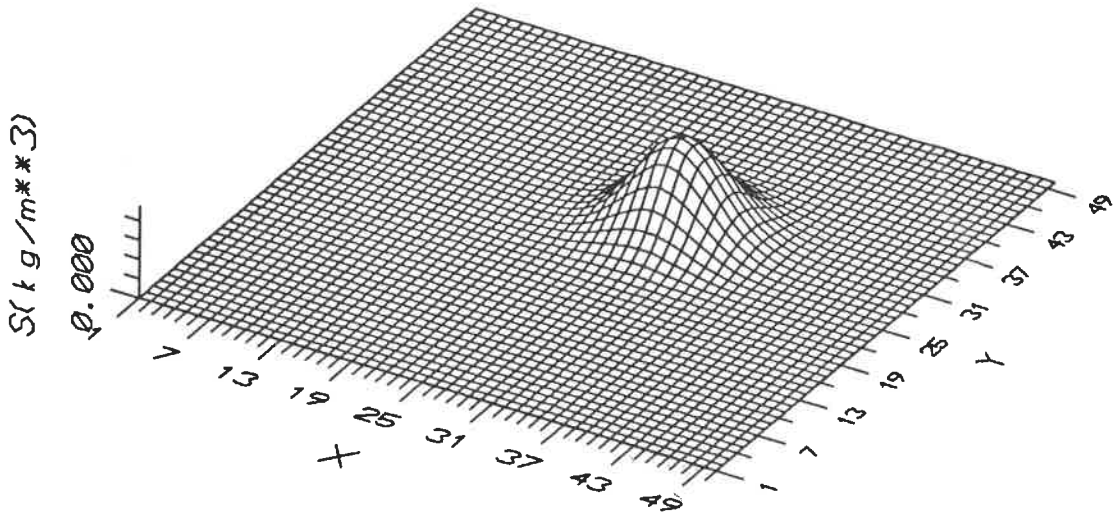

Figure 5.2.4 The Migration of Pollutant
in Overland Flow (2-D)
T=1477.85s, Smax=0.0766kg/m**3

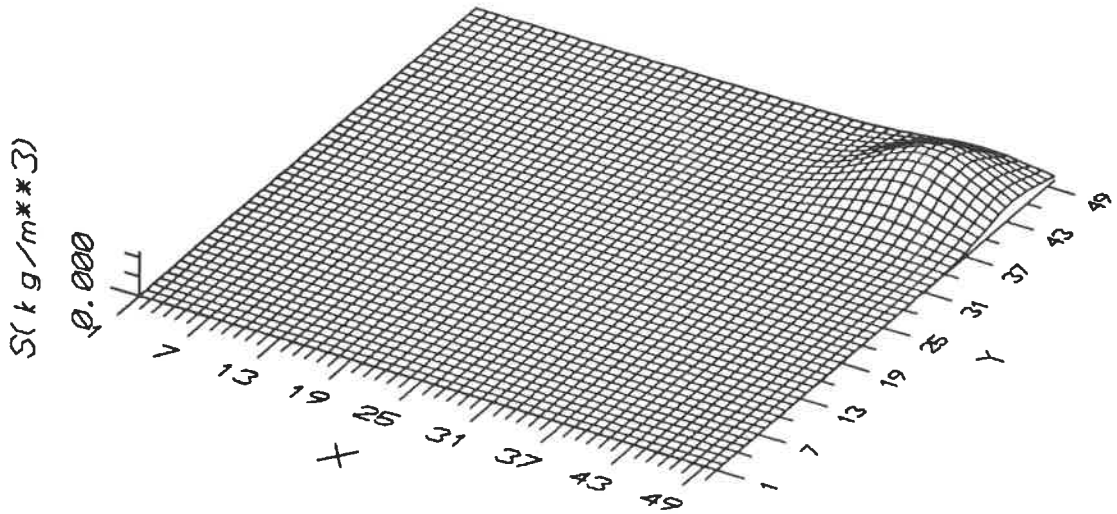

Figure 5.2.5 The Migration of Pollutant
in Overland Flow (2-D)
T=2227.85s, Smax=0.0364kg/m**3

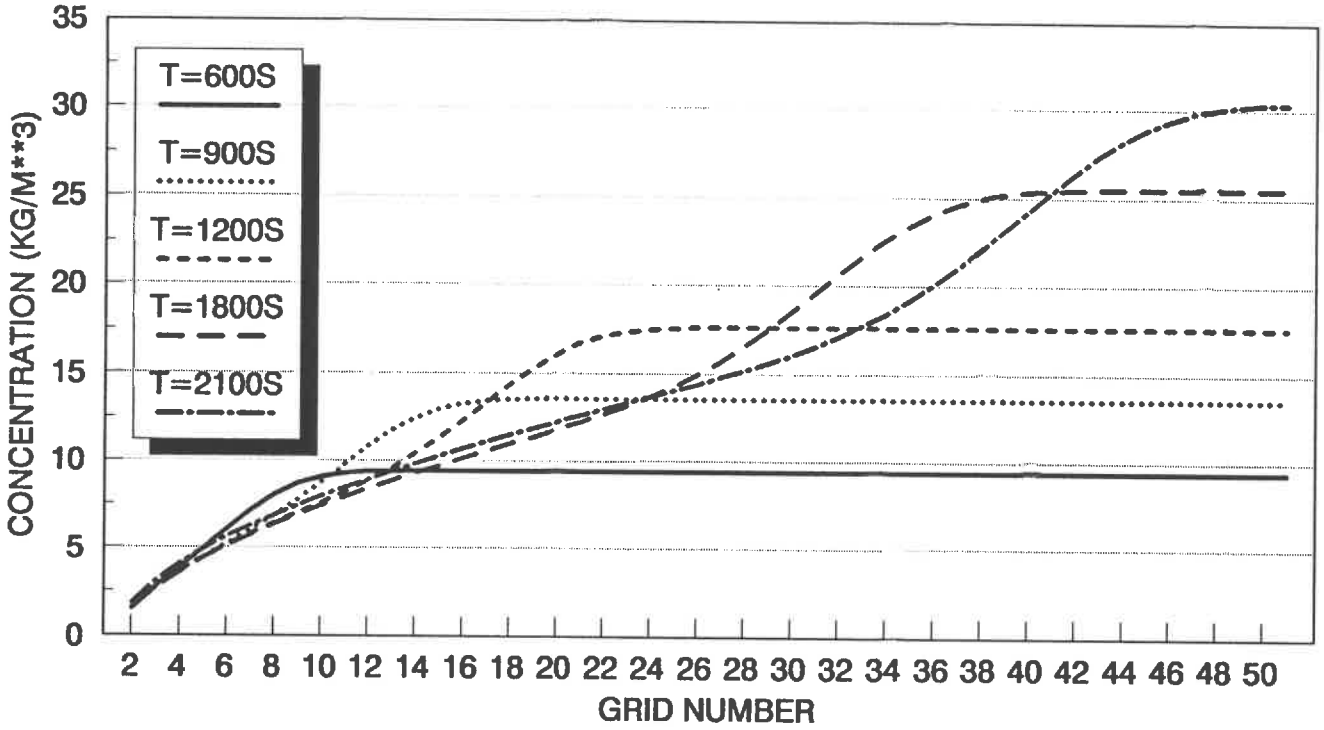

Figure 5.2.6 The Variation of Concentration (1-D)

Initial Pollutant Mass Uniformly Applied

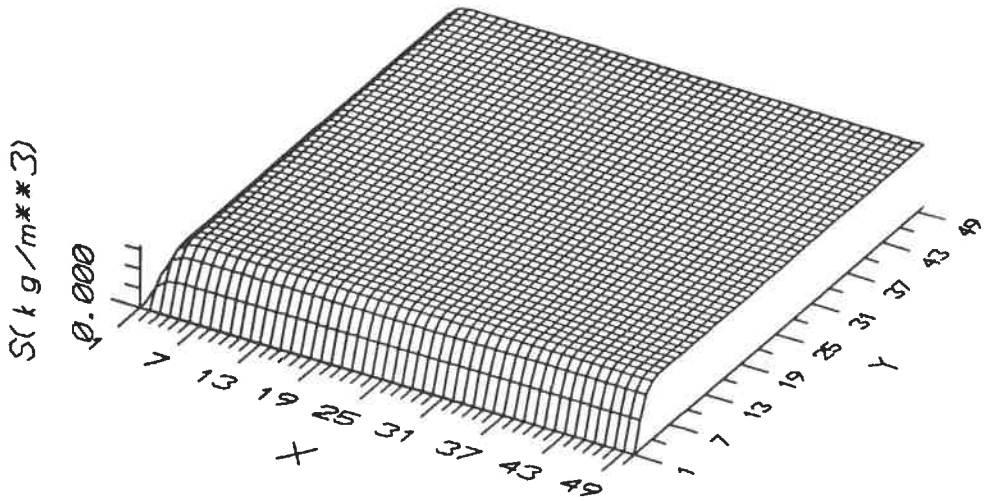

Figure 5.2.7 The Migration of Pollutant
in Overland Flow (2-D)
T=191.45s, Smax=20.0552kg/m**3

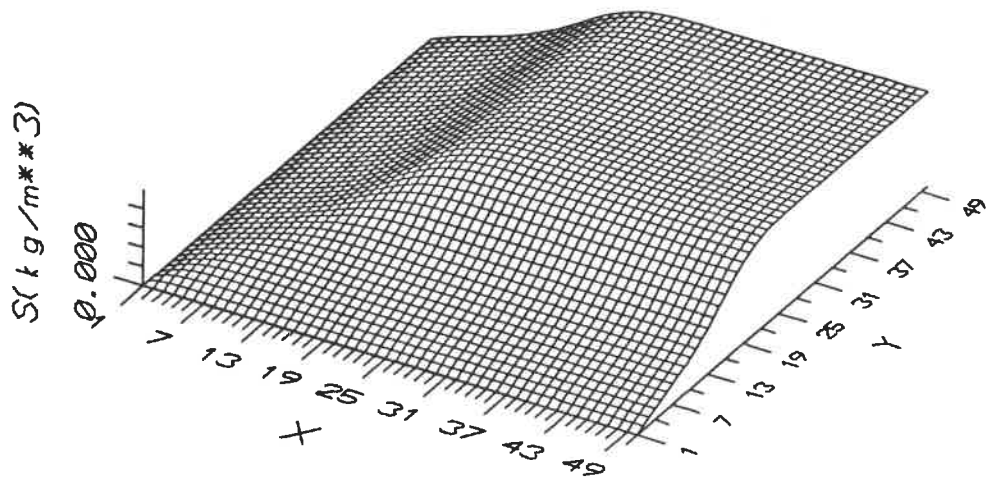

Figure 5.2.8 The Migration of Pollutant
in Overland Flow (2-D)
T=1227.85s, Smax=31.22kg/m**3

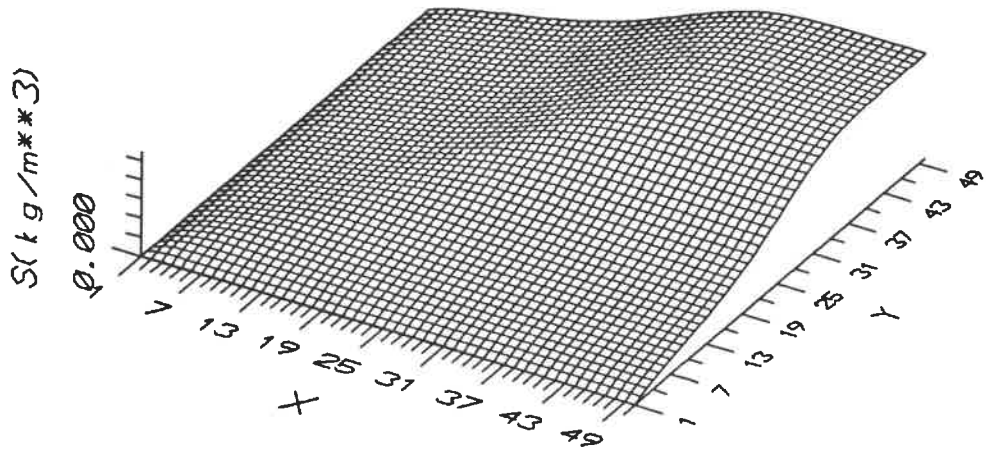

Figure 5.2.9 The Migration of Pollutant
in Overland Flow (2-D)
T=1727.85s, Smax=34.2072kg/m**3

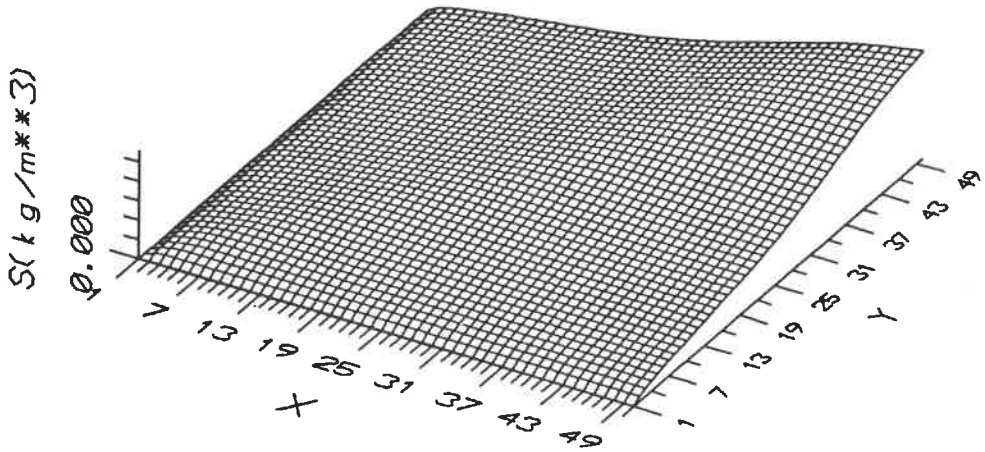

Figure 5.2.10 The Migration of Pollutant
in Overland Flow (2-D)
T=2227.85s, Smax=35.1082kg/m**3

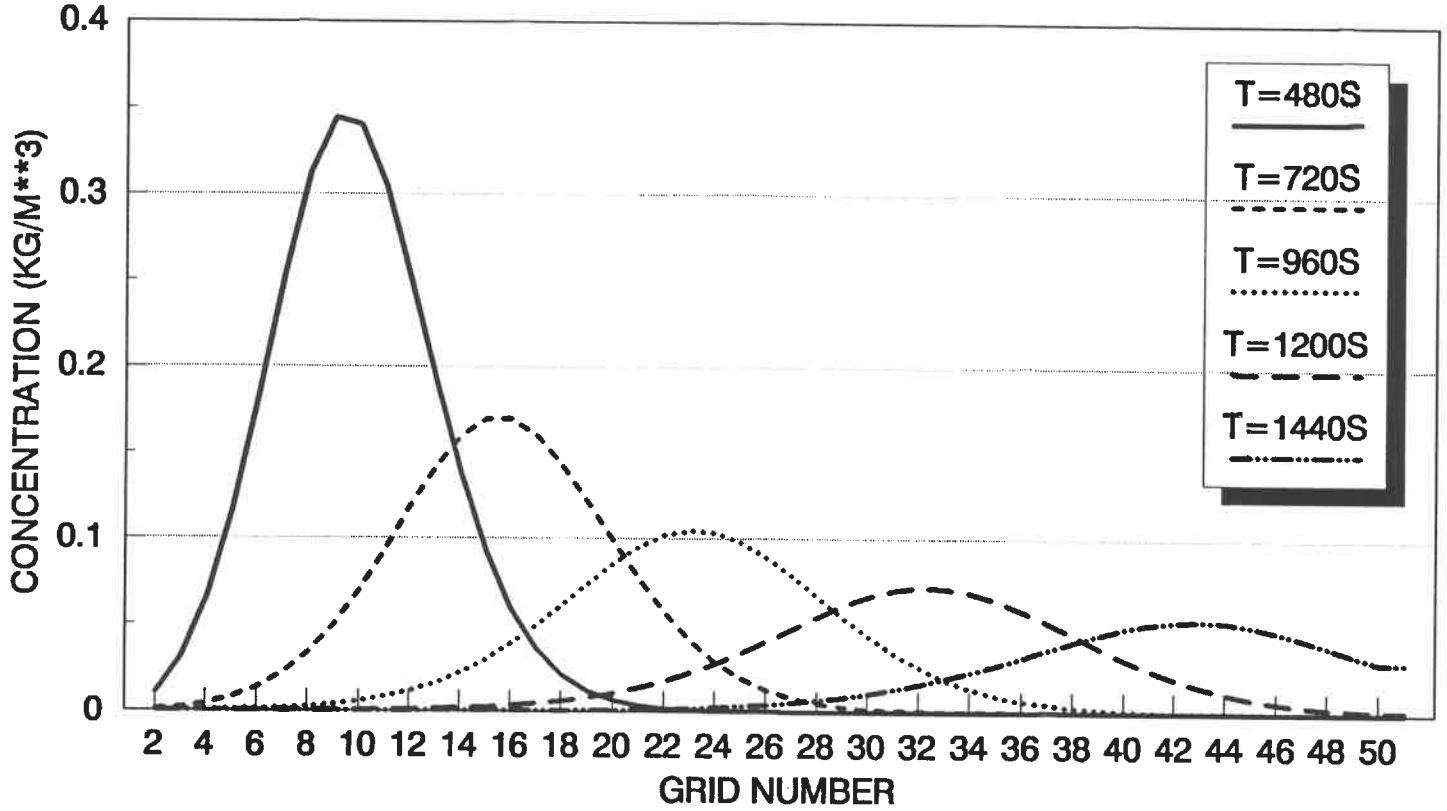

Figure 5.3.1 The Effect of Diffusion Coefficient, D=0.5m**2/s

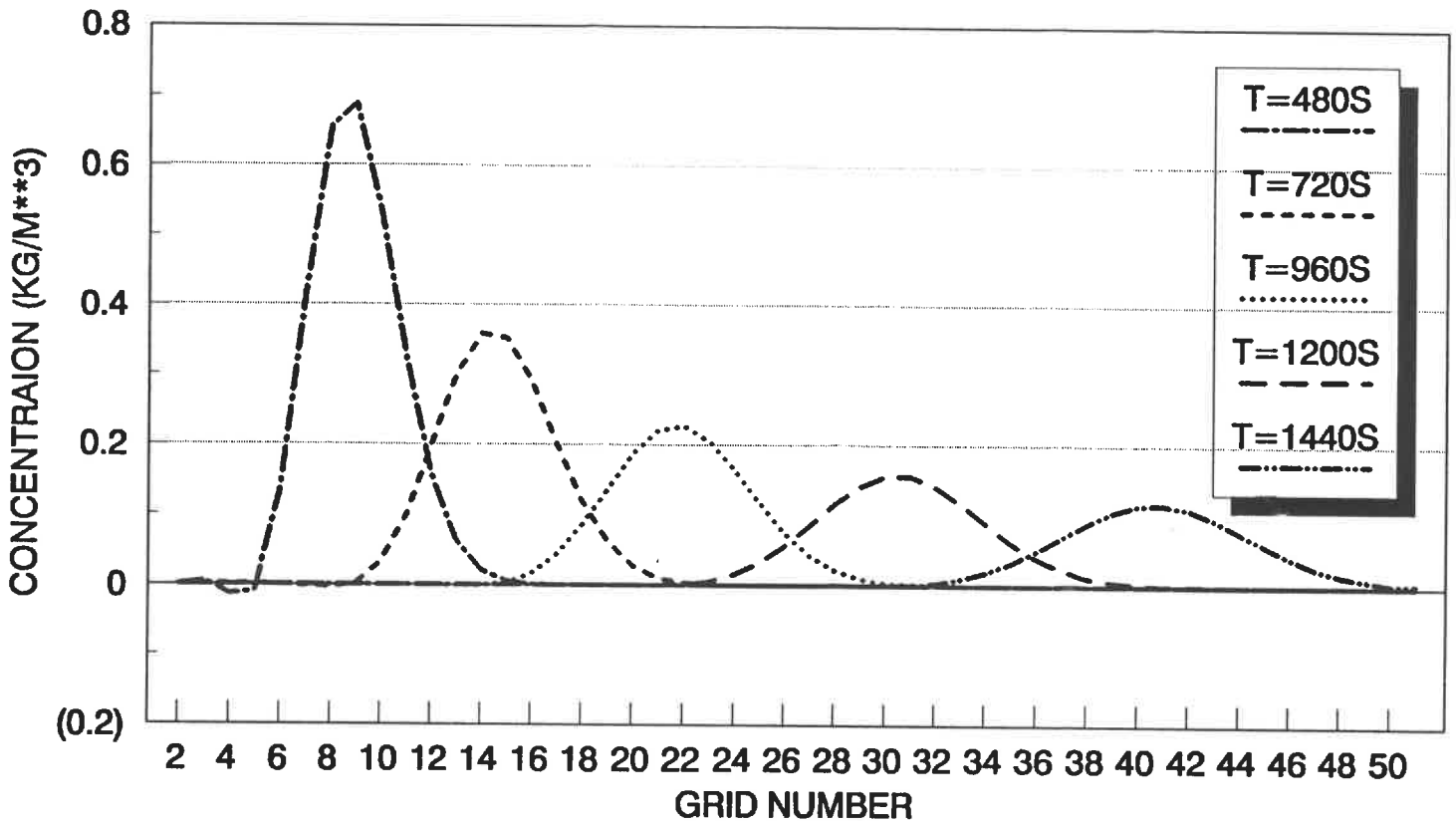

Figure 5.3.2 The Effect of Diffusion Coefficient, D=0.1m**2/s

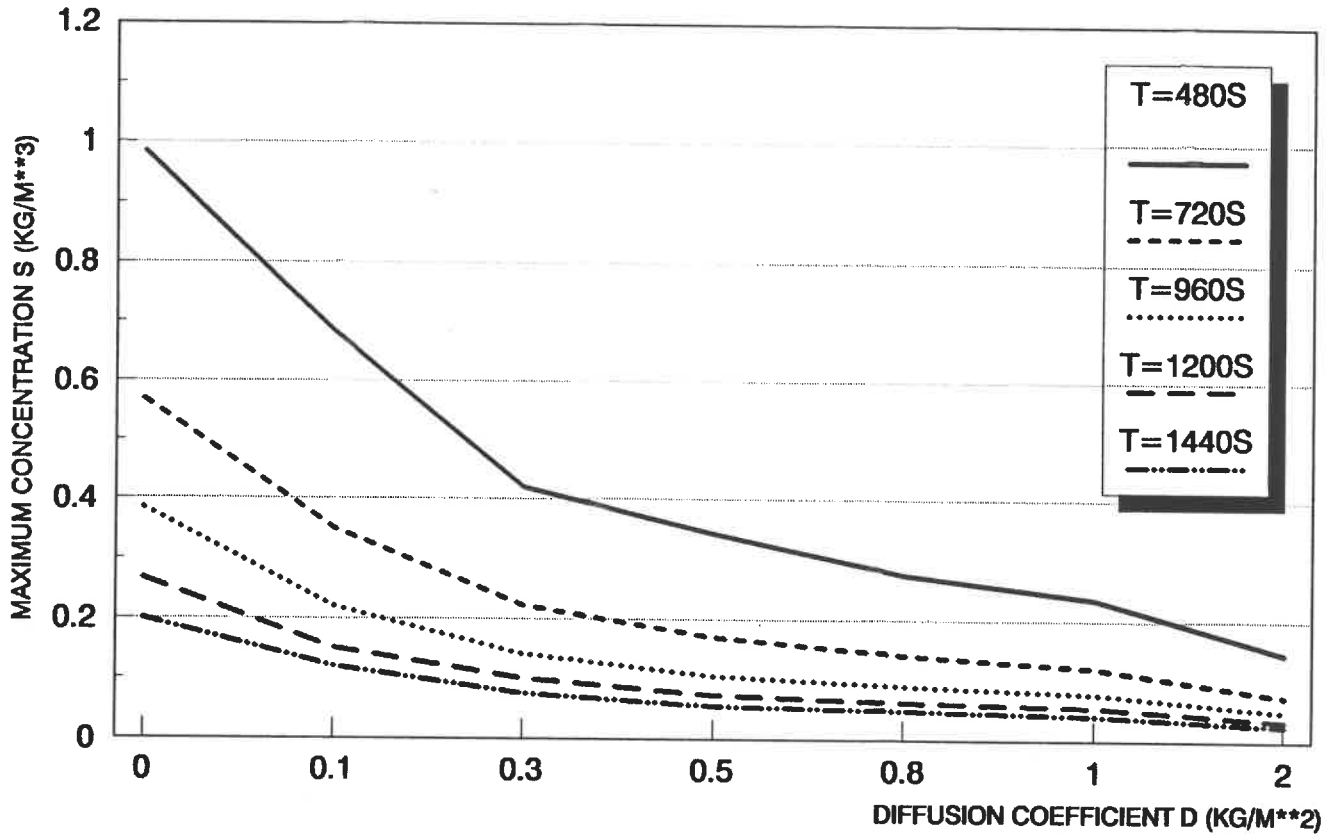

Figure 5.3.3 The Effect of Diffusion Coefficient

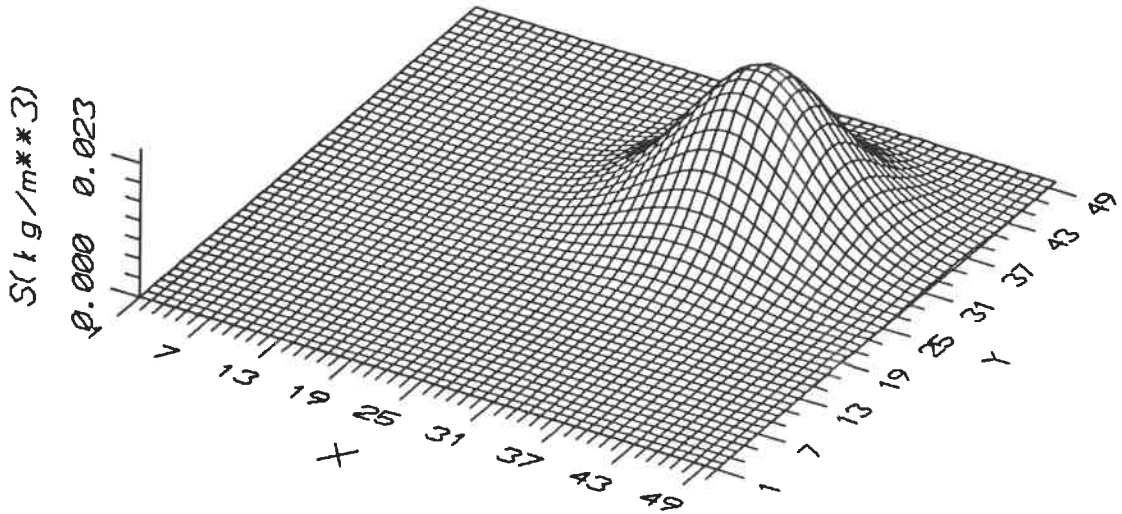

Figure 5.3.4 The Effect of Diffusion Coefficient
D=1m*2/s, Smax=0.023kg/m**3

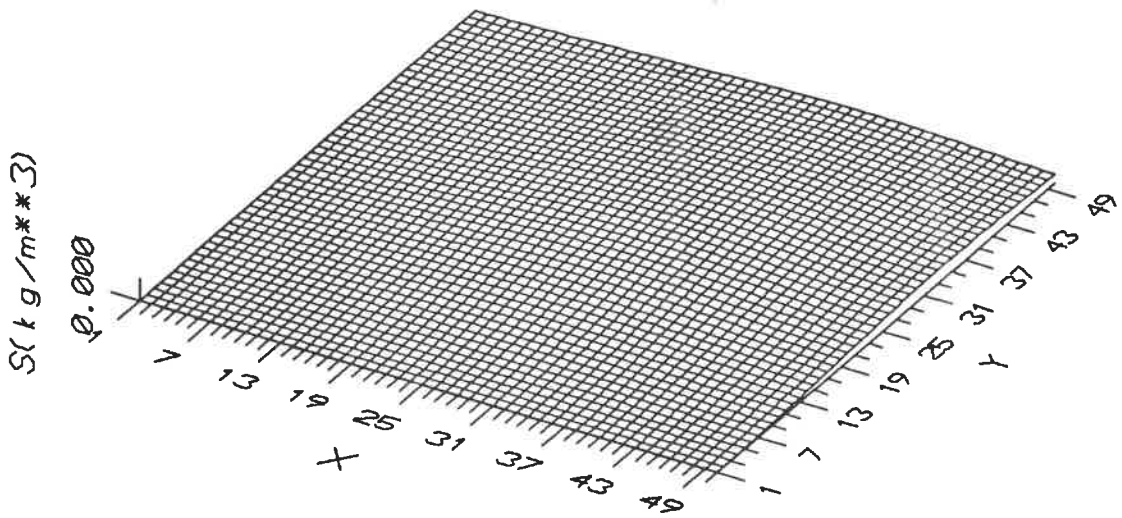

Figure 5.3.5 The Effect of Diffusion Coefficient
D=10 m**2/s, Smax=0.0037 kg/m**3

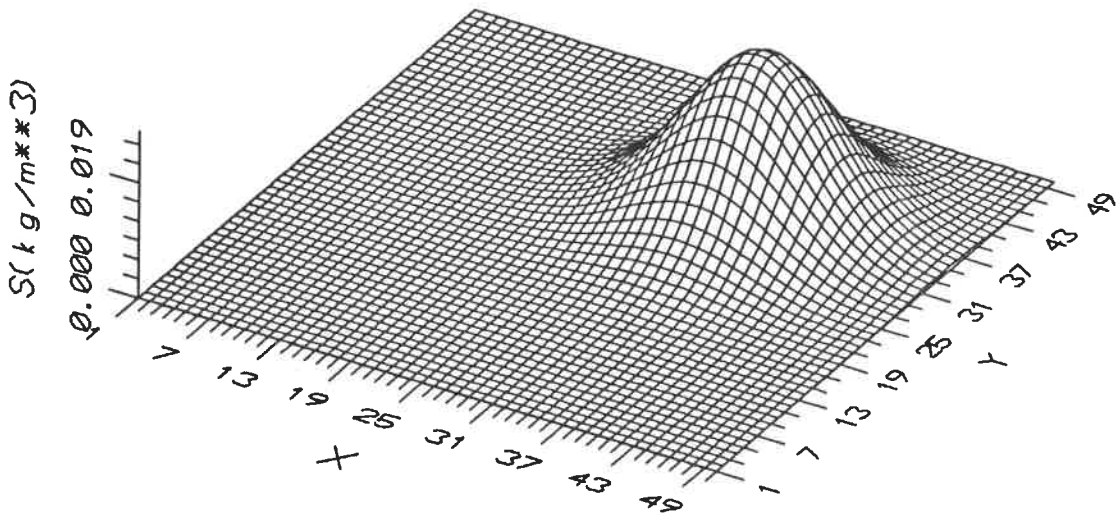

Figure 5.4.1 The Effect of Solubility
c*=745 kg/m**3, Smax=0.0259kg/m**3

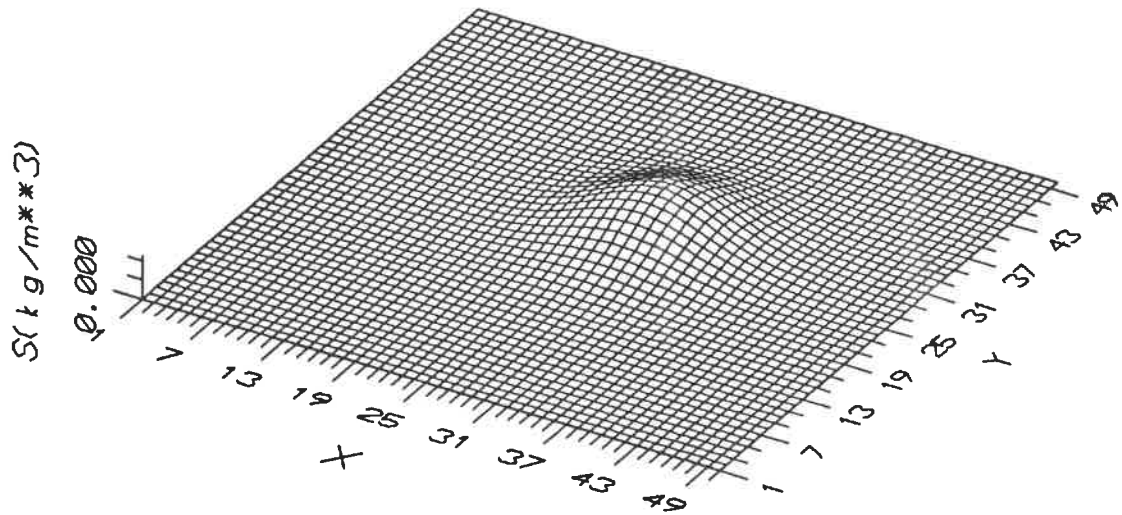

Figure 5.4.2 The Effect of Solubility
c*=34.8 kg/m**3, Smax=0.0073kg/m**3

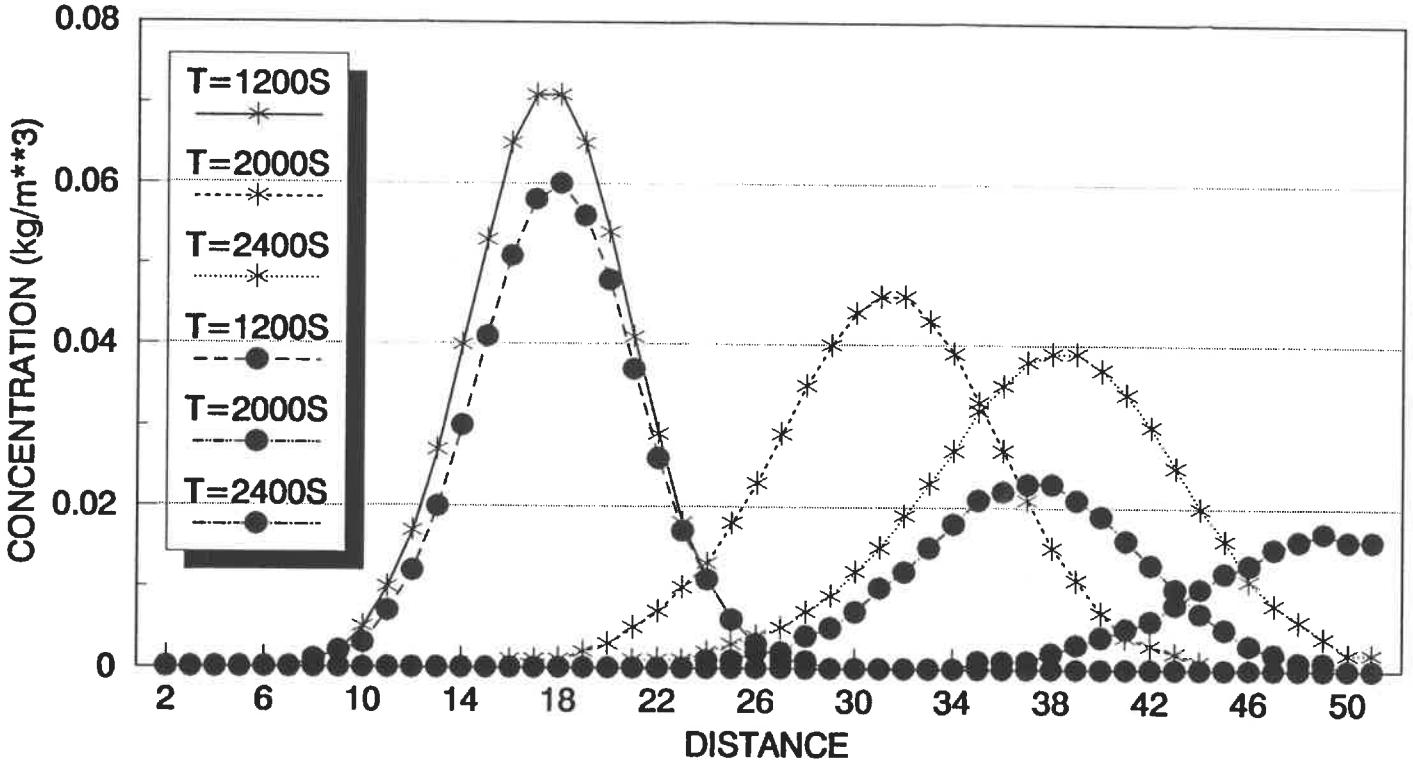

Figure 5.5.1 The Effect of Rainfall

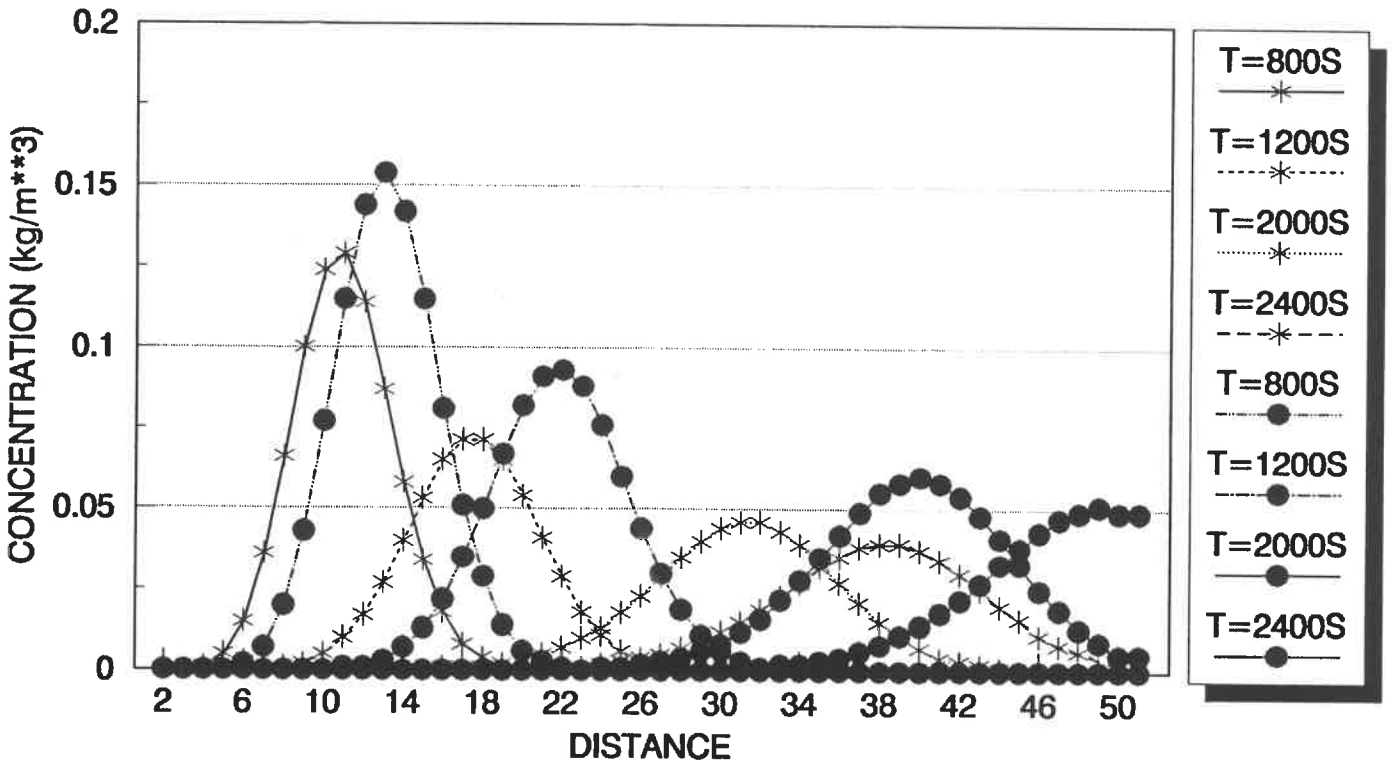

Figure 5.5.2 The Effect of Infiltration

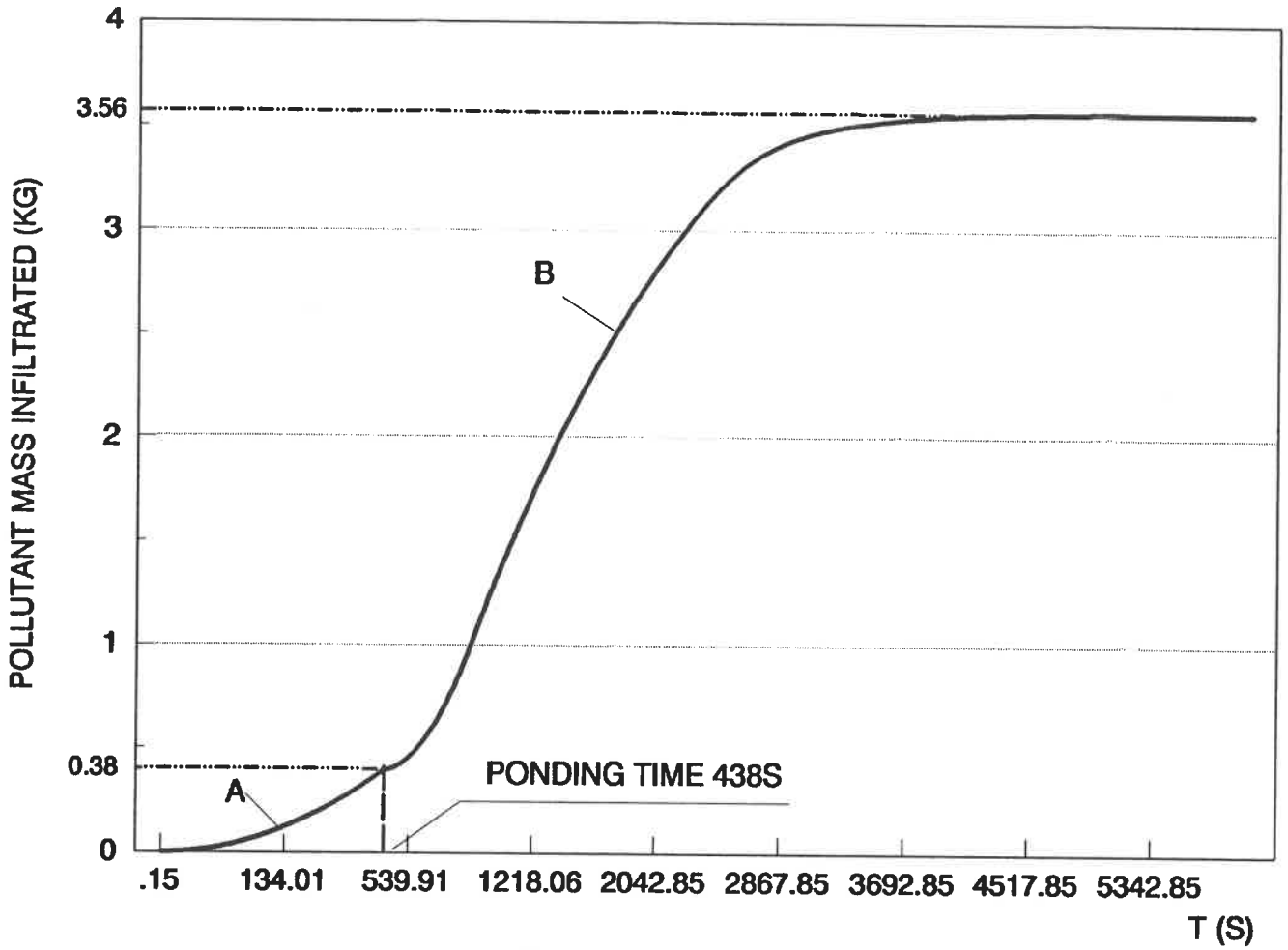

Figure 5.5.3 The Variation of Pollutant infiltrated

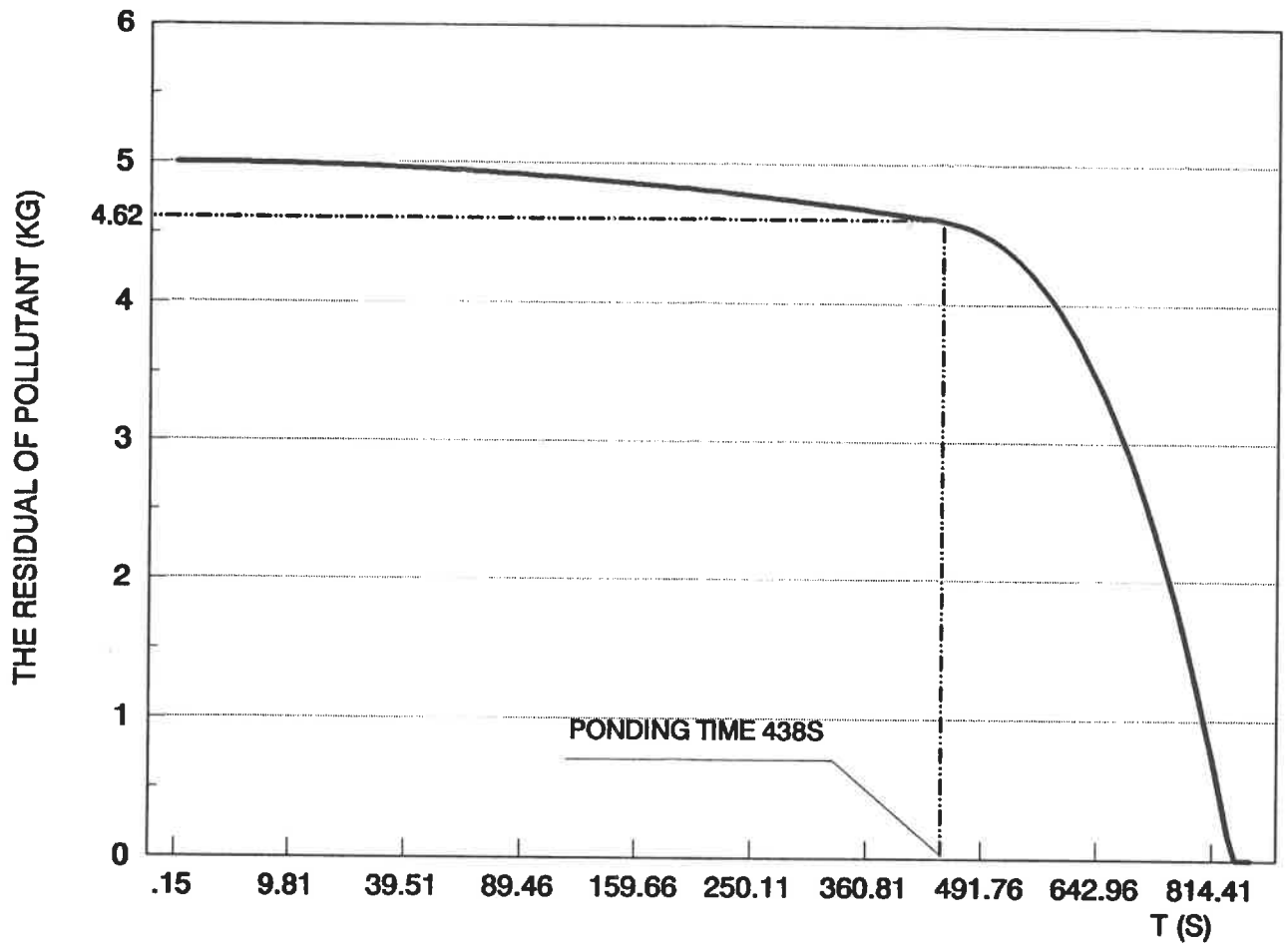

Figure 5.5.4 Time Evolution of Residual Pollutant

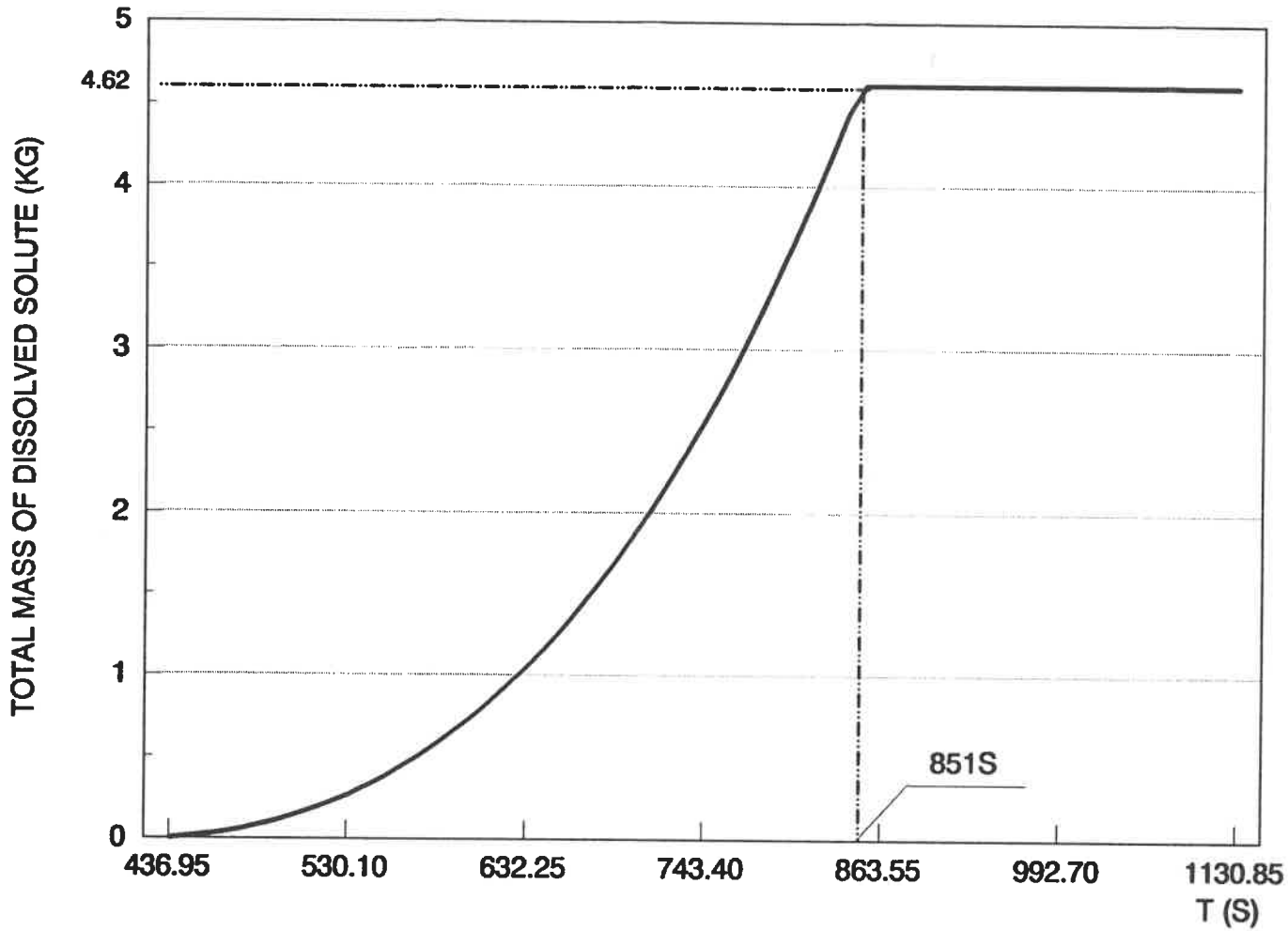

Figure 5.5.5 Time Evolution of Dissolved Solute

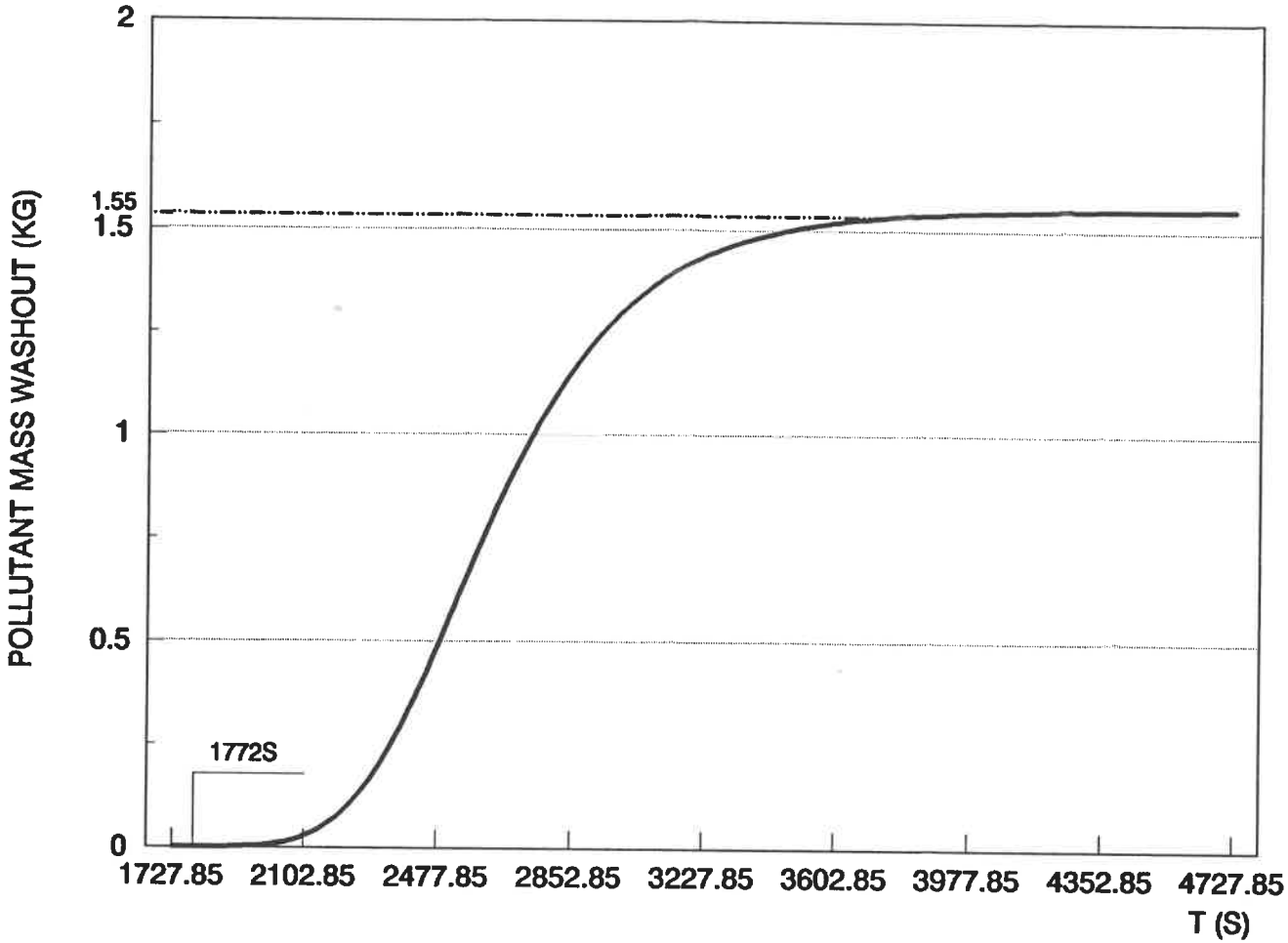

Figure 5.5.6 Time Evolution of Pollutant Washout

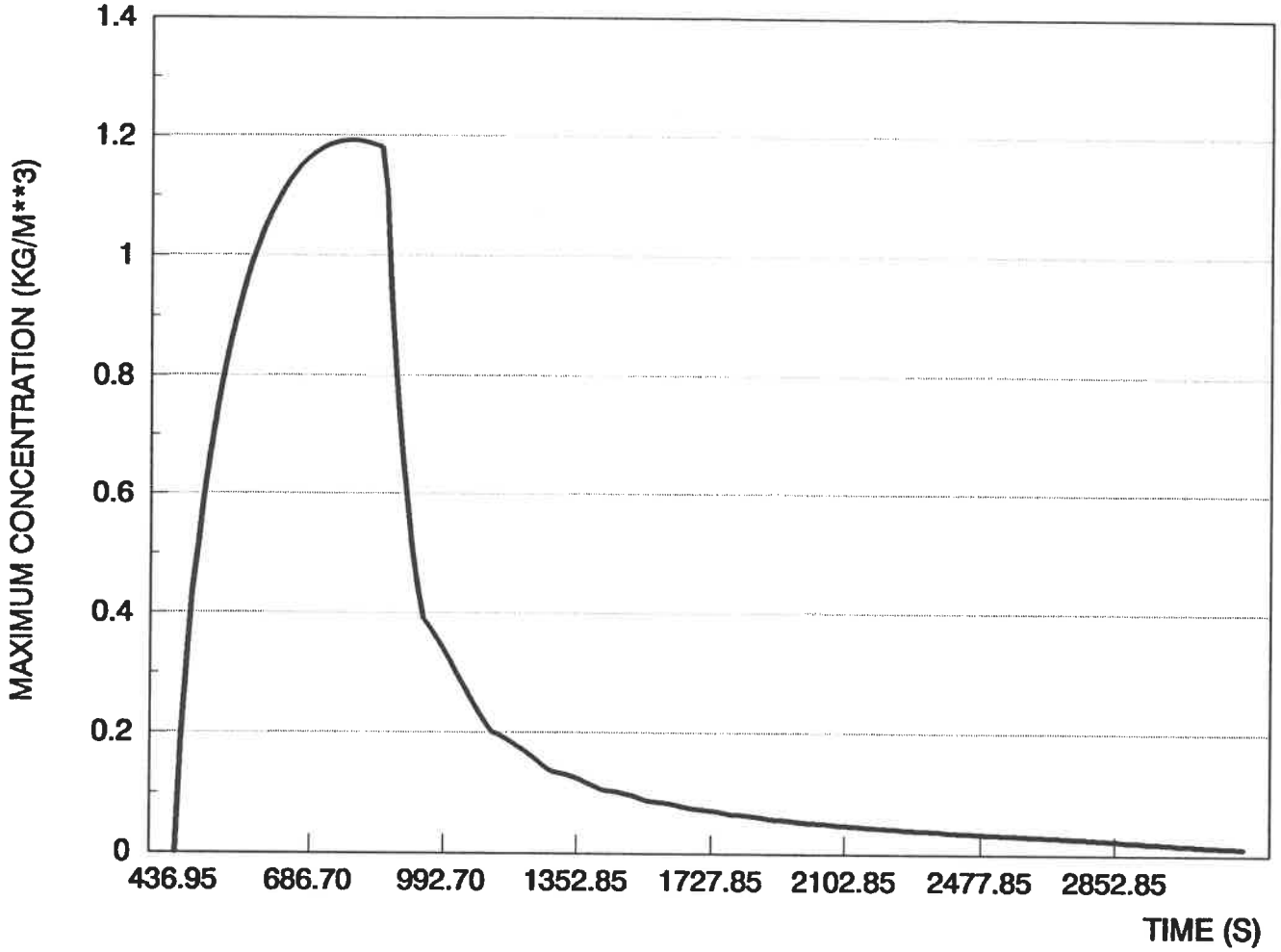

Figure 5.5.7 The Trace of Maximum Concentration

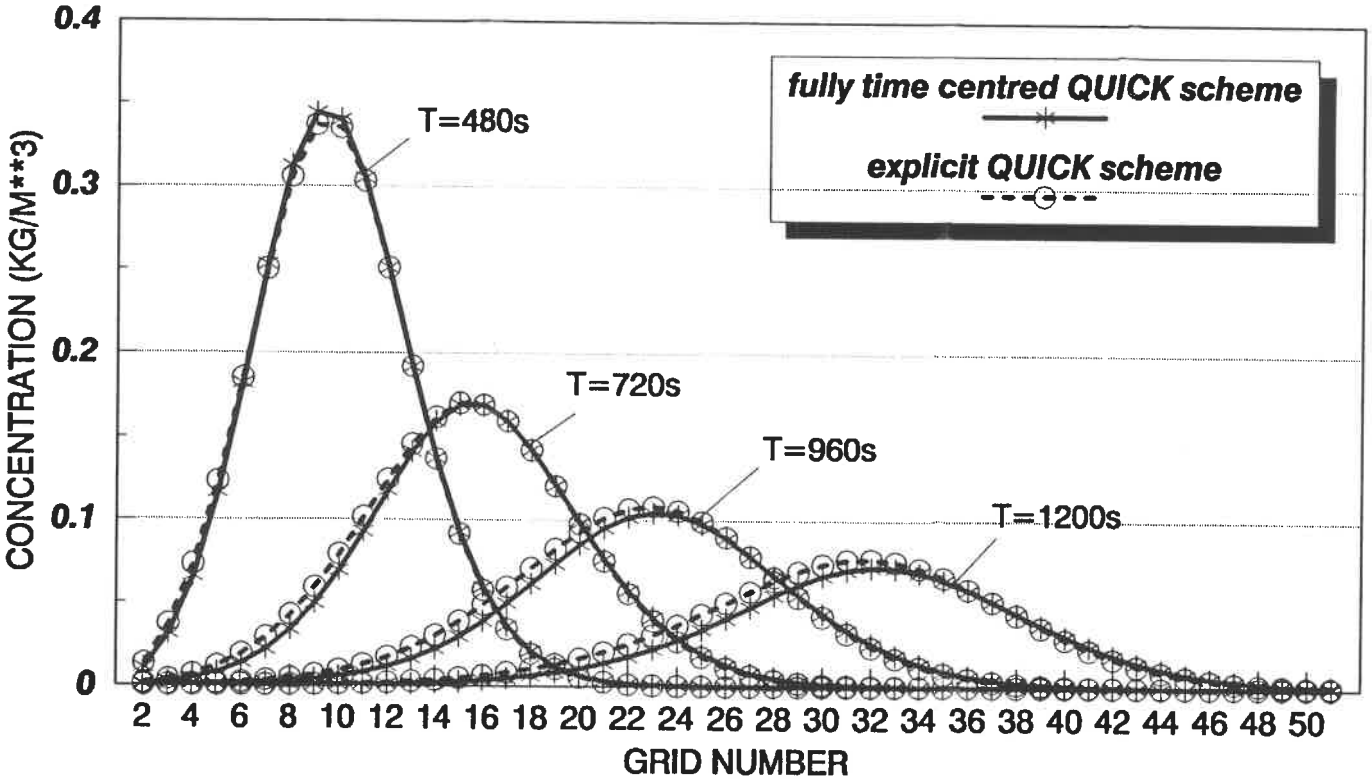

Figure 5.5.8 Comparison of the Different Scheme

CHAPTER 6
CONCLUSIONS AND RECOMMENDATIONS

A mathematical model based on physical reasoning for pollutant washout and transport in overland flow with infiltration, has been proposed in this study. The hydraulic behaviour of overland flow with infiltration and pollutant transport have been modelled individually using the results from the overland flow and infiltration to calculate the pollutant transport. The set of equations governing the complete system have been integrated numerically using various finite difference algorithms. A new formulation for the pollutant washout based on bed shear stress, reaction constant and ambient concentration of pollutant in the overland flow has been proposed. Several test computations indicated that the model provides reasonable results. The hydraulic portion of the model has been tested against pnblished field data with satisfactory agreement. Unfortunately, no field measurements of pollutant infiltration and washout are available for purposes of comparison.

In this study, a reaction rate constant k_2 appears in the solubility rate equation. For a given pollutant, k_2 is constant and has a physical basis. Its use lies in the fact that it may be treated as the only calibration parameter in the solubility rate equation which expresses the rate of mass transfer of a solid

pollutant to an aqueous solution. Actual values may be obtained by experiment.

Another parameter introduced in this study is the delay time coefficient k_4 introduced into the infiltration process before ponding time. It describes the time required for the solution containing the pollutant to become saturated. It directly affects the amount of infiltrated pollutant, especially during the initial period of rainfall. It is thus necessary to investigate the values of delay time coefficient by experiment, especially at the initial period during which saturated concentration is reached.

In this study, the effects of adsorption and any chemical reactions have not been considered, which may also be important factors in the pollutant transport. Further refinement of the model should incorporate these two important effects.

REFERENCES

AKAN, A. O., (1986) *Time of Concentration of Overland Flow*, Journal of Irrigation and Drainage Engineering., ASCE, Vol.112, No.4, pp283-292.

AKAN, A. O., (1987) *Pollutant Washoff by Overland Flow*, J. Environmental. Eng., Vol.113, No.4, pp811-823.

AKAN, A. O., and B. C. YEN., (1981) *Mathematical Modelling of Shallow Water Flow Over Porous Media*, J. Hydraul. Div., ASCE, Vol.107, No.HY4, pp 479-494.

AMEIN, M., (1968) *An Implicit Method For Numerical Flood Routing*, Water Resources Research., Vol.4, No.4, pp719-726.

BEDIENT, P.B., and W. C. HUBER, (1988) Hydrology and Floodplain Analysis Addison-Wesley Publishing Company, pp41.

BOUWER, H., (1966) *Rapid Field Measurement of Air Entry Value and Hydraulic Conductivity of Soil as Significant Parameter in Flow System Analysis*, Water Resources Research., Vol.2, No.4, pp729-738.

BRUTSAERT, W., (1971) *De Saint-Venant Equations Experimentally Verified*, J.Hydraul.Div., ASCE, Vol.97, No.9, pp1387-1401.

CHEN, Y., and R. A. FALCONER., (1992) *Advection-Diffusion Modelling Using The Modified QUICK Scheme*, Department of Civil Engineering, University of Bradford, Bradford BD7 1DP U.K. pp1171-1196.

CHOW, V.T., and BEN-ZVI, A., (1973) *Hydrodynamic Modeling of Two-Dimensional Watershed Flow*, J. Hydraul. Div., A SCE, Vol.99, No.HY11, pp2023-2040.

CHU, S. T., (1978) *Infiltration During an Unsteady Rain*, Water Resources research., Vol.14, No.3, pp461-466.

CLAPP, R. B., and G. M. HORNBERGER., (1978) *Empirical Equations for Some Soil Hydraulic Properties,* Water Resources Research., Vol.14, No.4, pp.601-604.

GOVINDARAJU, B. S., and M. L. KAVVAS., (1990) *Approximate Analytical Solutions for Overland Flows,* Water Resources Research., Vol.26, No.12, pp2903-2912.

HOLLY, F. M., and A. PREISSMANN., (1977) *Accurate Calculation of Transport in Two Dimensions*, J.Hydraul.Div., ASCE, Vol.103, No.HY11, pp1259-1277.

HROMADKA, T. V., MCCUEN, R. H., and C. C. YEN., (1987) *Comparison of Overland Flow Hydrograph Models*, J. Hydraul.Eng., Vol.113, No.11, pp1422-1440.

John A.B., (1977) Water Pollution Technology, Reston Publishing Company. Inc., pp110.

JOLIFFE, I. B., (1984) *Computation of Dynamic Waves in Channel Networks*, J. Hydraul. Div., ASCE, Vol.110, No.10, pp1358-1369.

KATOPODES,N., and T. STRELKOFF., (1979) *Two-Dimensional Shallow Water-Wave Model*, J. Eng. Mech. Div., ASCE., Vol.105, No.EM2, pp317-334.

KAWAHARA, M. and T. YOKOYAMA., (1980) *Finite Element Method For Direct Runoff Flow*, J. Hydraul. Div., ASCE, Vol.106, No.HY4, pp519-534.

KIRKBY, M.J., (1979) Hillslope Hydrology, John Wiley & Sons, Ltd., pp369.

LEONARD, B. P., (1979) *A Stable and Accurate Convective Modelling Procedure*

Based On Quadratic Upstream Interpolation, Computer Methods In Applied Mechanics and Engineering., Vol.19, No.1, pp59-98.

Li, C. W., (1990) *Advection Simulation by Minimax-Characteristics Method*, J. Hydraul. Eng., ASCE, Vol.116, No.9, pp1138-1244.

LIGGETT, J. A., and D. A. WOOLHISER., (1967) *Difference Solutions of The Shallow-Water Equation*, J. Eng. Mech. Div., Am. Soc. Eng., Vol.93, No.EM2, pp39-71.

MCCUEN, R. H., RAWLS, W. J., and D. L. BRAKENSIEK., (1981) *Statistical Analysis of The Brooks-Corey and The Green-Ampt Parameters Across Soil Texture*, Water Resources Research., Vol.17, No.4, pp1005-1013.

MEIN, R. G., and C. L. LARSON., (1973) *Modeling Infiltration during a Steady Rain,* Water Resources Research., Vol.9, No.2, pp384-394.

MOORE, I. D., and G. R. FOSTER., (1989) Hydraulics and Overland Flow, Process Studies in Hillslope Hydrology., John Wiley & Sons, Sussex, England, pp1-34.

MORRIS, E. M., (1979) *The Effect of Small-Slope Approximation and Lower Boundary Conditions on Solutions of the Saint-Venant Equations*, J. Hydr., Vol.40, No.1/2, pp31-47.

MULLEM, J. A. V., (1991) *Runoff and Peak Discharges Using Green-Ampt Infiltration Model,* Journal of Hydraulic Engineering., Vol.117, No.3, pp354-370.

RAWLS, W. J., BRAKENSIEK, D. L. and N. MILLER., (1983) *Green-Ampt Infiltration Parameters From Soils Data.*, J. Hydraul. Eng., Vol.109, No.1, pp62-70.

SIEMONS, J., (1970) Numerical Methods for the Solution of Diffusion- Advection Equation, Delft Hydraulics Laboratory. Ecole Polytechnique, pp3.

TAYFUR, G., KAVVAS, M. L., GOVINDARAJU, R. S. and D. E. STORM., (1993) *Applicability of St.Venant Equations for Two-Dimensional Overland Flows Over Rough Infiltrating Surfaces*, Journal of Hydraulic Engineering., Vol.119, No.1, pp51-63 .

VIESSMAN, W., KNAPP, J. W., LEWIS, G. L. and T. E. HARBARGH., (1989) Introduction To Hydrology, Third Edition, Harper & Row, Publishers, Inc., pp60.

WILLIAM, A. N., (1967) General Chemistry, McGraw-Hill Book Company, pp301.

WOOD, W. L., and P. D. ARNOLD., (1990) *On the Box Scheme for Overland Flow Calculations*, Communications in Applied Numerical Methods., Vol.6, pp.323-325.

WOOLHISER, D. A., (1975) Simulation of Unsteady Overland Flow, Unsteady Flow in Open Channels, Water Resources. Publications, Fort Collins, Colo., pp485.

ZHANG, W., and T. W. CUNDY., (1989) *Modeling of Two-Dimensional Overland Flow,* Water Resources Research., Vol.25, No.9, pp2019-2035.

ECOLE POLYTECHNIQUE DE MONTREAL
3 9334 00200396 8